UNIVERSIDADE DO ALGARVE

On the solvation in lipid bilayers measured by pyrene fluorescence: Thermal and molecular composition influence on equivalent polarity in lipidic mixtures

Dalila Lopes Arrais

Dissertação de Doutoramento em Ciências Biológicas (especialidade de Bioquímica)

Trabalho realizado sob a orientação de Prof. Doutor Jorge Manuel Martins
e co-orientação de Prof. Doutor Eurico Melo

2013

On the solvation in lipid bilayers measured by pyrene fluorescence: Thermal and molecular composition influence on equivalent polarity in lipidic mixtures.

Declaração de Autoria de Trabalho

Declaro ser a autora deste trabalho, que é original e inédito. Autores e trabalhos consultados estão devidamente citados no texto e constam da listagem de referências incluída.

Dalila Lopes Arrais

Copyright © 2013
Dalila Lopes Arrais (A Universidade do Algarve tem o direito, perpétuo e sem limites geográficos, de arquivar e publicitar este trabalho através de exemplares impressos reproduzidos em papel ou de forma digital, ou por qualquer outro meio conhecido ou que venha a ser inventado, de o divulgar através de repositórios científicos e de admitir a sua cópia e distribuição com objectivos educacionais ou de investigação, não comerciais, desde que seja dado crédito ao autor e editor).

Acknowledgements

"I have no special talent. I am only passionately curious." said Albert Einstein. I feel exactly the same. The need to question and find answers has driven me to these particular circumstances. The past years have been all about learning, not only in the scientific field, but also in life. I am truly thankful for the chance I have been given.

I would like to show my sincere appreciation to Prof. Jorge Martins, for all the support, friendship and wise advices throughout these (sometimes very demanding) years and for being an example in life. He once told me that fulfilling our purposes is as important as the path that leads us there and that being aware of this will make us rise above our (known) abilities. This is absolutely true! I also thank Prof. Eurico Melo for co-orienting this project.

I gratefully acknowledge FCT (Fundação para a Ciência e a Tecnologia) for the grant SFRH/BD/41607/2007 and IBB-CBME and Universidade do Algarve, Faro – Portugal, for their financial support and for providing all the necessary conditions so that this work could be performed.

But my overall gratitude goes to every single person who has been a part of my life until the present moment. Every living creature that touches (or touched) our lives has (or had) the power to contribute to the (never ending) creation of a better version of ourselves. It is up to us to read the signs and interpret them in the best way possible as everything is a positive lesson if seen through the right perspective. This will give us the chance to live plentifully, to accept ourselves and everyone who crosses our lives. I gratefully thank my family, Bruno and all my friends and dear ones, for showing me constantly how it feels to be truly loved.

This work is dedicated to those who are always
in my heart and bring light to my life!

(Este trabalho é dedicado a todos aqueles que, estando longe
ou perto, numa base diária ou menos constante,
me aquecem o coração e enchem a minha vida de luz!)

Abstract

Phosphatidylcholine (PC), sphingomyelin (SM) and cholesterol (CHOL) are major constituents of mammalian cell membranes. DPPC/CHOL and DPPC/DMPC are well-known binary mixtures. POPC/CHOL, DOPC/CHOL, egg-SM/CHOL, egg-SM/POPC and egg-SM/DOPC are less studied, but also important for the comprehension of the POPC/egg-SM/CHOL mixtures. These provide complex media for which polarity is hard to access. It is mainly determined by the water penetrating the bilayer (unevenly distributed creating a polarity gradient), though the influence of the dipoles from phospholipids (e.g. –PO, –CO, –OH) and the double bond in the steroid ring of CHOL cannot be neglected. CHOL derivatives are an interesting tool to verify the influence of the double bonds in the polarization of its surroundings. Pyrene fluorescence was used to access an equivalent polarity (associated to the dielectric constant) near the lipid/water interface of lipid bilayers. POPC/CHOL and DOPC/CHOL have similar thermal behavior and variation with CHOL content, though for lower CHOL content the equivalent polarity is higher for the DOPC/CHOL mixtures. The studies with DPPC and DMPC showed that pyrene does not seem to have a marked preference for either ordered or disordered phases. For DPPC/CHOL and egg-SM/CHOL the highlight goes to the behavior of the mixtures at higher CHOL amounts, where there is a substantial change in the thermal behavior and polarity values especially for the egg-SM/CHOL mixture. Egg-SM/POPC and egg-SM/DOPC show different behavior depending on which phospholipid has a higher molar proportion. The ternary mixtures analyzed do not exhibit significant differences, though there is the indication of the existence of a more ordered environment at lower temperatures and a less ordered environment for higher temperatures. The presence of 7DHC or DCHOL in egg-SM bilayers showed a tendency for the same behavior detected upon mixing higher amounts of CHOL.

Keywords: Pyrene, Fluorescence, Equivalent polarity, Model membranes, Lipid mixtures, Phase coexistence.

Resumo

As fosfatidilcolinas (PC), esfingomielinas (SM) e colesterol (CHOL) são os principais constituintes das membranas celulares de mamíferos. A presença deste esterol numa bicamada reflete-se através de algumas modificações ao nível das propriedades da mesma, das quais são exemplo, alterações na permeabilidade, espessura da bicamada, empacotamento das moléculas, difusão lateral dos lípidos. Hoje sabe-se que a bicamada lipídica que as compõe é um meio bastante complexo. Além de apresentar um gradiente de fluidez (da zona da interface, na qual os segmentos das cadeias metilénicas estão mais ordenados, para a zona do interior hidrofóbico, onde estão mais desordenados), apresenta ainda um gradiente de polaridade (que depende maioritariamente da presença de moléculas de água, mais concentradas na zona da interface e em muito menor quantidade no interior hidrofóbico). No entanto, é bastante difícil medir a polaridade em sistemas lipídicos. Um método muito utilizado é o uso de sondas sensíveis a alterações no meio, que particionam para o interior da bicamada. Embora as grandes diferenças na polaridade se devam à entrada e saída de água da bicamada, há que ter em conta a existência de dipolos provenientes dos diversos grupos moleculares dos lípidos (*e.g.* grupos fosfato, carbonilo, hidroxilo) e ligações duplas (como a que se encontra no sistema de anéis do colesterol). Muitos estudos sobre bicamadas lipídicas são feitos em sistemas modelo, segundo determinadas condições experimentais, e apenas dão uma ideia geral sobre as propriedades dos lípidos em misturas. O foco principal, na maioria das vezes, está nas interações entre lípidos, de modo que o papel desempenhado pelos dipolos é geralmente negligenciado. Sistemas binários e ternários como os estudados neste trabalho, podem parecer demasiado simples, mas dada a complexidade da membrana, são um bom método para isolar as partes para tentar compreender o todo. As misturas DPPC/CHOL e DMPC/DPPC já foram extensivamente estudadas, mas misturas como POPC/CHOL, DOPC/CHOL, egg-SM/CHOL, egg-SM/POPC e egg-SM/DOPC são menos conhecidas. No entanto, são um bom ponto de partida para aumentar um pouco mais a complexidade do sistema em estudo e partir para misturas ternárias, como a mistura POPC/egg-SM/CHOL, que é conhecida como sendo a mistura canónica que mimetiza a formação de domínios lipídicos (ou "rafts") em membranas biológicas. O uso de derivados de colesterol, também pode ser útil, no caso de se pretender uma melhor perceção sobre as interações lípido-esterol, como aconteceu neste trabalho, particularmente em relação à influência da ligação dupla do colesterol na polaridade sentida pela sonda.

Para aceder à polaridade nas misturas estudadas, foi utilizada a molécula de pireno, um hidrocarboneto aromático policíclico. Muito se tem especulado acerca deste tipo de sondas e sobre a consistência dos resultados que produzem, em especial, sobre o facto da inserção de uma molécula rígida poder trazer efeitos a nível estrutural, e sobre a possível existência de movimentos transversais consideráveis, que possam de certa forma alterar os resultados. O pireno inserido na bicamada localiza-se na zona mais ordenada das cadeias metilénicas. É certo que apresenta pequenos movimentos transversais, mas segundo estudos recentes em misturas POPC/CHOL, estes parecem ser negligenciáveis, bem como os possíveis efeitos estruturais provocados pela inserção desta sonda. O facto de esta sonda proporcionar uma média da polaridade nesta zona e ainda poder reportar uma média de diferentes zonas no plano da bicamada, devido à sua difusão lateral e ainda devido à difusão lateral dos lípidos,

revela-se como uma vantagem na sua utilização. Geralmente, os dados são obtidos sob a forma de uma razão entre a intensidade da primeira banda (altamente sensível à polaridade do solvente) e a intensidade da terceira banda (praticamente insensível à polaridade do solvente) do espetro de emissão do pireno (normalmente representada como I_1/I_3). Através da escala de polaridade do pireno (baseada no efeito de Ham) é possível relacionar esta razão diretamente com a constante dielétrica de um meio.

Com base nos diagramas de fases conhecidos para as misturas analisadas neste trabalho, foi possível obter um conjunto de resultados bastante completos, através da caracterização, em termos de polaridade (equivalente), de sistemas com diferentes composições lipídicas, a diferentes temperaturas.

No caso das misturas que envolvem fosfolípidos insaturados, verificou-se que os perfis de variação térmica de POPC/CHOL e DOPC/CHOL são equivalentes e semelhantes aos verificados para solventes homogéneos polares. No entanto, é possível detetar diferenças na polaridade para altas concentrações de colesterol (os valores de I_1/I_3 baixam com a adição de 40 mol% de colesterol no caso da mistura POPC/CHOL e com a adição de 20 mol% do mesmo esterol na mistura DOPC/CHOL).

A mistura (quase) ideal entre DPPC e DMPC revelou que a sonda parece não ter uma preferência marcada por fases mais fluidas ou fases mais ordenadas, sendo que esta poderá depender da composição da bicamada.

Para as misturas de fosfolípidos saturados com colesterol, a análise dos resultados é um pouco mais complexa. No entanto, observa-se um comportamento semelhante para as duas misturas (embora com valores de polaridade, no geral, ligeiramente mais elevados para a mistura DPPC/CHOL): para baixas concentrações de colesterol, obtiveram-se resultados parecidos aos correspondentes às fases fluidas, e um comportamento semelhante a solventes homogéneos polares; aumentando a quantidade de esterol, os valores de I_1/I_3 passam a não depender da temperatura, ou a depender de forma inversa (que é o caso da mistura egg-SM/CHOL).

As misturas fosfolípido-fosfolípido estudadas mostram que os perfis de variação da polaridade com a temperatura dependem de qual dos fosfolípidos está em excesso.

No caso das misturas ternárias, verificou-se que não há diferenças significativas entre os valores de polaridade para cada composição escolhida, no entanto, a variação térmica aponta no sentido da existência de uma fase mais ordenada a baixas temperaturas e uma fase menos ordenada a elevadas temperaturas.

Por sua vez, os efeitos da adição de 7DHC ou DCHOL à egg-SM, verificaram-se, de um modo geral, como sendo semelhantes aos efeitos do colesterol. Deste modo, o comportamento da mistura egg-SM para elevadas concentrações de colesterol pode não ser um efeito específico da presença da ligação dupla.

Palavras-Chave: Pireno, Fluorescência, Polaridade equivalente, Modelos de membrana, Misturas lipídicas, Coexistência de fases lamelares.

Contents

Abbreviations and Symbols

ΔG	Gibbs free energy variation
ΔH	Enthalpy variation
ΔS	Entropy variation
7DHC	7-Dehydrocholesterol
7DHCR	7-Dehydrocholesterol reductase
Abs	Absorbance / Absorption
CAC	Critical aggregation concentration
$CHCl_3$	Chloroform
CHOL	Cholesterol
CMC	Critical micelle concentration
D	Distance
DCHOL	Cholestanol
DMPC	1,2-dimyristoyl-*sn*-glycero-3-phosphocholine
DOPC	1,2-dioleoyl-*sn*-glycero-3-phosphocholine
DPPC	1,2-dipalmitoyl-*sn*-glycero-3-phosphocholine
DSC	Differential scanning calorimetry
E	Applied electric field
egg-SM	Natural egg yolk sphingomyelin
EPR	Electron paramagnetic resonance
ER	Endoplasmatic reticulum
ESR	Electron spin resonance
EtOH	Ethanol
F	Fluorescence emission
F'	Fluorescence emission after solvent relaxation
G	Correlation factor that characterizes the relative orientations between neighboring molecules
GPI	Glycosylphosphadidylinositol
GUV	Giant unilamellar vesicles
I_1/I_3	Ratio between the intensities of fluorescence of the first and third band of the pyrene emission spectrum
IC	Internal conversion
IR	Infrared spectroscopy
ISC	Intersystem crossing
k_B	Boltzmann constant
L_α	Liquid crystalline or fluid lamellar phase
L_β	Gel lamellar phase
$L_{\beta'}$	Gel lamellar phase for phosphatidylcholines
L_c	Sub-gel phase
l_d	Liquid disordered phase for phospholipid-cholesterol mixtures
l_o	Liquid ordered phase for phospholipid-cholesterol mixtures

LAURDAN	2-dimethylamino-6-lauroylnaphthalene
LUV	Unilamellar vesicles
$\boldsymbol{M}$	Molar mass
MD	Molecular dynamics
MeOH	Methanol
MLV	Multilamellar vesicles
$\boldsymbol{N_A}$	Avogadro Number
NMR	Nuclear magnetic resonance
^{2}**H-NMR**	Deuterium nuclear magnetic resonance
$\boldsymbol{p}$	Polarization
$\mathbf{P_{\beta'}}$	Ripple phase for phosphadidylcholines
PAH	Polycyclic aromatic hydrocarbons
PC	Phosphatidylcholine
PE	Phosphatidylethanolamine
PI	Phosphatidylinositol
PG	Phosphatidylglycerol
$\boldsymbol{P_m}$	Molar polarizability
POPC	1-palmitoyl-2-oleoyl-*sn*-glycero-3-phosphocholine
PRODAN	6-propionyl-2-dimethylaminonaphthalene
PS	Phosphatidylserine
PSM	N-pamitoyl-sphingomyelin (N-palmitoyl-D-*erythro*-sphingosylphosphorylcholine)
$\boldsymbol{Q}$	Charge (+q or –q) of a particle
$\mathbf{S_0}$	Singlet ground electronic state
$\mathbf{S_1}$	First singlet electronic excited state
$\mathbf{S_2}$	Second singlet electronic excited state
So	Solid-ordered state of lipid bilayers
$\mathbf{So_1}$	POPC-rich solid-ordered state in PSM/POPC mixtures
$\mathbf{So_2}$	PSM-rich solid-ordered state in PSM/POPC mixtures
SLOS	Smith-Lemli-Opitz syndrome
SM	Sphingomyelin (1-ceramide-phosphorylcholine)
SUV	Small unilamellar vesicles
$\mathbf{T_1}$	First triplet state
$\mathbf{T_2}$	Second triplet state
$\boldsymbol{T_m}$	Main phase transition temperature
$\boldsymbol{T}$	Temperature
UV-vis	Ultra-violet visible range of the electromagnetic spectrum
$\boldsymbol{v_0}$	Vibrational ground state
$\boldsymbol{v_1}$	First vibrational excited state
$\boldsymbol{v_2}$	Second vibrational excited state
$\boldsymbol{V}$	Molar volume

Greek Letters

$\boldsymbol{\alpha}$	Molecular polarizability
$\boldsymbol{\varepsilon_0}$	Permittivity in vacuum
$\boldsymbol{\varepsilon}$	Dielectric constant or relative permittivity (also noted as ε_r) / molar absorption coefficient
$\boldsymbol{\varepsilon_r}$	Dielectric constant or relative permittivity (also noted as ε**)**
$\boldsymbol{\lambda_{exc}}$	Excitation wavelength
$\boldsymbol{\mu}$	Dipole moment of a molecule in the ground state
$\boldsymbol{\mu^*}$	Dipole moment of a molecule in the excited state
$\boldsymbol{\mu_i}$	Induced dipole moment
$\boldsymbol{\pi}$	Bonding *pi* molecular orbital
$\boldsymbol{\pi^*}$	Antibonding *pi* molecular orbital
$\boldsymbol{\rho}$	Mass density
$\boldsymbol{\tau}$	Fluorescence lifetime
$\boldsymbol{\Phi_F}$	Fluorescence quantum yield

Chapter I

INTRODUCTION

I – 1 *A general view over biological membranes*

Membranes play a key role in structure and function of cells. They are complex structures that are involved in several biological events, *e.g.* the permeation of small molecules in and/or out of compartments, and the information transfer mostly through conformational changes induced in protein membrane components. They also provide the ideal conditions for cellular enzymes to catalyze numerous transmembrane reactions (such as molecular transport), in plane sequential reactions (electron transport chains) and to participate in the maintenance or biosynthesis of the membrane [1].

One (very) simple way to look at biological membranes is to picture them as flexible boundaries that form a permeability barrier and provide compartmentalization, *i.e.* sealing specific environments [2]. Essentially, it is their ability to control the nature of all communications between the inside and outside media that made them such an interesting object of study. Its barrier properties became evident in the early studies involving cells. With the advance in membrane study techniques, soon there was the notion that the membrane supporting structure was mainly of lipidic nature, it was disposed in the form of a bilayer and that there was the presence of biologically relevant proteins [3]. Singer and Nicolson [4] then collected the available information to formulate the famous "fluid mosaic model" in which biological membranes were seen as a lipid bilayer where globular proteins could diffuse freely and could be inserted into the membrane or loosely attached to it (Figure 1.1 – A). They also accounted the fact that some proteins may prefer a specific lipidic surrounding in order to be fully functional. This idea was later refined by Mouritsen and Bloom [5], giving rise to the Mattress Model: protein and lipid interactions are based in the hydrophobic matching, which leads to the accumulation of certain lipidic species around the proteins, resulting in their aggregation and clustering (Figure 1.1 – B) [3]. These views describe the basic interaction between the two major components of biological membranes: lipids and proteins. Carbohydrates account for about 10% of the weight of plasma membranes, but are invariably bound to either proteins or lipids. It is now known that membrane composition is highly variable from cell to cell and even between organelles inside the same cell [1, 3, 6].

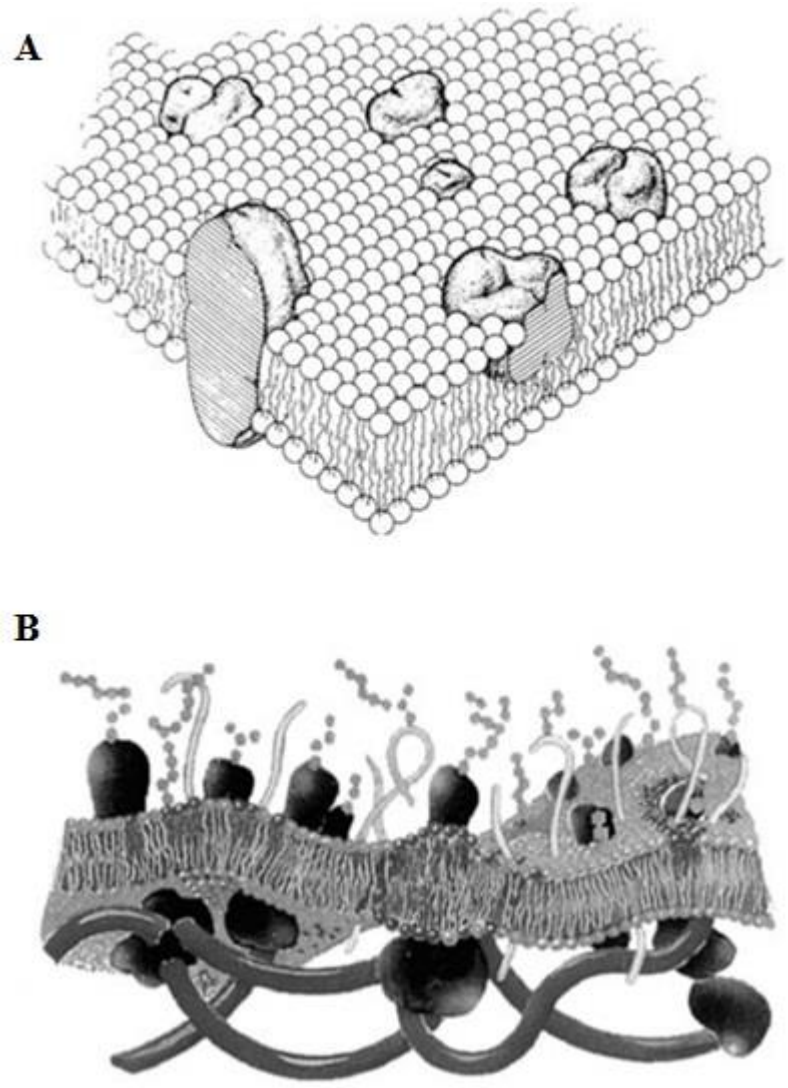

Figure 1.1 – (A) Singer and Nicolson fluid mosaic model: the membrane proteins are "floating in a fluid sea" of lipids and are grouped in two classes (integral and peripheral); (B) Mouritsen and Bloom mattress model: a lipid bilayer subjected to undulations that is sandwiched between polysaccharides on the outside and the cytoskeleton in the inside and displays lateral heterogeneity, lipid domains formation and thickness variation close to integral proteins (adapted from reference [3]).

Nowadays, there is much available information mostly achieved by studying the physicochemical properties of membrane components on its own or through the assembly of model membranes with varying lipidic and/or proteic compositions, under different thermodynamic parameters (*e.g.* temperature, pressure).

I – 1.1 *Lipid bilayer structure*

I – 1.1.1 Water

Water is an important component of lipidic membranes as it stabilizes membrane structure. It plays a major role in physiological processes of great significance, such as membrane fusion, and the association with proteins and small molecules with the lipid bilayer [3, 7]. Lipids need high amounts of water to fully hydrate. The dissimilar distribution of water in biological membranes (higher amounts at the lipid/water interface and lower amounts in the hydrocarbon region) gives rise to different polarity environments (with different dielectric constants), therefore creating a polarity gradient.

Due to this, the role of water will be addressed several times throughout this work, every time it is relevant to the matter. A more detailed description on how water interacts with lipid bilayers and influences the polarity and the dielectric constant in these lipidic systems will be given in Section I – 1.4.

I – 1.1.2 Membrane lipids

Lipids are responsible for the formation of the matrix which is the base for the structure of biological membranes. The membrane response to several physiological events (like high curvature regions, membrane fusion, cytokinesis, biosynthetic pathways) as well as the selective interaction with membrane proteins (assisting on the correct folding or on the achievement of optimal enzyme activity) may require the presence of different lipidic species. At the same time, as these changes in the lipidic environment are performed, the main bilayer physical properties are still maintained. This is only possible due to the existence of a great variety of lipidic chemical structures [1, 2, 8]. Lipids are small amphiphilic molecules with a polar head group and a hydrophobic hydrocarbon region [3]. Most of the information on the properties of lipid bilayers results from studies with glycerophospholipids (or just "phospholipids"), sphingolipids and sterols, so the next lines will be focused on them.

I – 1.1.2.1 Glycerophospholipids

The glycerophospholipids are the main lipid constituents in biological membranes, usually found in most eukaryotic and prokaryotic organisms. They are glycerol-based lipids for which generally there is a phosphate group linked in the third position (*sn*-3) and two hydrocarbon chains attached (through ester linkages) to the first and second positions (*sn*-1 and *sn*-2,

respectively). These are the so-called 1,2-diacylphosphoglycerides or phospholipids. The hydrocarbon chains vary widely in length, branching, and degree of unsaturation. Lipids containing double bonds in their methylenic chains are called unsaturated phospholipids, while the ones without double bonds are called saturated [1, 3]. The phosphate is usually linked to one functional group thus constituting the polar head group that categorizes such lipids into phosphatidylcholines (PC), phoshatidylethanolamines (PE), phosphatidylserines (PS), phosphatidylglycerol (PG) and phosphatidylinositol (PI). From these, PC are of particular interest as they are a major component in animal cell membranes. Many of these molecules have one saturated and one unsaturated chain (in animal cells, the unsaturated chain is usually esterified to the *sn*-2 position of glycerol). Natural occurring PC commonly display *cis*-double bonds [1, 8]. Figure 1.2 shows the structures of the PC used in this work: 1,2-dimyristoyl-*sn*-glycero-3-phosphocholine (DMPC); 1,2-dipalmitoyl-*sn*-glycero-3-phosphocholine (DPPC); 1-palmitoyl-2-oleoyl-*sn*-glycero-3-phosphocholine (POPC); 1,2-dioleoyl-*sn*-glycero-3-phosphocholine (DOPC).

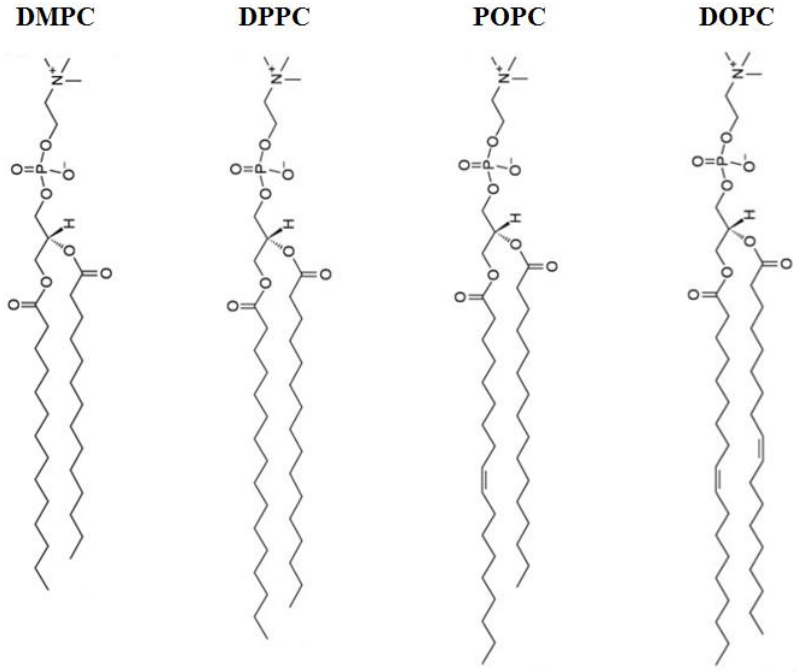

Figure 1.2 – Schematic representation of the structure of the phospholipids used in this work. For DMPC, the two sterified fatty acids are myristic acid (Abbreviated notation: 14:0). For DPPC, the two sterified fatty acids are palmitic acid (16:0). For POPC, the *sn*-1 position is sterified with palmitic acid and the *sn*-2 position with an oleic acid, with a *cis*-double bond in carbon 9 (16:0-18:1, Δ9-*Cis*). For DOPC, the two sterified fatty acids are oleic acid (18:1, Δ9-*Cis*).

I – 1.1.2.2 Sphingolipids

One of the fundamental structures that are common to sphingolipids is the ceramide (N-acyl-sphingosine). The sphingolipids basically contain the same polar substituents as the glycerophospholipids, but they are ceramide-based. Due to their similarities regarding physicochemical properties, these two lipidic species are frequently grouped together. Sphingomyelin (SM) or ceramide 1-phosphorylcholine is one of the most important phosphosphingolipids (Figure 1.3). The terminal–OH group of ceramide is esterified with a choline group. It is widely found in animal cell membranes, generally in the outer leaflet of the plasma membrane [1, 2, 6].

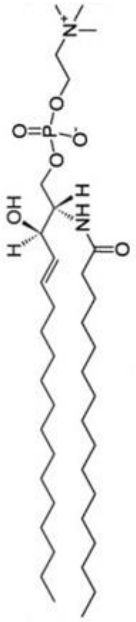

Figure 1.3 – Schematic representation of PSM (N-palmitoyl-1-phosphorylcholine) (Abbreviatied notation: 16:0 SM) which is the predominant lipidic specie in the egg-SM used in this work.

I – 1.1.2.3 Sterols

Sterols are found in the composition of plant, animal and fungal membranes. Most have the same ring skeleton, but differ in their side chains, peripheral structure features,

stereochemistry and number of double bonds in the ring system [6]. Cholesterol (CHOL) (Figure 1.4) is by far the most commonly found sterol in eukaryotic cell membranes.

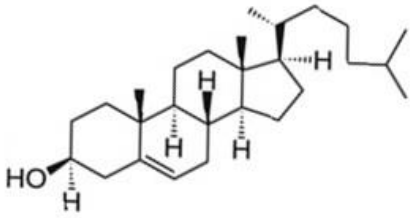

Figure 1.4 – Schematic representation of the structure of CHOL.

It is present in animal cell plasma membranes (20 mol% - 50 mol% of its mass), lysosomes, endosomes, mitochondrial membranes (< 5 mol%), Golgi (≈ 8 mol%) and endoplasmatic reticulum (ER) (≈ 10 mol%) [9]. Sterols are a major mean through which eukaryotic cells modulate and refine membrane properties [10]. Other important sterols are sitosterol, campesterol and stigmasterol, usually found in higher plants; ergosterol, an important component in fungal plasma membranes, and lanosterol, the sterol of some procaryotes [1, 3, 8].

I – 1.1.2.3.1 Cholesterol is a "special" lipid

CHOL is a very important biomolecule with various important biological functions. It is involved in several physiological events, *e.g.* biogenesis, cell growth, steroid hormone and bile salt synthesis and embryonic development [10, 11, 12]. Further, CHOL acts as a precursor of the active form of vitamin D. Its synthesis is mainly confined to the ER and includes the presence of acetyl coenzyme A in a series of enzymatic steps (CHOL is indeed the regulator of some enzymes in its metabolic pathway) [2]. These are highly regulated as any deviation from its physiological concentrations may cause pathological situations. Elevated cholesterol levels have been observed in membranes of living cells and are associated with the formation of atherosclerotic plaques (in the form of CHOL monohydrate) [13], depletion of ER calcium supplies [14] and obstruction of the small bowel [15, 16]. The Alzheimer's disease also seems to

be related to the levels of CHOL and lipids as its distribution may be related to the formation of amyloid deposits [17].

The involvement of CHOL in membrane organization and structure characterizes it as a "membrane active sterol". It has a major contribution in the control of membrane passive permeability to small polar molecules, by reducing average "fluidity" and free volume of the lipid bilayers. Plus, it has an important role on lateral organization, modulation of membrane thickness, enhancement of mechanical strength [18, 19] and free volume distribution (involved in controlling membrane protein activity and "raft" formation) [7, 10, 11]. Basically, these effects in membrane structure and function are the result of the molecular structure and the interactions of this sterol with neighbor lipids (and proteins). As it is shown in Figure 1.4, CHOL is also an amphiphilic molecule, though it is not similar to a "regular" phospholipid. It is constituted by a small hydrophilic hydroxyl (–OH) group and a planar rigid hydrophobic structure (in a *trans*-configuration) with a short branched (isooctyl) chain segment. Its ring system has a smooth face (α-face), regular and tight, and a rough face (β-face) irregular and less tight due to the presence of the protruding methyl groups [9, 20, 21]. The smooth and rough sides of CHOL are indicated as responsible for the molecule tilt, when inserted in lipid bilayers [21]. This sterol seems to adjust its tilt angle for a better accommodation in the membrane: at low CHOL concentrations, the molecule has a large tilt, while at higher CHOL concentrations it has a smaller tilt [22, 23]. This was observed in the cases of saturated lipid bilayers and unsaturated lipid bilayers, though the molecular tilt appears to be lower in the latter case [23] [24]. This feature is believed to be essential for the ordering and condensing effect exerted by CHOL on neighbor lipids [25]. The general aspects of phospholipid-sterol interactions in lipid bilayers will be further described in Section I – 1.2.2.2.

I – 1.1.2.3.2 Cholesterol derivatives

The so-called CHOL derivatives may be a useful tool when it comes to understand certain lipid bilayer properties, especially by comparing its effects on membrane structure and function with the ones exerted by CHOL. In this work, the attention goes to 7-dehydrocholesterol (7DHC) and cholestanol (or dihydrocholesterol – DCHOL), which are represented in Figure 1.5 – A and B, respectively. Structurally, the main difference between these sterols is in the number of double bonds in the ring system: 7DHC has two double bonds, CHOL has one and DCHOL has none. 7DHC may be more rapidly oxidized than

CHOL [26], due to its loss of planarity [27, 28], while DCHOL is similar to CHOL, in terms of planarity, condensation ability and molecular areas at air-water interface [28].

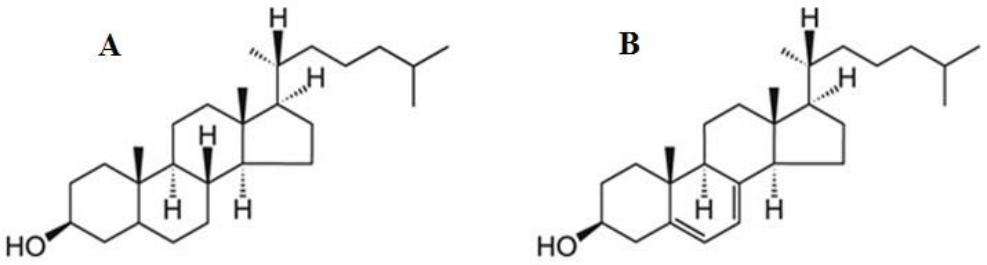

Figure 1.5 – Schematic representation of the structures of the CHOL derivatives used in this work: (A) DCHOL; (B) 7DHC.

7DHC is a biogenic intermediate in the biosynthesis of CHOL [28]. It is converted into CHOL *via* an enzymatic step performed by 7-dehydrocholesterol reductase (7DHCR). A defect in this enzyme leads to the accumulation of 7DHC in all tissues and this is associated with the Smith-Lemli-Opitz syndrome (SLOS) [26, 28, 29]. There are some indications that 7DHC may participate in raft formation [28, 30] and that its presence can affect the protein raft composition [31]. DCHOL also seems to promote the formation of membrane domains [28].

I – 1.1.3 How do lipids behave in aqueous solution?

Above a critical concentration (referred in literature as "Critical Aggregation Concentration" – CAC, an extended notion of the classical "Critical Micelle Concentration" – CMC), lipids tend to form amphiphilic aggregates in order to shield the hydrocarbon chains of the amphiphiles from contact with water, while exposing their polar and/or charged groups to it. The hydrocarbon parts of these molecules do not interact favorably with water through dipole-dipole interactions and they are also not able to form hydrogen bonds. Due to this hydrophobic effect (liberated water molecules from the solvent cages formed around the hydrocarbon chains to stabilize them in a hydrogen-bond forming medium), the overall entropy of the amphiphile/water mixture is higher (the increase in entropy in aqueous solvent

largely compensate the formation of amphiphilic aggregates), and the stability of the system is ensured ($\Delta G < 0$). So, the association of the hydrocarbon parts of the lipids will contribute to minimize the total surface area in contact with water, while the polar domains interact with it or with other lipid head groups either through hydrogen bonding or ionic interactions, constituting an energetically stable structure in the aqueous environment [1].

I – 1.1.3.1 Assembly of lipid aggregates

The lipid aggregation in the presence of water results in various lipid-water polymorphic arrangements for which the predominant lipidic form depends mainly on temperature, pressure, ionic strength and pH. Generally, they can be found as: micelles (which may assume different shapes); lamellar phases (extended two-dimensional sheets in the form of bilayers, at very high lipid concentrations); and, at very high temperatures, cubic phases (unilamellar structures with periodic three-dimensional order) or inverted hexagonal phases (mostly for PE) [1, 3].

From these, lamellar phases are of great interest, as the lipid bilayer is a self-aggregate "sheet" of amphiphiles (usually two molecules thick) in which the polar portions of the constituent molecules are exposed to water at the two surfaces and the apolar portions are excluded from water in the volume between these two surfaces [1, 2, 3, 8].

I – 1.1.3.2.1 Experimental model membrane systems

Model membrane systems are a useful tool to study the properties of pure lipids, lipid mixtures and reconstituted lipid-protein mixtures. These form spontaneously on hydration of the amphiphiles and are represented in Figure 1.6. Usually, they are studied as monolayers (using a Langmuir trough to accurately measure lipid properties like surface area and lateral pressure) or liposomes (lipid structures that usually enclose an aqueous volume). According to the already mentioned properties of lipids, when they disperse in water a heterogeneous mixture of vesicular structures is formed, with these containing concentric bilayers separated from the inside and the outside by a thin layer of water (approximately 10-20 Å) due to a strong force of repulsion (usually referred to as "hydration force") [3, 6, 8]. These are called multilamellar vesicles (MLV). They can be transformed into unilamellar vesicles of different diameters: small unilamellar vesicles (SUV) with about ≈ 20 nm of diameter; large

unilamellar vesicles (LUV) with about ≈ 100 nm and giant unilamellar vesicles (GUV) in the order of 10-50 μm [1, 8].

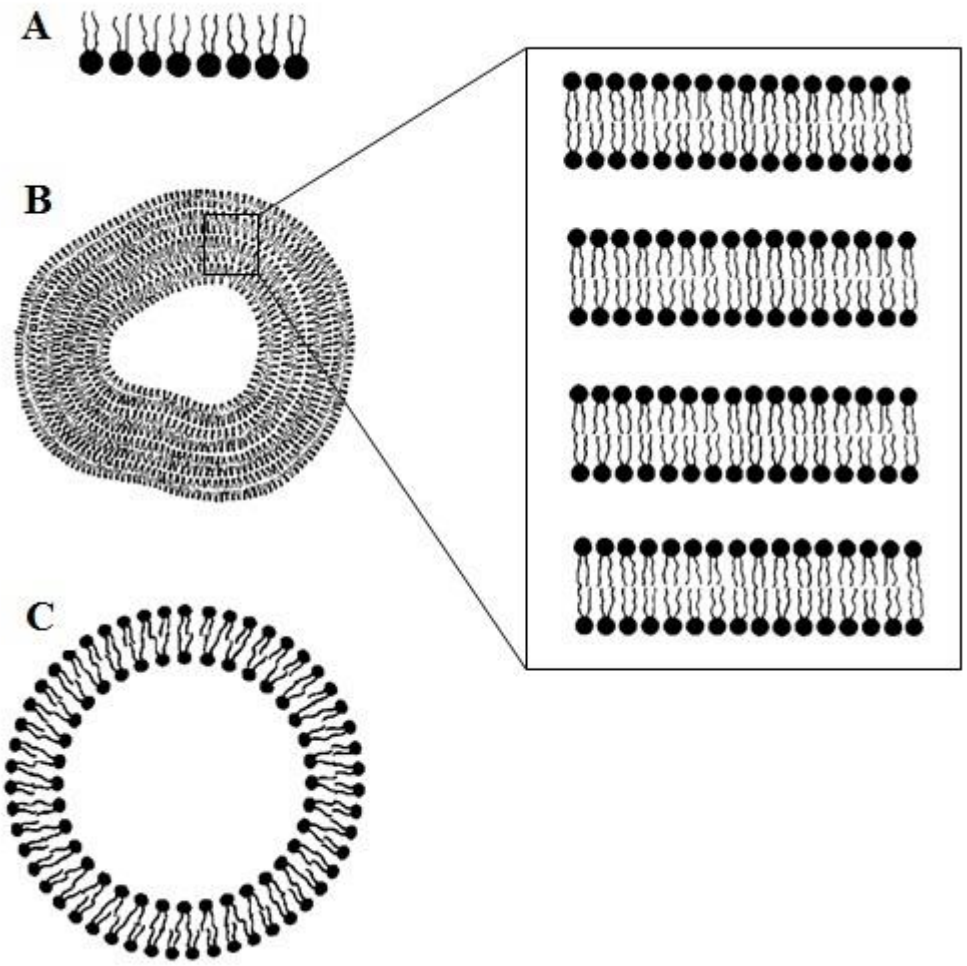

Figure 1.6 – Schematic illustration of lipid molecular aggregates used as model membrane systems. (A) Monolayer; (B) Multilamellar vesicle or liposome (with the representation of multilamellar lipid bilayers in a stack); (C) Unilamellar vesicle or liposome (adapted from reference [9]).

I – 1.2 *Lipid bilayer physical properties*

Lipid bilayers are condensed phases that with many characteristics of simple lipids though simultaneously structured. Their transbilayer profile was characterized by a number of techniques, *e.g.* X-ray and neutron scattering techniques, NMR (nuclear magnetic resonance),

EPR (electron paramagnetic resonance) or ESR (electron spin resonance), molecular probing through optical spectroscopies and computer simulations (Figure 1.7). Roughly, lipid bilayers can be divided into four zones: (from the outside to the inside) a zone where "structured" water is deprived of forming all possible hydrogen bonds; a hydrophilic/hydrophobic region that includes the polar head groups and the upper segment of the hydrocarbon chains (where the membrane/water interface is found); a region of ordered fatty-acid segments; and a hydrophobic core with disordered methylenic chains segments [9].

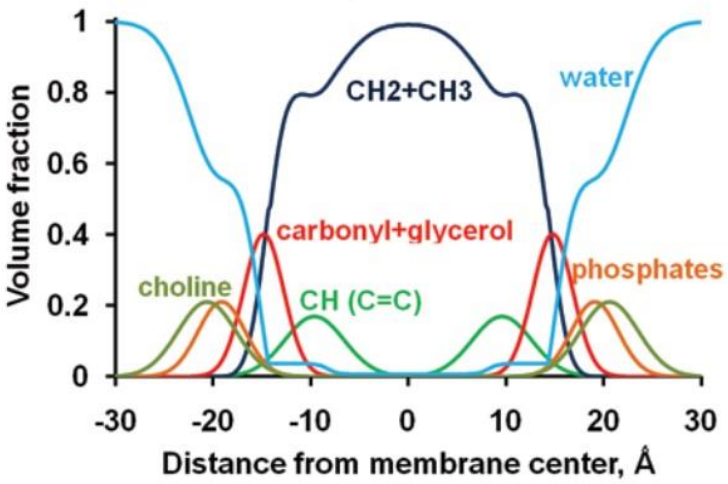

Figure 1.7 – Volume fractions of lipid segments for a fluid DOPC bilayer (determined by X-ray and neutron scattering). The volume fractions of individual lipid components are represented as colored solid lines for alkyl groups ($CH_2 + CH_3$, dark blue), double bonds (green), water (blue), carbonyls with glycerols (red), phosphates (orange), and choline (olive) groups (adapted from reference [32]).

Data from X-ray crystallography shows that lipid bilayers are closely related to liquid crystals, as the lipid molecules display a preferential orientation within the membrane [3]. The lipid polar head groups (in PC) are generally parallel to the plane of the bilayer, which seems to be the most stable arrangement as the positive and negative charges are located in a plane that is nearly parallel and electrostatically neutral [1, 6]. On the other hand, the acyl chains are usually aligned perpendicular to the membrane surface though they can have a tilt angle (the angle between the hydrocarbon chain axis and the bilayer normal). The glycerol backbone is the least flexible region of phospholipids. The acyl chains linked to the *sn*-1 position of

glycerol have higher order parameters for carbons up to the middle of the chain. Then they rapidly decay toward the terminal methyl group (the region of high chain order is referred as the "order parameter plateau") as there is the increase on the probability of carbon-carbon (C–C) *trans-gauche* isomerization. In contrast, chains linked to the *sn*-2 position have lower order parameters (due to differences in chain orientation near the glycerol) [6, 33]. The orientational and positional order of phospholipid acyl chains is the basis for the existence of a fluidity gradient [34].

Generally, the lipids that constitute lipid bilayers are polymorphic: they have different modes of hydrocarbon packing. These are mainly dependent on their chemical identity, degree of hydration, pressure, ionic strength, pH and temperature, which basically defines their final form [6]. The temperature dependent change in hydrocarbon chain order is called order or melting transition (generally addressed as a solid-to-liquid transition). These transitions occur over a very narrow temperature regime, as a consequence of the cooperativity between large clusters of *n* lipids (cooperative unit) that form under the influence of temperature [3]. In this particular case, we can observe different phases (*i.e.* fixed and well-defined physical states) [35]. In order to better understand this phenomenon, it is helpful to first consider a single lipid bilayer.

I – 1.2.1 Phase transitions in single lipid bilayers

At very low temperatures, phospholipid chains may be arranged in a rigid and highly ordered state (all-*trans*), easily comparable to a crystalline structure (the "sub-gel" or L_c phase). As the temperature increases, the molecules will be arranged tightly in a two dimensional lattice in the membrane plane that corresponds to the gel phase (L_β). These are phases of higher bilayer thickness due to the all-*trans* state of the methylenic chains (oriented perpendicular to the bilayer plane). When the temperature is raised, there is still in the existence of a two-dimensional ordered system, but the hydrocarbon chains are mostly disordered (increase in the *gauche* conformers) and the lattice order is lost (Figure 1.8). At this point, we are in the presence of a fluid phase, often called the liquid-crystalline phase (L_α). This form is usually thought to represent the bulk of the lipids in the biological membrane [1, 3].

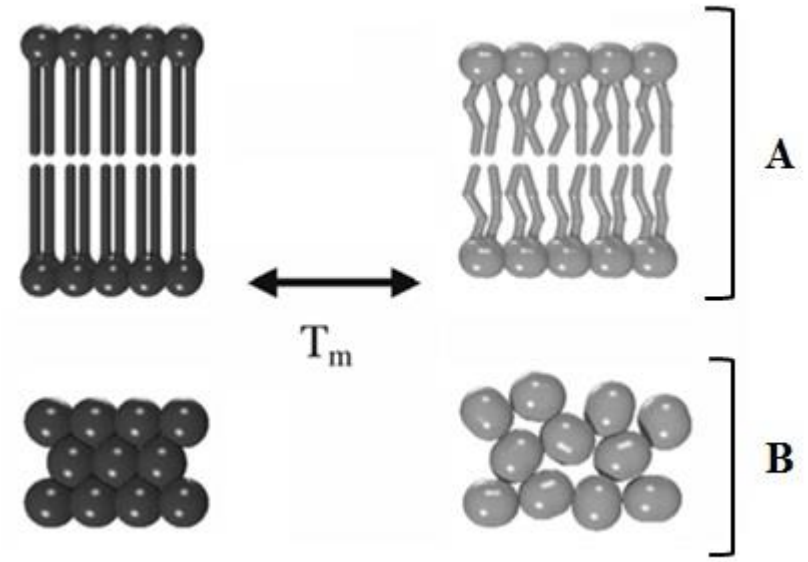

Figure 1.8 – Representation of the melting transition from a solid (ordered) phase to a liquid (disordered) phase (from left to right). (A) Reduction of the hydrocarbon chain order upon increasing temperature. (B) Loss in lattice order in the polar head group region when the temperature is higher (adapted from reference [3]).

The temperature for which there is the transition from the gel to the liquid crystalline phase is called the main phase transition temperature (T_m). Table 1.1 represents the T_m for the lipids used in this work. This process is endothermic and is usually monitored through differential scanning calorimetry[1] (DSC). It occurs exclusively in the plane of the membrane and is observed in all lipid bilayers regardless of the chemical identity of the lipids. At the T_m, the lipid is partially in the gel state and partially in the liquid crystalline state. The temperature at which this phase transition occurs is mostly dependent on the chemical identity, length and degree of unsaturation of the fatty acyl chains, but the nature of the polar head group is also important. In this matter, the intermolecular forces (van der Waals interactions) play an significant role in contributing for the relative stability of the referred phases: longer chain lengths result in higher T_m values and *vice versa*. The existence of *cis*-double bonds reduces the T_m as this will disrupt the ability of the chains to interact optimally in the gel state [1, 3].

1 Diffential scanning calorimetry is based on the changes of heat flow in the sample and the reference cells [6].

Table 1.1 – Main phase transition temperatures (T_m) for the phospholipids used in this work.

Phospholipid	T_m (ºC)
POPC	– 20*
POPC	– 2.6*
DMPC	23*
DPPC	41*
PSM	41.3**

* reference [36]
** reference [6]

It is also important to notice that phase transitions are accompanied by lateral expansion and consequent decrease in bilayer thickness, increase on the number of water molecules bound to the surface of the bilayer and nonmonotonic changes in bilayer volume. This free volume increases with the bilayer depth and is higher in the L_α phase, due to the disorder of the hydrocarbon chains deep in the bilayer [1, 3, 6, 20].

Phospholipids with a large area requirement for the polar head group such as PC and PI, show a pretransition between the gel and liquid-crystalline states (Figure 1.9). This happens because the acyl chains are tilted with respect to the bilayer normal. This is why in PC, the gel phase is noted as $L_{\beta'}$. The "second" gel state is referred to as the ripple phase ($P_{\beta'}$), where the acyl chain order is lower than in the L_β and L_c phases. This is a consequence of the periodic one-dimensional ripples that were detected on the membrane surface (probably formed by periodic arrangements of linear gel and fluid domains in atomic microscopy studies). So, this can be seen as a partially melted lipid phase that forms prior to the melting transition. In these cases as the temperature increases we may be in the presence of a subtransition from the L_c to the $L_{\beta'}$ phase, a pretransition from the $L_{\beta'}$ to the $P_{\beta'}$ and the main transition from the $P_{\beta'}$ to the L_α phase [1, 3].

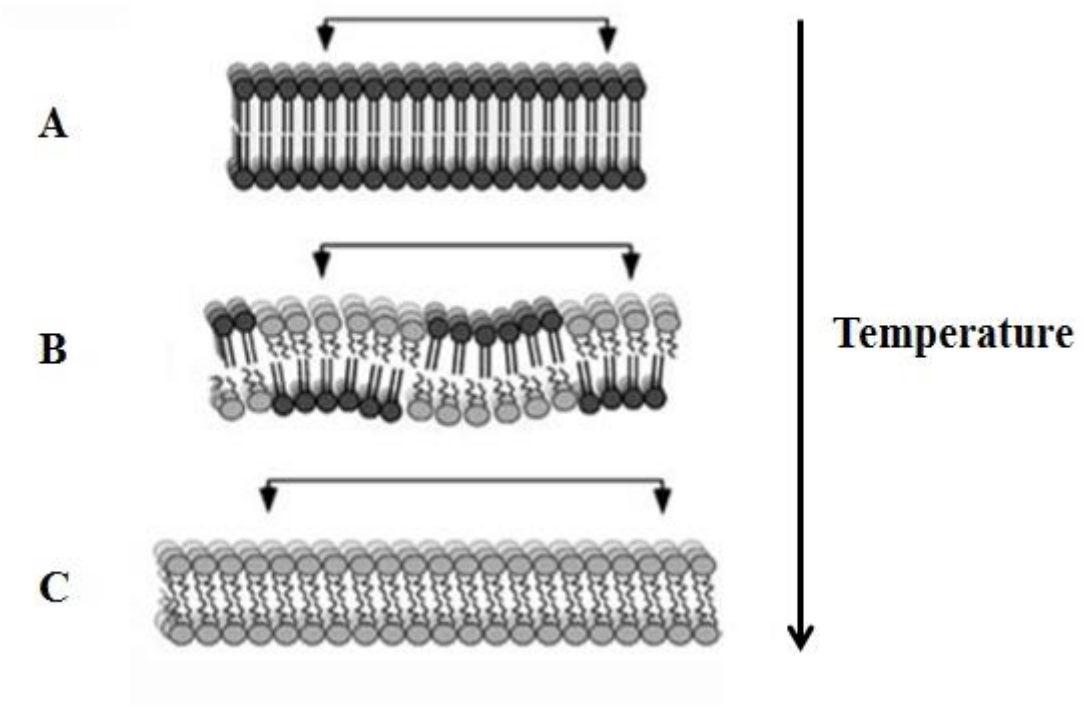

Figure 1.9 – Schematic representation of thermal phase behavior for an experimental system composed of phosphatidylcholines. (A) gel phase (B) ripple phase; (C) liquid crystalline phase (adapted from reference [3]).

Biological membranes seem to adapt their lipid composition such that the temperature distance between room temperature and melting transition is maintained, so they do not display phase transitions. However, the basic physical-chemistry of lipid mixtures is relevant to the understanding of biological membrane properties, especially when it regards possible lateral inhomogeneities [1, 3]. That explained some relevant lipidic mixtures will be considered.

I – 1.2.2 Lipidic mixtures and the observation of phase coexistence

I – 1.2.2.1 Phospholipid-phospholipid mixtures

In lipidic mixtures, the melting of a certain lipid is influenced by the melting behavior of neighboring lipids of different chemical nature. When the lipids randomly distribute in each of the lipid phases (*i.e.* exchanging lipids within the gel phase or the fluid phase will not change the free energy of the lipid matrix) one is in the presence of ideal mixing [3].

Thermodynamic studies have clearly demonstrated that dissimilar phospholipids do not mix ideally, but many times an ideal mixing (based in the Regular Solution Theory[2]) is assumed in order to obtain a quantitative description of complicated experimental phase diagrams [3].

A phase diagram (exemplified in Figure 1.10) is a graphic representation of conditions at which thermodynamically distinct phases can occur. They may be calculated (theoretical) or experimentally obtained through DSC or spectroscopic techniques. Nonideal mixing of lipids is often identified by comparing the experimental phase diagram with the one predicted theoretically [1, 3]. Disaturated PC that differ only in the length of two methylenic groups in their acyl chains exhibit an almost ideal behavior in phospholipid-water dispersions, *e.g.* DMPC/DPPC binary mixtures [37, 38]. The phase diagram for this mixture is represented in Figure 1.10 – A, along with the one for another binary mixture used in this work, the egg-SM/DOPC mixture (Figure 1.10 – B). The latter shows an overall behavior similar to the DMPC/DPPC mixture, though with some differences.

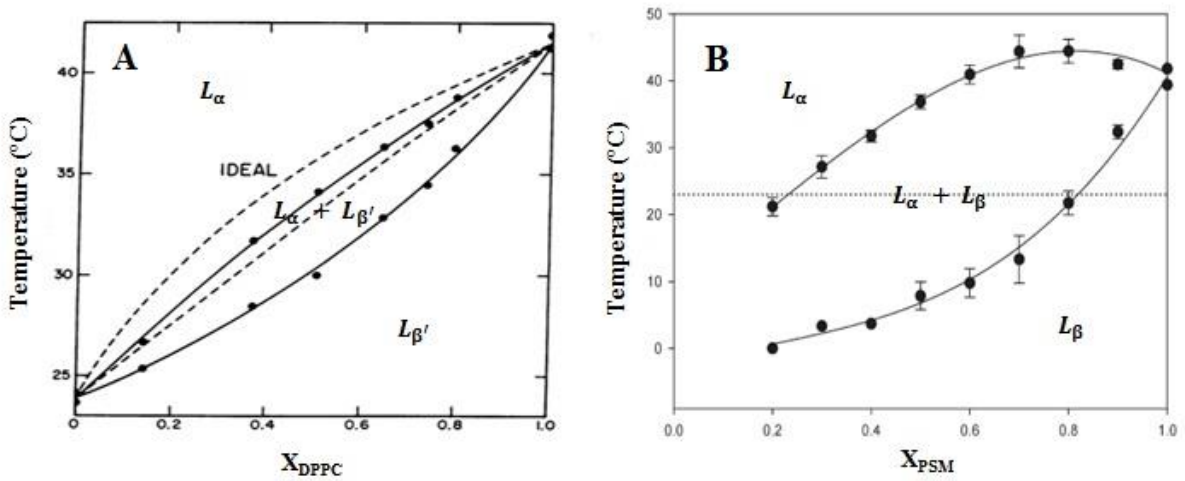

Figure 1.10 – Phase diagrams for phospholipid-phospholipid mixtures used in this work. (A) Representation of a DMPC/DPPC phase diagram (adapted from reference [37]) where the behavior of the mixture is close to ideal; (B) Representation of a PSM/DOPC phase diagram (adapted from reference [39]), for which the overall behavior is similar to the one observed for the DMPC/DPPC mixture.

2 The components in each phase are assumed to mix randomly as in an ideal solution theory, with $\Delta S = 0$, though neighboring lipids still contribute to the enthalpy (ΔH) of the system [3].

So, in the gel phase, the packing requirements may prevent two lipids from being miscible, resulting in clustering or lateral phase separations, and even in the liquid crystalline phase, the two lipids may be miscible and still behave nonideally [1]. The differences in the head group constitution and mainly in chain length, may lead to lipid preferences in the nearest neighbors both in gel and liquid crystalline phases [8].

I – 1.2.2.2 Phospholipid-sterol binary mixtures

CHOL has an amphiphilic structure, but it does not form bilayers of its own (it forms crystals) [3]. The miscibility of CHOL in the lipid bilayer depends both on structure of the phospholipid polar head groups and hydrocarbon chains, on temperature and phase state of the bilayers [20], but it can go as high as ≈ 67 mol % (different experimental conditions from those used in this work) [40]. When inserted in a lipid bilayer, the –OH group of CHOL is near the ester carbonyls of the phospholipids and its long axis is oriented parallel to the bilayer normal. The position of the sterol relative to the bilayer interface is mainly determined by a hydrophobic/hydrophilic balance [20, 41]. At the lipid/water interface, CHOL can lead to an even higher orientational polarization[3] of the water molecules when compared to pure phospholipid bilayers [42]. On the other hand, CHOL can penetrate deep into the hydrophobic interior, which depth will depend on the sterol content of the bilayer [42]. In some cases, it can also protrude into the opposite monolayer and even cross the membrane by (passive) diffusion across the bilayer, unspecific diffusion in the presence of proteins or at the boundary of membrane domains, or through active protein-mediated transport [11]. CHOL has a highly dynamic motion parallel to the bilayer normal and displays a very rapid transbilayer motion (flip-flop) rate in liposomes [11].

Phospholipid-sterol interactions are complex. In a simple description, CHOL interacts with the phospholipids in different ways: in the polar head group zone, the –OH group of this sterol interacts mainly with the phosphate (–PO) and carbonyl (–CO) groups, participating in hydrogen bonding (it can either be a donor and an acceptor) and also in charge pairing (electrostatic interactions between the partial positive charged choline nitrogen moiety and the negatively charged CHOL oxygen) [7, 21, 24]; at the hydrocarbon region, CHOL interacts with the methylenic chains of the phospholipids mainly through van der Waals interactions and short range electrostatic effects [20].

3 Water molecules at air/water surface are highly polarized. This orientational polarization can occur in substances composed of molecules that have permanent electric dipoles. The alignment of the dipoles is temperature dependent and leads to an orientational polarizability [43], see Section I – 2.1.

This is a consequence of the amphiphilic nature of both molecules: this way, the –OH group of CHOL and the polar head groups are in contact with water and the hydrocarbon chains and the steroid ring system are "shielded" from this contact. However, when considering phospholipid-sterol interactions the nature of CHOL as bulky rigid molecule inserted into a lipid bilayer (containing flexible phospholipid molecules) cannot be overlooked.

At this point, it is interesting to consider the phase diagram for the DPPC/CHOL mixture (Figure 1.11). This is one of the most studied and well-known phospholipid-sterol mixtures [44, 45, 46, 47]. In the specific case of PC, the electrostatic interactions between the head groups are weak and there are only hydrogen bonding acceptor groups. The interaction with CHOL may lead to the increase of the distance between the phospholipid head groups and a consequent decrease in the electrostatic attractions or a reduction of its potential to hydrogen bond [20]. At lower CHOL (and higher temperatures) this may not be evident: the phospholipid chains are still "disordered" (translational disorder, rapid lateral diffusion, substantial degree of chain conformational disorder) as in the case of a pure phospholipid bilayer [19]. So, this is many times described as a liquid disordered phase (l_d). But, as the sterol content in the mixture is gradually raised, there will be a substantial effect on the order parameters measured along the lipid hydrocarbon chain. Generally, there is an enhancement of the lipid packing increasing the molecular order of the lipid chains and a reduction of the surface area per molecule occupied by phospholipids at the air/water interface [6].

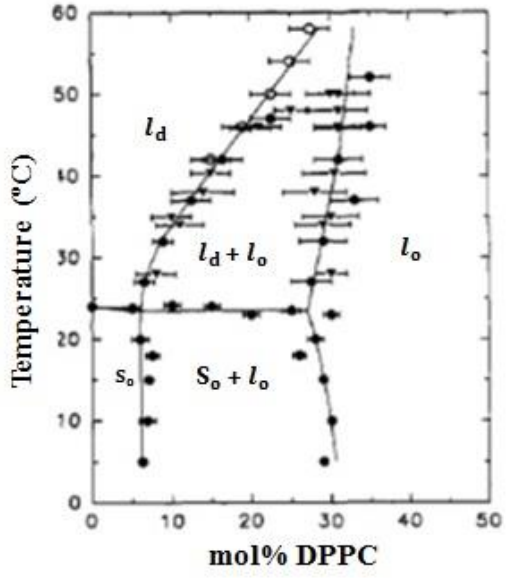

Figure 1.11 – Phase diagram for the DPPC/CHOL mixtures (adapted from reference [45]).

This condensing effect is the result of CHOL steroid ring interactions with the acyl chains that force them to assume a more ordered conformation and is stronger in the case of saturated phospholipids. As a consequence, there is an increase of the conformational order and a decrease in the translational diffusion (2-3 fold up to about 10 fold) [8, 48]. These conformational constraints give rise to the formation of a fluid phase distinct from the L_α and l_d phases, the so-called liquid-ordered phase (l_o). This is usually seen as a state of "intermediate fluidity" between the familiar gel and fluid phases formed by pure glycerophospholipids and sphingophospholipids. In the l_o phase, the molecules can exhibit a degree of translational freedom (in a simple way viewed as lateral mobility) and translational diffusion similar to the one for the conventional fluid bilayer state, while at the same time, the configurational freedom (order) of the lipid hydrocarbon chains more closely resembles the one observed for the gel state [49, 50].

This said it is worth considering three important models that illustrate the interaction between CHOL and phospholipids: the condensed complex model, the superlattice model and the umbrella model. The condensed complex model [51, 52, 53] was proposed to explain the phospholipid-CHOL mixture properties that become highly nonideal at higher CHOL content. The phospholipid-CHOL interactions are treated as reversible chemical reactions at chemical equilibrium and it assumes that there is the formation of lipid-sterol complexes with defined stoichiometry to account for deviations from the regular solution thermodynamics. The "condensed" term indicates that complexes are formed as a consequence of the condensing effect of CHOL: the average area per phospholipid in the complex is less than would be expected for ideal mixing and the methylenic chains are in the all-*trans* configuration, closely packed, making this complexes, a thicker "region" in the lipid bilayer. The superlattice model [54] affirms the existence of regularly distributed lattices (within the matrix lattice formed by membrane acyl chains and CHOL molecules) and irregularly distributed lattices that coexist in fluid sterol-containing membranes. This model states the existence of critical CHOL concentrations (20, 22.2, 25, 33.3, 40 and 50 mol %). In regular solutions, this sterol is distributed into either hexagonal or centered rectangular superlattices, whose shape and size fluctuates with time. In this case, the long range repulsive forces between the bulky steroid rings and the short range interaction between sterols and the neighboring hydrocarbon chains are invoked as being crucial for superlattice formation. The umbrella model [55] asserts that the polar head group must help to cover the nonpolar body of CHOL to avoid the unfavorable free energy that arises from the sterol's exposition to water. The lipid head groups reorient

and expand at the bilayer aqueous interface in order to cover CHOL (as its concentration is raised and as long as the polar head groups are capable of "shielding" the interaction of water with the steroid ring of CHOL) [48].

There was another saturated phospholipid-CHOL mixture used in this work, the PSM/CHOL mixture (for which the phase diagram will be presented in Section I – 1.2.2.3). It is interesting to notice that DPPC and SM (Figure 1.2 and Figure 1.3, respectively) display structural similarities like the identical zwitterionic hydrophilic head group, the existence of an interface section and two methylenic chains which form the hydrocarbon core. The main difference between these two species is the fact that the SM head group and interface section has hydrogen bond donor and acceptor groups (while PC only have acceptor groups), and only one variable alkyl chain [56, 57]. Though, it appears that the charge pairing interactions may be more frequent between SM and CHOL than the conventional hydrogen bonds [21, 24]. This mixture has not been extensively studied as the DPPC/CHOL mixture but its phase diagram also illustrates the existence of the already mentioned l_{d} and l_{o} phases as well as a large liquid-liquid coexistence regime between these two phases ranging (roughly) from 15 to about 35 mol % of CHOL, above the T_{m}. [1, 3].

I – 1.2.2.2.1 Phase coexistence

The formalisms applied for the construction of phase diagrams for mixtures of homogeneous solvents are also applied in the case of lipid mixtures. The phase coexistence is the result of lateral phase separation that seems to occur under certain conditions. In these cases, it is usual to consider one of the phases as physically continuous (or percolative) and the other as physically discontinuous or dispersed as isolated domains. An interconversion between these phases may occur as a result of changes in physicochemical properties of the bilayer (as lateral pressure, temperature, chemical composition). By crossing the critical mass ratio of phases (the percolative threshold) previously disconnected domains and their constituents can be connected as well as other can be disconnected. Systems with phase coexistence may experience interfacial or surface tension (line tension, in two-dimensional systems) between phases that drives the system toward a minimization of the free energy at the interface. Line tension (macroscopically) is the result from both hydrophobic and chain ordering mismatch at the boundary between domains [8]. Hybrid lipids are lipids that can lower this tension to zero and still have minor effects on the thermodynamics (phase diagram,

critical temperature, *etc*.) of the system. This designation comes from the fact that they have a fully saturated chain and a partially unsaturated one. They are soluble in the equilibrium phases, but also interfacially active (*e.g.* when added to a typical saturated/unsaturated/CHOL system, they adsorb to the interface between two coexisting bulk l_d and l_o phases phases) [58]. Their molecular orientation is energetically favorable (*e.g.* POPC) [59]. Tension plays an important role in the stability of the membranes (not just tension as local pressure, but the whole distribution of local pressure determines the functioning of membranes, including functioning of proteins) [60]. A strong surface tension may lead to the separation of phases into macroscopic domains or rafts [8] (Section I – 1.3.2). In homogeneous solvents, the dielectric constant plays an important role in the miscibility, so it is possible that it will also be relevant in the case of lipidic mixtures and lipid organization into domains [61] (further considerations in this matter in Section I -2.1). Now, one has the tools to proceed to a more complex system.

I – 1.2.2.3 Ternary mixtures

In the recent decade, ternary mixtures of PC, SM and CHOL (three major components of the exoplasmatic leaflet of the mammalian plasma membranes) have often been investigated. Based in the studies from PSM/CHOL, POPC/CHOL and PSM/POPC (Figure 1.12 – A, B and C, respectively), the first diagram to be published for a ternary mixture (POPC/ PSM/CHOL) was the one from de Almeida et al. [62] represented in Figure 1.12 – D and E. These diagrams have a triangular representation and the compositions in mole fractions/molar proportions are given by the set of points contained within an equilateral triangle of unit side [3].

It is interesting to notice that CHOL seems to interact differently with saturated and unsaturated lipids [21, 24], as fully saturated PC and SM are known to have the strongest interactions with this sterol [9, 63] and seem to have a preference for its smooth side [24]. Indeed, there are experimental evidences that indicate that CHOL partitions with roughly two-fold greater affinity into vesicles prepared from saturated PC or SM than into vesicles prepared from unsaturated PC [50]. Even between saturated phospholipids, this sterol shows preferential association. It is thought to interact more strongly with sphingolipids (mainly due to the ability of charge pairing and hydrogen bonding between CHOL hydroxyl group and the neighboring SM molecules), triggering lateral separation of lipids into l_d and l_o domains which have been extensively characterized in model membranes [11, 64, 65, 66].

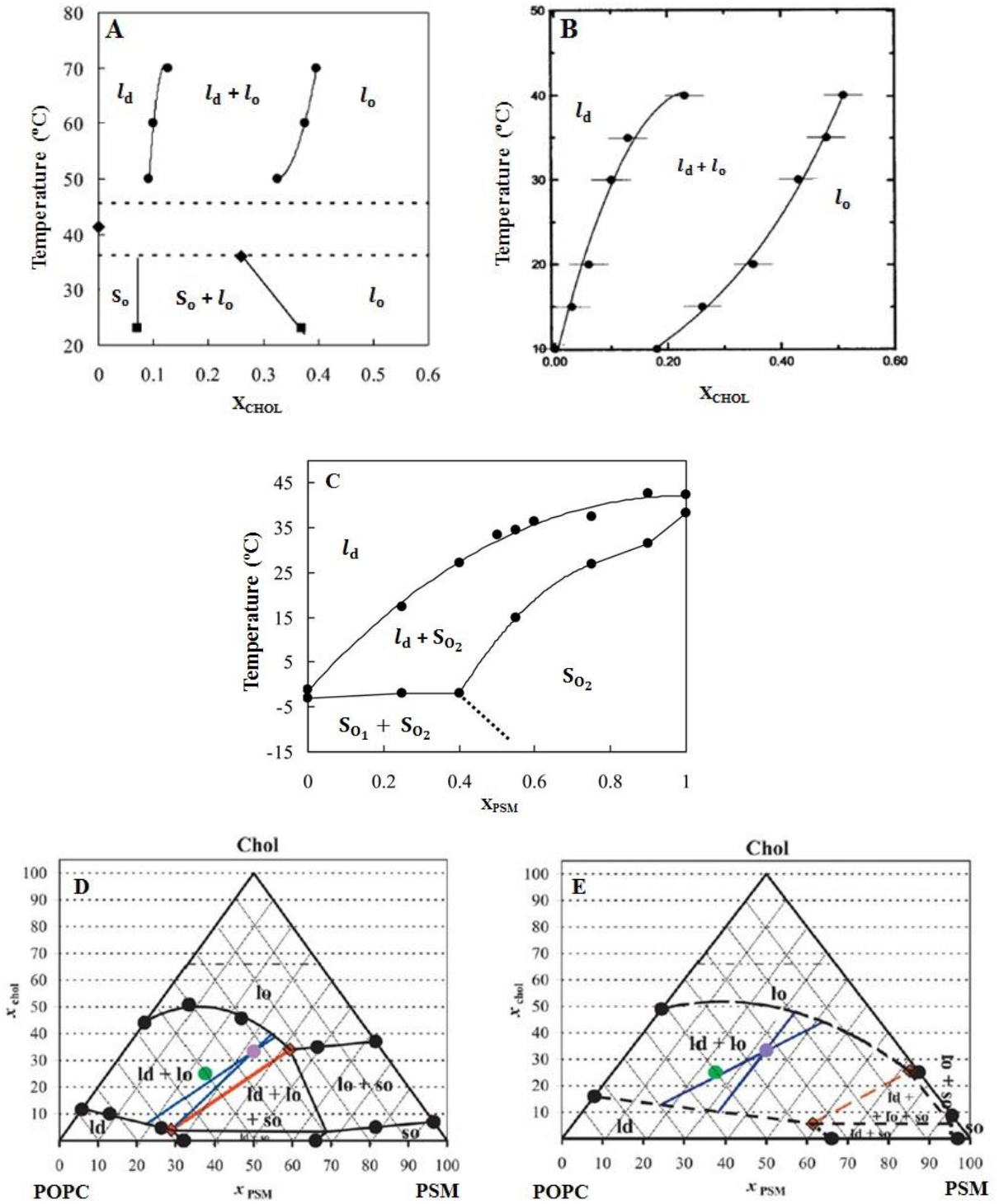

Figure 1.12 – Phase diagrams for phospholipid-cholesterol binary and ternary mixtures used in this work. (A) PSM/CHOL (adapted from reference [62]); (B) POPC/CHOL (adapted from reference [71]); (C) PSM/POPC, So_1 is POPC-rich and So_2 is PSM-rich (adapted from reference [62]); (D) POPC/PSM/CHOL at 23 ºC (adapted from reference [62]) (E) POPC/PSM/CHOL at 37 ºC (adapted from reference [62]).

So, phase separation can also be observed in ternary mixtures containing one low T_m phospholipid (*e.g.* POPC, DOPC), CHOL and a high T_m phospholipid (*e.g.* SM, DPPC) [3].

While the condensed complex model points toward that fact that these mixtures, under certain conditions, will be composed fundamentally by a SM/CHOL complex (l_o) and POPC (l_d) [67], other studies indicate there may be the existence of domains enriched in unsaturated lipids with low CHOL content (l_d) coexisting with other domains with large amounts of saturated lipids and CHOL (l_o) [68, 69, 70].

The POPC/PSM/CHOL mixture is considered the canonical raft mixture [72], as it seems to represent the essential characteristics of the lipidic components of membranes that contain rafts, as these l_d and l_o phases seem to coexist at concentrations that mimic the composition of the outer leaflet of the mammalian plasmatic membrane [65, 73, 74]. In compositional terms, it may be rather simple when compared to the complexity of the plasma membrane, though it is a good starting point to understand the properties for the mixing of more than two different lipids [65].

I – 1.3 *Lateral and transversal asymmetry in biological membranes*

Membrane lipids exhibit relatively rapid transbilayer motion (flip-flop), which is usually negligible due to the half times on the order of several days or longer. The lipid biosynthesis in the ER and Golgi complex, relatively slow membrane translocation of lipids, asymmetrical chemical composition of aqueous compartments, spontaneous curvature or the existence of "flippases" may contribute to membrane transversal asymmetry. An example of transverse lipid asymmetry is the human erythrocyte, with PC and SM on the outer surface and PE and PS in the inner half of the membrane. Membranes also exhibit lateral asymmetry (or lateral heterogeneity), as there are domains or regions within some membranes which have distinct compositions and which may separate from other portions of the membrane with respect to the diffusional exchange of components [1].

I – 1.3.1 Membrane proteins

Membranes contain between 20% and 80% (w/w) protein. These are the biochemical active membrane components thorough the form of enzymes, transporters, receptors, pores, *etc.*, which distinguishes each particular membrane. Nowadays, membrane proteins are generally viewed as being folded in a way that the nonpolar hydrophobic surfaces can interact

with the nonpolar portions of the lipid bilayer and the polar or charged regions can interact with the lipid head groups at the surface. These proteins are generally bound to the membrane through noncovalent forces such as the hydrophobic driven interactions (based on the hydrophobic effect), van der Waals forces or electrostatic interactions. Many of these proteins present themselves in the form glycoproteins, with the carbohydrate residues always being located on the extracytoplasmatic side of the membrane. They are usually categorized as intrinsic (or integral) and extrinsic (or peripheral). These are weakly bound to the membrane surface by electrostatic interactions either with the lipid head groups or with other proteins. Intrinsic membrane proteins are in contact with the membrane interior. Proteins can recruit lipids of similar hydrophobic length around them or change their conformation to adjust to the hydrophobic thickness of the membrane [1, 3].

I – 1.3.2 Lipid domains in biological membranes

The existence of rafts (Figure 1.13) was proposed in both model and biological cell membranes. The early classification of lipid domains[4] was based on an operational definition: they were not soluble in Triton X-100. However, soon it was noticed that this detergent-extraction method did not serve as a reliable tool to draw conclusions about the formation of rafts in biomembranes [75], as detergents may also extract subsets of proteins or lipids, giving rise to a compositional raft that does not resemble the original membrane domain [76]. As model membrane studies (not involving detergents) also supported the idea that these rafts could coexist in biological membranes [77], other methods of detection and extraction were than developed and perfected. Though, all led to the same conclusion: lipid rafts must be defined by its function and not by the method used to isolate it [76]. So, these have been proposed to be thermodynamically stable lipid domains consisting predominantly in CHOL and saturated long-chain sphingolipids (that can be formed as pure kinetic processes) [78], which are associated with specific proteins [79]. Lipid rafts have been shown to have an important role in signal transduction, membrane fusion, cytoskeleton organization, lipid sorting and protein trafficking/recycling [80, 81, 82]. Considering a simplistic point of view, rafts may act merely as platforms that support the co-localization of the signaling components facilitating their interaction or, on the other hand, they can disperse interacting components, preventing them to participate in a specific pathway, leading to signal termination [69, 83].

[4] A domain is defined as being a region that is distinctively marked from the surrounding medium through its physical properties [6] [3].

Proteins are suggested to be one of the major components of lipid rafts: some are attached to these ordered domains by a glycosylphosphatidylinositol (GPI) lipid anchor [84] (Figure 1.13) while others are palmitoylated and myristoylated, *e.g.* Src (Sarcoma)-family kinases [85].

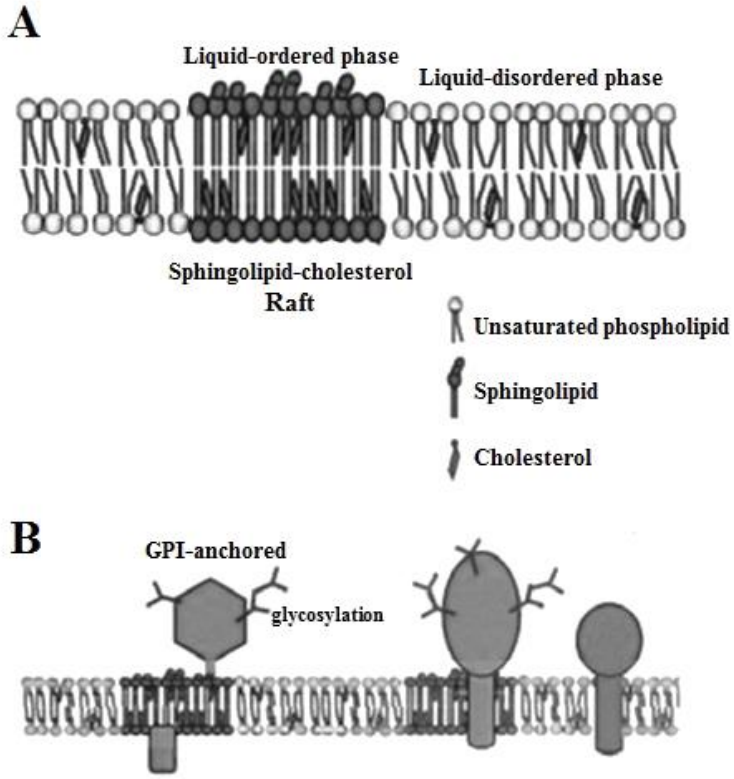

Figure 1.13 – Schematic representation of rafts in biological membranes: (A) Sphingolipid-cholesterol raft formation in a fluid environment of unsaturated phospholipids; (B) Proposed preferential association of membrane proteins to lipid rafts (adapted from reference [3]).

Generally, the interaction of proteins with membrane lipids provides a method to enlarge and stabilize these rafts, so that processes like enzyme activation, receptor cross-liking and even local changes in lipid concentrations can easily occur [69]. For example, fluctuations in cholesterol levels can lead to changes in enzyme activity and/or accessibility to their substrates (which are the cases for the Ca^{2+}–ATPase and the Na^{+}/K^{+}–ATPase), mainly as a consequence of the changes in bilayer thickness or chain order [10, 69, 82]. Studies in model membranes also show the presence of rafts in the inner leaflet. It has been proposed that the

SM and CHOL rafts in the outer leaflet are able to organize the lipids in the inner leaflet (it lacks sphingolipids, but it is rich in acidic phospholipids and unsaturated acyl chains). Many studies in model membranes rely on spectroscopic methods, so one has to be careful when interpreting the results, as they may be complex (due to the lifetimes of the probes, and of the molecular complexes) [82]. *In vivo* studies are difficult to perform due to the small dimensions of the lipid rafts (diameter less than 200 nm, but the size depends highly on the method used to measure) [68]. Since artificial lipids in the presence of high fractions of cholesterol form l_o phases it is believed that rafts may be of l_o nature [3, 11]. It is also important to understand that the final location of peptides in the membrane and the correct functioning of a variety of integral membrane proteins, including ion channels, membrane receptors and enzymes, are sensitive to the physicochemical properties of the local environment [86].

I – 1.4 *Lipid bilayers as permeability barriers*

The hydrophobic core is responsible for the barrier properties lipid bilayers exhibit against the diffusion equilibration of solutes between the two aqueous compartments that it separates. However, it has long been recognized that, in artificial membranes, the lipid bilayer is not strictly impermeable to water and sugar molecules. In particular, water exchanges rapidly between the exterior and the interior of lipid vesicles implying the presence of these molecules within the hydrophobic core of the lipid bilayer [33, 87]. The ability of most small molecules (molecular weight lower than 300 g/mol) to cross the bilayer is directly proportional to their ability to partition into hexadecane (or olive oil) from aqueous solution (Overton's Law). Permeation by these small molecules and ions may occur via one or a combination of both of the following mechanisms: solubility-diffusion mechanism (the bilayer is treated like a slab of liquid hydrocarbon packed in between two aqueous compartments and the permeant must partition into the bilayer from one of the compartments and then diffuse across the hydrocarbon part and leave by dissolving into the second aqueous compartment, *e.g.* water, glycerol, urea) and the pore mechanism (there is the formation of temporary water-filled pores across the bilayer through which the permeant diffuses to the other compartment, *e.g.* protons) [8, 33]. The lipid membranes display maximum in their conductance for ions and larger molecules close to the lipid melting transition, which is possibly related to area fluctuations [3]. The permeation profiles of water and polar solutes into lipid bilayer membranes are fundamental not only to transport studies but also to the energetics of insertion of proteins into membranes.

The polarity profiles are probably determined to a large extent by the penetration of water into the hydrophobic interior. This will probably contribute to modulate the energetics of burying amino acid residues in membranes, but has largely been neglected in favor of a uniform hydrophobic effect. In fact, the hydrophobic core is estimated to have a dielectric constant of around 2-4 [33]. The polar head group region, including the ester functions of the glycerol backbone, represents the interface between this hydrophobic region and the bulk of the water phase, with dielectric constants around 10-45 depending on the technique used [33] [88]. The permeability also depends on membrane lipid composition. CHOL modifies significantly the polarity profile mainly by increasing water penetration at the head group and reducing it in the middle of the membrane [89]. The existence of kinks in the hydrocarbon chains facilitates the diffusion due to the isomerization along the acyl chains of the phospholipids, creating packing defects. Thus, the addition of this sterol orders the hydrocarbon chains, reducing these defects and consequently the free volume [6, 33]. Studies with DOPC bilayers showed that the water concentration is quite significant at the head group level (1-2 M, depending on the degree of unsaturation and CHOL concentration), while in the middle of the membranes, it is about 0.2-0.4 M, depending to some extent in the degree of unsaturation [90, 91].

Water next to the surface is in contact with the phospholipids and water. The external plane is the so-called bulk water. The PC head groups interact with it mainly through ester, phosphate oxygens (primary hydration site), carbonyl oxygens (deeper in the bilayer) and tetramethylammonium groups (comparable to water-water interactions) [87]. There seems to be a small fraction of water molecules that are immobilized, while a larger fraction distributes in the polar head groups zone: typically, for PC, 20-30 molecules are sufficient to completely hydrate one single uncharged lipid [1, 8]. Water as a part of the membrane can be seen as confined water (loosely bound shell that dissolves low molecular weight compounds and it is thermodynamically different from bulk water, *i.e.* dissimilar translational and rotational properties, electrical conductivity and density) and hydration water (which is strongly attached to the groups promoting their stability and excluding water soluble compounds) [87] [92, 93, 94]. It is important to notice that there are two main features arising from this orientation: the surface charge potential (electrical double layer where there can be an arrangement composed by fixed charged groups, as the negative charges of phosphates and positive charges of the choline for PC) and the dipole potential (mostly determined by the orientation ordering of –PO and –CO groups, that extend to the water phase and polarize water) [42, 92].

The most specific water-head group interactions are those involving the unsterified phosphate oxygens (great contribution to the orientational polarizability) [42]. All additional water forms a separated aqueous phase, giving rise to the existence of a structure in equilibrium with bulk water [1, 8].

I – 2 *Polarity measurements in biological membranes*

The fact that the lipid bilayer in biological membranes presents a fluidity gradient, may result in structural heterogeneities in its structure that can correspond to different environmental micropolarities. In the presence of an essentially hydrophobic medium provided by the acyl chain region, a correct determination of these "polarities" may be more difficult than it appears at first sight and it will clearly depend on the technique used. So, the use of molecular probes may constitute an advantageous approach for characterizing membranes in terms of environmental micropolarity. Nevertheless, the choice of the "correct" probe has to take into account several important steps. The determination of the experimental approach and conditions along with the properties of the specific medium one wants to analyze are some of the aspects that worth considering in order to obtain reliable results.

I – 2.1 *Polarity is a complex physicochemical property*

Polarity plays a major role in many physical, chemical, biochemical and biological phenomena. In solution the solute-solvent interactions result not only from the permanent dipole moments of solute or solvent molecules, but also from their polarizabilities. There are four major dielectric interactions: dipole-dipole, solute dipole-solvent polarizability, solute polarizability-solvent dipole, polarizability-polarizability. These are non-specific interactions that should be distinguished from specific interactions, such as hydrogen bonding. The "polarity" of a solvent (or a microenvironment) is usually associated with the static dielectric constant or relative permittivity (ε_r)[5], a macroscopic quantity, or the dipole moment (μ)[6]. This is not satisfactory as in fact the term "polarity" should account the complex interplay between all types of solute-solvent interactions (*i.e.* specific and non-specific interactions) [95].

---

5 The relative permittivity ε_r can be defined as the ratio between the experimental permitivitty ε and the permittivity in vacuum ε_0 so that $\varepsilon_r = \varepsilon/\varepsilon_0$ [35] [43].

6 The dipole moment can be defined as $\mu = q\mathrm{d}$, where $+q$ and $-q$ are two equal charges separated by a distance d [35].

In this matter, the following lines will consider a "polar" molecule with a permanent dipole moment that arises from the partial charges of atoms mainly due to differences in their electronegativities [35, 95]. An applied electric filed can distort a molecule as well as align its permanent dipole, so the solute-solvent interactions also depend on the polarizability (α)[7] that is basically a change in the dipole moment induced for an external electric field [35, 43, 95]. The polarizability of a solvent is the result of both the mobility of electrons in the solvent and the dipole moment of the solvent molecules. It also depends on the dielectric constant, which includes the effect of molecular orientation of the solvent molecules [35]. The dielectric constant is normally dimensionless and it is large if the molecules are polar or highly polarizable. The Debye equation:

$$\frac{\varepsilon_r - 1}{\varepsilon_r + 2} = \frac{\rho\, P_m}{M} \tag{1}$$

for which P_m stands for molar polarizability:

$$P_m = \frac{N_\mathrm{A}}{3\,\varepsilon_0}\left(\alpha + \frac{\mu^2}{3\,k_\mathrm{B}\,T}\right) \tag{2}$$

can be transformed into an equation that gives us the relation between the dielectric constant (ε_r), the polarizability (α) and the dipole moment (μ) in a dielectric material whose molecules are free to rotate:

$$\frac{\varepsilon_r - 1}{\varepsilon_r + 2} = \frac{\rho\, N_\mathrm{A}}{3\,M\,\varepsilon_0}\left(\alpha + \frac{\mu^2}{3\,k_\mathrm{B}\,T}\right) \tag{3}$$

where ρ is the mass density of the sample, M is the molar mass of the molecules and ε_0 is the permittivity in vacuum [35, 43]. The term $\mu^2/3k_\mathrm{B}T$ (where k_B represents the Boltzmann Constant) accounts for the thermal dependence of the dipole in the presence of an applied field [35].

7 The polarizability α is related to the induced dipole moment μ_i and the applied electric field E so that $\mu_i = \alpha \mathrm{E}$ [35].

In the case of nonpolar molecules (considering μ = 0 and therefore $\mu^2/3k_BT = 0$), equation 3 can easily be transformed into the Clausius-Mossoti equation:

$$\frac{\varepsilon_r - 1}{\varepsilon_r + 2} = \frac{\rho\, N_A\, \alpha}{3\, M\, \varepsilon_0} \tag{4}$$

for which there is no thermal variation influencing the dielectric constant [35].

These formalisms can be applied to studies in model membranes. The dielectric constant (that from now on, will be denoted only as ε) of fluid mixtures using only one pure component is related to intermolecular interactions, through equation 5:

$$\frac{(\varepsilon - 1)(\varepsilon + 2)}{9\,\varepsilon} = \frac{4\,\pi\, N_A}{3\, V}\left(\alpha + \frac{\mu^2\, g}{3\, k_B\, T}\right) \tag{5}$$

where the first member corresponds to the polarization *p*, V is the molar volume and g is a correlation factor that characterizes the relative orientations between neighboring molecules [96]. It is known that most naturally occurring zwitterionic phospholipids and sphingolipids, like the ones used in this work, exhibit a permanent electric dipole moment [97]. This is quite significant, mostly in membranes with asymmetric leaflet composition, as it contributes to the formation of the dipole potential in the lipid bilayers which is of major importance in a variety of biological processes (*e.g.* enzyme regulation and its lateral distribution) [98]. Theoretical studies involving lipid bilayers also account for the electrostatic energy that arises from the contribution of the dipoles, though the dielectric constants for the hydrocarbon interior is needed in the majority of the cases [99]. It is important to account for this (inversely proportional) variation of the dielectric constant with temperature (as the different phases are temperature dependent) and molecular composition, but at the same time it is also difficult to analyze the results due to the contribution various polar moieties (mainly, –OH, –PO, –CO groups from lipids and/or solvents). For pure phospholipid bilayers, it is now known that the environment provided by a gel phase is significantly different from the one observed for a liquid crystalline phase: it is higher in the former case, even though the water amounts are lower when compared to a fluid phase [99, 100]. The results from a study with frozen glasses [101] may help to explain this observation. It is possible that this is a consequence of the different mobility of water molecules at dissimilar temperatures: in the gel phase (at lower

temperatures), there is less molecular motion and consequently the average dipoles are less randomly oriented; when the temperature is higher and we are in the presence of a liquid crystalline phase, the water molecules display a higher range of possible orientations, thus the average dipole moments appear lowered.

In this matter, it is important to consider that, when working with lipid mixtures, one is in the presence of polarity changes in a nonideal system that displays single phases and/or phase coexistence, depending mainly on the chemical composition and temperature, as we can see by observing a general phase diagram. In fact, most phase diagrams of lipid mixtures account for lipid characteristics as hydrocarbon chain length, degree of unsaturation or even the formation of hydrogen bonding, but only subtly (or not at all) refer the influence of these permanent dipoles [61]. The truth is that line tension and electrostatic dipolar interactions (as variations in the dielectric constant and polarizability of the dipoles) may in fact be an important issue in determining the size of lipid domains and they should be considered [99, 102].

These "local polarities" in lipid bilayers can be estimated by using various spectrometric techniques (UV-visible and infrared (IR) spectrophotometries, fluorescence spectroscopy, EPR (electron paramagnetic resonance), *etc.*). Due to the already mentioned complexity of biological membranes, it is easier to access information by using simple models like binary and/or ternary mixtures of lipids. Though this facilitates the acquiring of significant data, by varying few parameters, some attention must be paid to the conclusions about the way they affect the overall picture.

I – 2.2 *Polarity and solvent effects in fluorescence measurements*

I – 2.2.1 General features of fluorescence spectroscopy

The processes that occur between the absorption and emission of light are usually illustrated by the Jablonski diagram (Figure 1.14). Typically, the singlet ground, first and second electronic states are represented as S_0, S_1 and S_2 respectively. At each of these electronic energy levels, a number of vibrational energy levels can exist ($v = 0, v = 1, v = 2$, *etc.*). The transitions between states are depicted as vertical lines in order to demonstrate the instantaneous nature of light absorption. These can occur in about 10^{-15}s so that the nuclei in a molecule remain essentially stationary during the transitions (Franck-Condon principle) [43, 103].

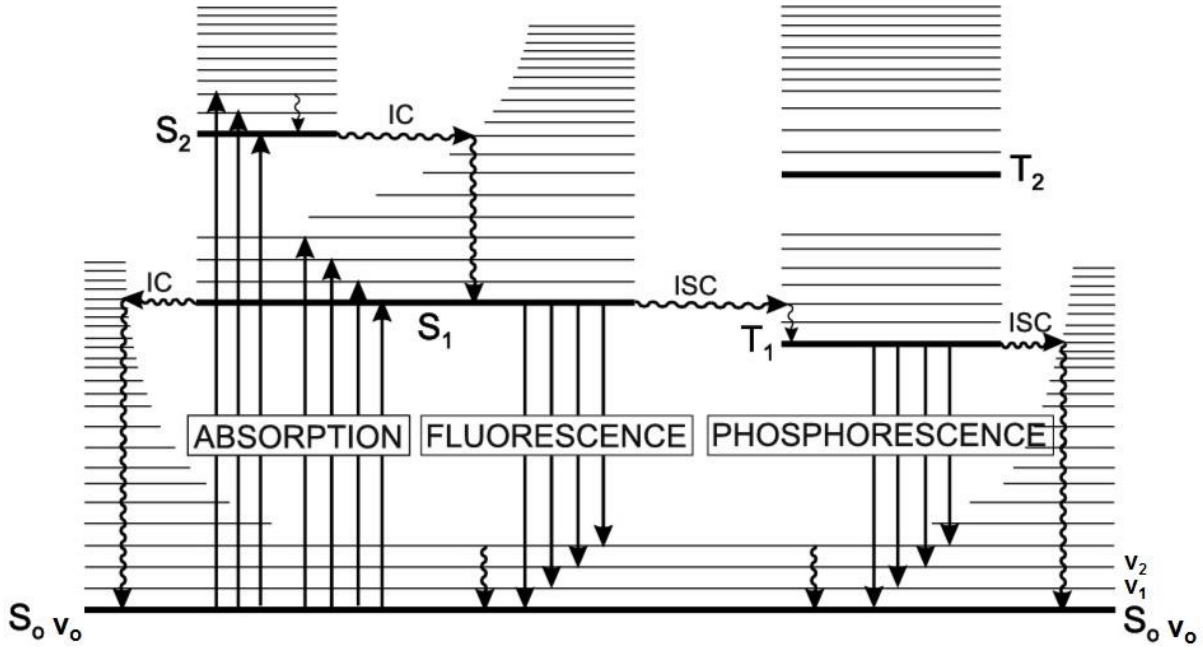

Figure 1.14 – Representation of a Jablonski Diagram. (S_0) singlet ground electronic state; (S_1) first singlet excited electronic state; (S_2) second singlet excited electronic state; (v_0) vibrational ground state; (v_1) first vibrational excited state; (v_2) second vibrational excited state; (T_1) first triplet state; (T_2) second triplet state; (IC) internal conversion; (ISC) intersystem crossing (adapted from reference [95]).

Following the absorption of light, several processes usually occur. A molecule is usually excited to some higher vibrational level of either S_1 or S_2. In general, in condensed phases there is a rapid relaxation (10^{-12}s or less) to the lowest vibrational level of S_1. This process is called internal conversion (IC) (Figure 1.14). Since fluorescence lifetimes are typically near 10^{-8} s, internal conversion is generally completed prior to emission. The emission of photons associated to a transition from a thermally equilibrated excited state (*i.e.* the lowest energy vibrational state of S_1 to the ground state S_0) is called fluorescence and the fluorescent molecules are called fluorophores [103]. Molecules in the excited state can also undergo a spin conversion (intersystem crossing) to the first triplet state T_1 (Figure 1.14). Emission from this state is called phosphorescence [103].

The fluorescence emission spectrum is typically a mirror image of the absorption spectrum which is a consequence of the identical nuclear geometry during electronic excitation (the spacing of the vibrational energy levels of the excited states is similar to that of the ground state) and its characteristics are generally independent of the excitation wavelength due to the rapid relaxation of the fluorophores (Kasha's Rule) [95, 103]. Emission usually occurs over a

longer period of time when compared to absorption. The average time for which fluorescent molecules remain in the excited state, after the excitation by a very short pulse of light, is the excited-state or fluorescence lifetime (τ). The number of emitted photons relative to the number of absorbed photons is known as the fluorescence quantum yield (Φ_F). These are perhaps the most important characteristics of a fluorophore as they determine the time available for it to interact with or diffuse in its environment, and hence the information available from its emission [95, 103]. The interaction of the fluorophore with the surrounding medium may occur in the form of collisional quenching (when the excited-state fluorophore is deactivated upon contact with some other molecule in solution), fluorophore-solvent interactions and rotational diffusion (*e.g.* complex formation and/or energy transfer). In this timescale, the solvent molecules are able to reorient around the excited-state dipole [103]. Typically, the fluorophore has a larger dipole in the excited state (μ^*) than in the ground state (μ). Following excitation the solvent dipoles can reorient or relax around μ^*, lowering the energy of the excited state. This is represented in Figure 1.15. As the solvent polarity is increased, this effect becomes larger, resulting in emission at lower energies or longer wavelengths and consequent substantial spectral shifts (also known as Stokes shifts) [95, 103].

Steady-state fluorescence is the most common type of measurement, due to the fluorescence timescale. Usually it is performed under constant illumination and observation (when the sample is first exposed to light, "steady-state" is reached almost immediately). The second type of measurement usually applied is time-resolved fluorescence, which is used measuring intensity decays or anisotropy decays. In these cases, the sample is exposed to a pulse of light and the intensity decay is recorded with a high-speed detection system [103].

Fluorescence spectroscopy is a highly sensitive spectroscopic technique, though fluorescence measurements are indeed more difficult than they appear at first sight. The proper correction of the emission spectra may not be simple, due to some aspects intrinsic to the spectrofluorometer. Also, there may be contamination of the signal by scattered light (Rayleigh or Raman), especially in the case of turbid samples or even by fluorescent impurities of the solvent if the samples are not prepared within the use of careful experimental conditions [95, 103].

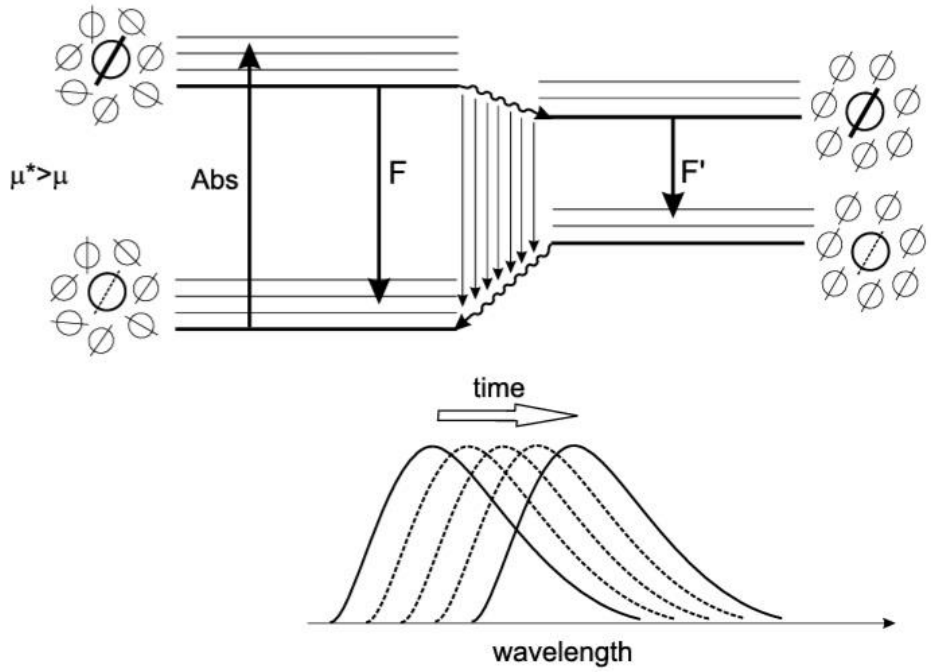

Figure 1.15 – Example of solvent relaxation for a probe with a weak dipole moment in the ground state μ and a large dipole moment in the excited state μ*. The spectrum is dislocated to higher wavelengths (adapted from reference [95]).

I – 2.2.2 The use of fluorescent probes

Fluorescent molecules are often used to investigate physicochemical, biochemical and biological systems, due to the fact that fluorescence emitted by most molecules is indeed extremely sensitive to their microenvironment. There are many factors that can affect the fluorescent measurements (*e.g.* solvent polarity and viscosity, probe conformational changes, rigidity of the local environment, probe-probe interactions) [95, 103]. Generally, the use of extrinsic probes is criticized due to the fact that the exact location of the probe may not be known. Plus, in many cases, a possible local perturbation induced by the probe itself has to be considered. The choice of a fluorescent probe is an important step and it is crucial for obtaining unambiguous interpretations. Analytical techniques based on fluorescence detection are very popular because of their high sensitivity and selectivity, together with the advantages

of spatial and temporal resolution. An example of widely used fluorescent probes is the aromatic hydrocarbons [95, 104]. Most fluorescent compounds are aromatic, normally displaying $\pi \rightarrow \pi^*$ type transitions. They are generally characterized by high molar absorption coefficients and relatively high fluorescence quantum yields [95].

I – 2.2.2.1 Empirical scales of polarity

When the absorption and emission spectra of some compounds is dependent on solvent polarity, they are said to be solvatochromic. The consequent shifts when they are inserted in solvents of different polarities can be used to build empirical polarity scales. The Z-scale was the first (single parameter) approach in this matter and it was developed based on the solvatochromic shift of 4-methoxycarbonyl-1-ethylpyridinium. Later, there was the introduction of the E_T scale based on the negative solvatochromism (a shift toward the blue in the UV-vis light spectrum) of 2,6-diphenyl-4-(2,4,6-triphenyl-1-pyridino)-phenolate. It was then realized that the specific solute-solvent interactions have to be considered in protic solvents like alcohols. As a consequence, they began to follow two distinct lines: one for non-protic solvents and one for protic solvents. Soon it was realized that due to the already mentioned complexity of the term "polarity", the empirical scales would not be of great use if they kept focused on a single parameter approach. Plus, many of the used dyes were not fluorescent [95]. From then, many efforts were focused on the design of fluorescent probes and Kamlet and Taft [105] developed a multi-parameter approach, the π^* scale. The π^* parameter is a measure of the polarity/polarizability effects of the solvent that includes both non-specific and specific solute-solvent interactions. This has been successfully applied to IR, NMR, ESR, UV-vis absorption and fluorescence spectra, and many other physical or chemical parameters (as reaction rate, equilibrium constants, *etc.*) [95].

In the matter of fluorescent probes, there were also studies with aromatic molecules with a high degree of symmetry (*e.g.* benzene, triphenylene, naphthalene, pyrene, coronene). Their first singlet absorption ($S_0 \rightarrow S_1$) may be symmetry forbidden, so that the intensities of the various forbidden vibronic bands are highly sensitive to solvent polarity (Ham effect) [106, 107]. In polar solvents, the intensity of the $S_0 v_0 \leftarrow S_1 v_0$ band increases at the expense of the others. In particular, the changes in the fluorescence spectrum of pyrene in solvents with different polarities (Figure 1.16) show that the polarity of an environment can be estimated by measuring the ratio between the first and third vibronic bands (I_1/I_3) [108, 109]. This ratio

ranges from ≈ 0.6 in hydrocarbon media and ≈ 2 in dimethylsulfoxide. These values provide a polarity scale called the *Py* scale. When dividing solvents by class (aprotic aliphats, protic aliphats, aprotic aromatics) each class gives an excellent correlation between the *Py* scale and the π^* scale. Plus, the *Py* scale seems to be insensitive to hydrogen bonding for protic solvents [95].

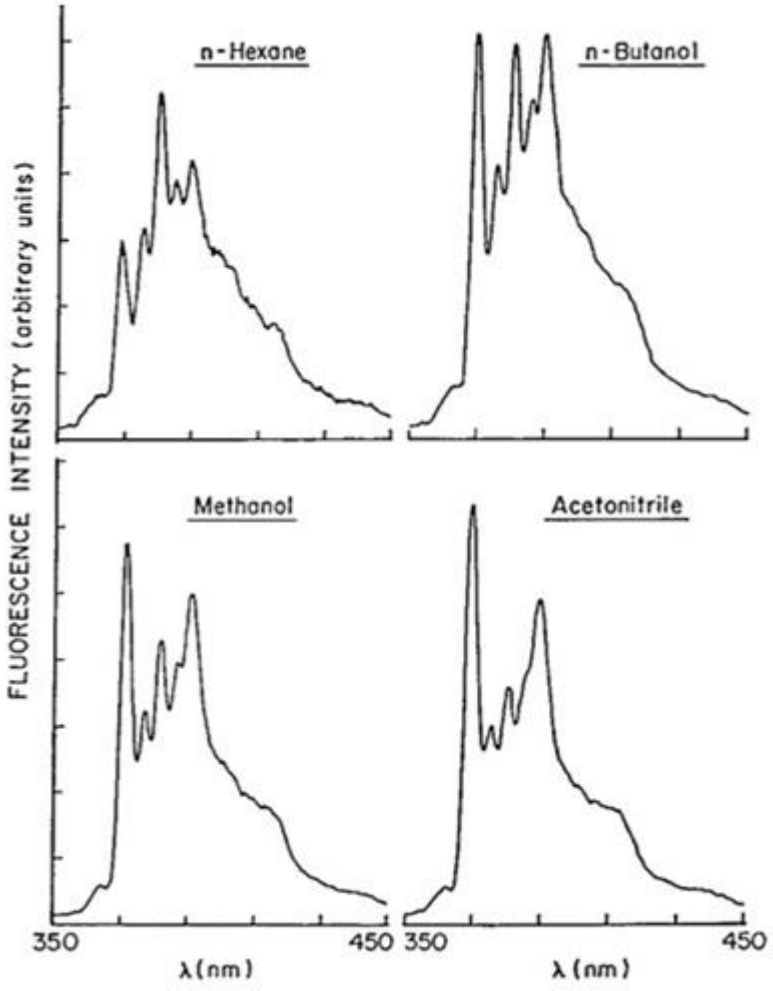

Figure 1.16 – Emission spectra of pyrene in polar solvents demonstrating the probe sensitivity to solvent polarity (represented by the increase of the intensity of the first band of the emission spectrum from an apolar medium like n-hexane to a polar medium provided by acetonitrile) (Adapted from reference [108]).

I –2.3 *Pyrene: a well-known and widely used polarity probe*

I – 2.3.1 Pyrene absorption and emission characteristics

Polycyclic aromatic hydrocarbons (PAH) do not exhibit spectral shifts similar to solvatochromic molecules, but they exhibit a variation in the ratio of the emission band intensities that has been correlated to the polarity of the local environment [110].

Pyrene (Figure 1.17) is an example of that type of molecules. In the absorption spectrum, the first absorption band is localized between 380 nm and 350 nm and corresponds to the singlet absorption $S_0 \rightarrow S_1$. This transition is very weak and the transition moment is polarized along the short axis of the molecule. It is a symmetry forbidden[8] transition. The second absorption band is localized between 350 nm and 290 nm and corresponds to the singlet absorption $S_0 \rightarrow S_2$. This transition is highly allowed and the transition moment is polarized along the long axis of the molecule [110] [111]. This is represented in Figure 1.17. This molecule exhibits a well-defined emission spectrum composed by five peaks that go from 373 nm to 384 nm and correspond the vibrational transitions (Figure 1.17). The first peak (373 nm) corresponds to the $S_0 v_0 \leftarrow S_1 v_0$ transition, and is sensitive to the polarity of the solvent. The third peak (corresponding to the $S_0 v_1 \leftarrow S_1 v_0$transition) is relatively insensitive to the solvent polarity. It is the ratio between the intensities of these two bands (I_1/I_3) that allows the "quantification" of the pyrene sensitivity to the local environment. In this particular case, the stability of the solute-solvent complex is controlled mainly by dispersion forces. The dipolar nature of the medium determines the extent to which there is the formation of an induced dipole moment that is responsible for a symmetry distortion (as a consequence of the solvent dipole – solute induced dipole interactions). This is the basis for the pyrene absorption and emission sensitivity to the polarity of the medium [110, 111, 112]. The emission spectrum exhibits mixed polarization, which indicates that there is a vibronic[9] coupling between the closely spaced S_1 and S_2 states (involving specific vibrational levels) [110, 111]. Pyrene has a fluorescence lifetime of 410 ns in degassed ethanol (20 ºC) [95] and ≈ 150 ns in lipid bilayers (POPC bilayers in aerated aqueous suspension, at 25 ºC) (unpublished results).

---

8 For molecules with a high degree of symmetry, transitions within certain p or d orbital are forbidden, as they only involve a redistribution of the electrons within a given subshell [35].

9 The term vibronic arises from the condensation of the terms "vibrational" and "electronic" [35].

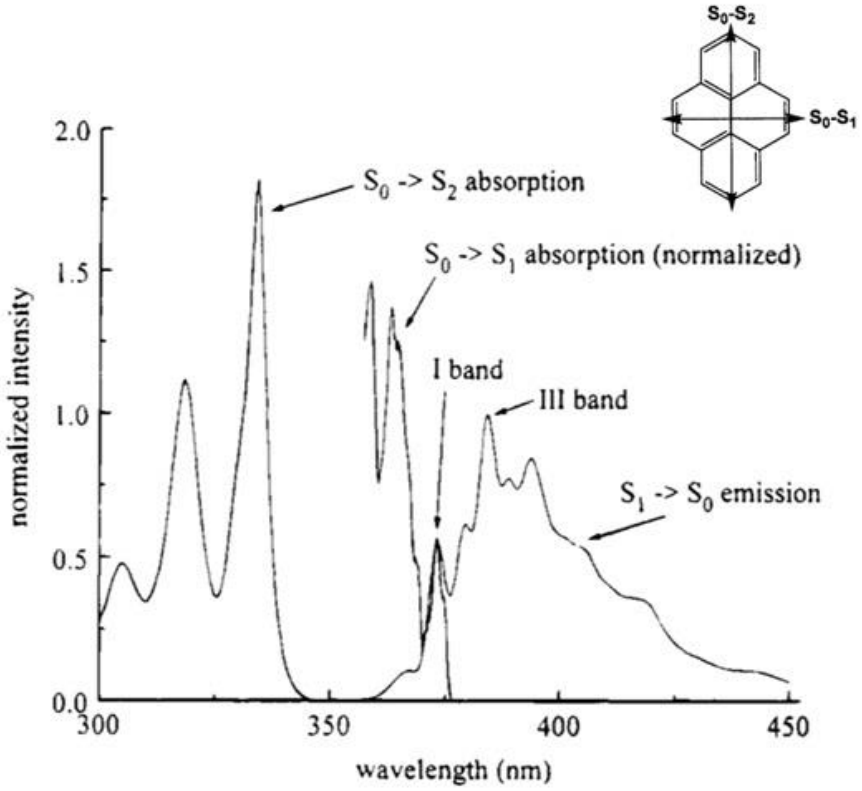

Figure 1.17 – Representation of the pyrene molecule and its absorption and emission spectra (adapted from reference [110]).

I – 2.3.1.1 Pyrene fluorescence measurements must be free of experimental and instrumental artifacts

I – 2.3.1.1.1 The appropriate experimental conditions

One must undergo a careful choice of the experimental conditions in order to obtain reliable I_1/I_3 values. An important requirement when working with pyrene fluorescence is that the working solutions have a concentration below 10^{-6} M, *i.e.* with an absorbance < 0.02 (obtained through the Bouger-Beer-Lambert Law[10]), in order to avoid primary (excitation) and secondary (emission) inner filtering effects [113]. The former happens when a significant part of the incident light is absorbed before reaching the central part of the cuvette.

10 This states that, for low concentration solutions, the fraction of light absorbed by a thin layer is proportional to the number of absorbing molecules [95].

On the other hand, the emission inner filter effect (or self-absorption) is mainly the result of the absorption of fluorescence photons that are emitted in the region overlapping the absorption spectrum, distorting the shape of the fluorescence spectrum in this region [95, 113].

Another issue related with samples having a high probe concentration is the formation of excimers[11]. These form by collision between the excited molecule and an identical molecule in the ground state. The fluorescent band corresponding to an excimer is located at wavelengths higher than that of the monomer and does not show vibronic bands [95]. Though, its band intensity can overlap the monomer emission, giving rise to erroneous I_1/I_3 values [114].

Furthermore, pyrene is a photosensitive molecule. It was already proven that pyrene instability due to photochemical effects may lead to the formation of secondary products that can affect the precision of the overall fluorescence measurements, and these are proportional to the time of exposure to light [115]. As this kind of studies involve the use of an intense light source and, in some cases, through long periods of time, it is also important to adjust the spectrofluorometer parameters. So the use of slit widths[12] of 1 nm (for excitation and emission) or less is recommended [113].

I – 2.3.1.1.2 Raman scattering

Obtaining solvent blanks may not be necessary in some cases. Though in other cases it is essential, in order to obtain accurate I_1/I_3 values. For some types of solvent (*e.g.* homogeneous alcoholic solvents) another emission band may appear due to scattered light, in particular the Raman scattering. This happens as the result of the inelastic collision of a photon (in a population of about 10^7 photons) with the solvent molecules. This leads to the gain or loss of energy and, as consequence, the scattered light has either a lower frequency (Stokes radiation) or a higher frequency (anti-Stokes radiation) than the incident light [35, 43], many times overlapping the first band of the fluorescence spectrum of pyrene.

---

11 Excimers are dimers in the excited state. The term excimer results from the contraction of the terms "excited" and "dimer" [95].

12 The slit widths are generally variable, and a typical monochromator of a spectrofluorometer will have both an entrance (excitation) and an exit (emission) slit. Larger slit widths yield increased signal levels, and therefore, higher signal-to-noise ratios. Smaller slit widths yield higher resolution, however at the expense of light intensity [95].

I – 2.3.1.1.3 The I_1/I_3 ratio depends on temperature

It is important to determine how the I_1/I_3 values vary with temperature, as there is the use of a wide range of temperatures in this work. The dependence of the dipole moments and dielectric constant on temperature has already been discussed (Section I – 2.1).

Figure 1.18 is a graphic representation of the inversely proportional variation of I_1/I_3 (and, consequently, of the dielectric constant) with increasing temperature, for homogeneous polar solvents [100]. This variation is higher in polar solvents, *e.g.* methanol, ethanol, which may be the result of hydrogen bonding between the solvent molecules that can lead a different orientation of the solvent dipoles around pyrene molecules [111]. On the other hand, for more apolar solvents, the I_1/I_3 values are nearly insensitive to solvent polarity.

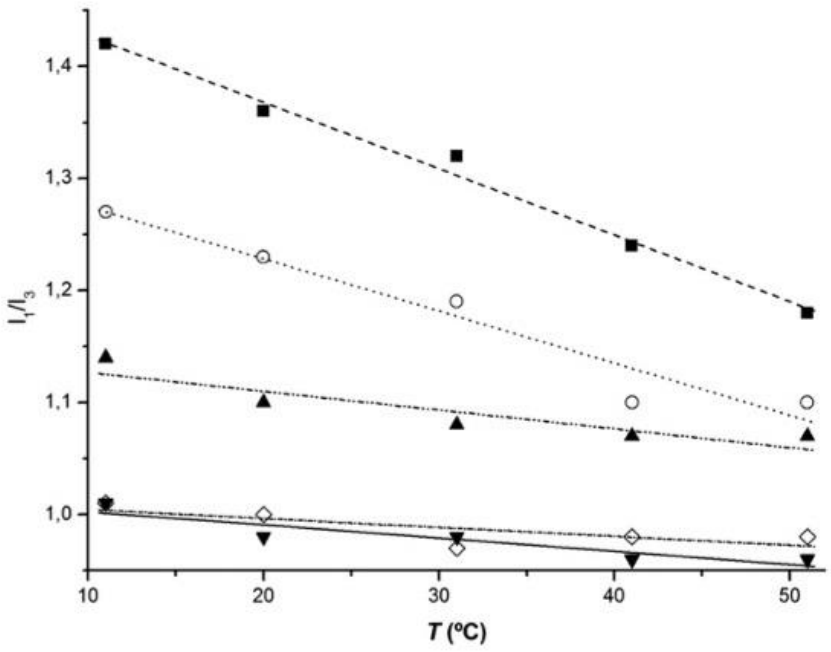

Figure 1.18 – Thermal dependence of the I_1/I_3 ratio of pyrene in alcoholic solvents: (■) Methanol; (○) Ethanol; (▲) 1-Propanol; (◊) 2-Butanol; (▼) 1-Hexanol (adapted from reference [100]).

I – 2.3.2 Studies using Pyrene

Pyrene has been used to investigate the extent of water penetration into micelles and to accurately determine critical micellar concentrations [108]. In lipid vesicles, measurement of the I_1/I_3 ratio provides a simple tool for determination of phase transition temperatures and also the effect of cholesterol addition [95]. In liposomes, the use of fluorescence probes is often accomplished by simple partitioning of water-insoluble probes into nonpolar region of membranes [103]. Through the years many experimental approaches were applied in order to determine bilayer polarity values, but there are some concerns when it comes to obtaining accurate results. In fluorescence-based studies, one of the problems is the fact that the probes only report average polarity values. Additionally, molecules like PRODAN (6-propionyl-2-dimethylaminonaphthalene) [116], LAURDAN (2-dimethylamino-6-lauroylnaphthalene) [116], Nile Red [117], 3-hydroxyflavones and derivatives [118], may contain groups (*e.g.* carbonyl, carboxyl, nitroxide) that display the ability to form hydrogen bonds with water at different bilayer depths [119]. Pyrene has limited spatial resolution in measuring the polarity gradient. Results from ^{2}H-NMR and molecular dynamics (MD) studies [120] indicate that free pyrene, in lipid bilayers, is located near the headgroup region, in the more ordered zone of acyl chains, due to entropic reasons as the insertion of a rigid molecule in the disordered section of the hydrocarbon chains would imply its ordering and as a consequence a decrease in entropy. Another issue relating the reliability of pyrene as a polarity probe is its rigid structure and its possible effects in the organization of the surrounding medium along with the possibility of transversal displacements of the molecule along the hydrocarbon length during its excited-state lifetime. In that matter, recent MD studies [121] pointed out to the fact that for POPC/CHOL mixtures, the effects of pyrene in the order of the methylenic chains of the phospholipids are modest and mainly felt locally. Additionally, the lipid composition does not seem to significantly affect the transverse location of pyrene. Though, this probe displays a relatively minimal dipole moment in the excited state and it is not sensitive to the formation of hydrogen bonds. The long axis of pyrene (≈ 1 nm) and its small scale up-and-down motions allows the averaging of an equivalent polarity (mainly determined by the local water density) in the more ordered section of the methylenic chains. Plus, its lateral diffusion along with the lateral diffusion of membrane components, during the excited-state lifetime of the molecule, allows for an averaging of the polarity in different zones in the bilayer plane [121]. This makes pyrene is a reliable tool when it comes to describe the polarity of the environment

through the dipolarity/polarizability mode [100]. Calibration plots such as the one represented in Figure 1.19 can be used as a polarity index to estimate equivalent dielectric constants with pyrene incorporated in model membrane systems [100].

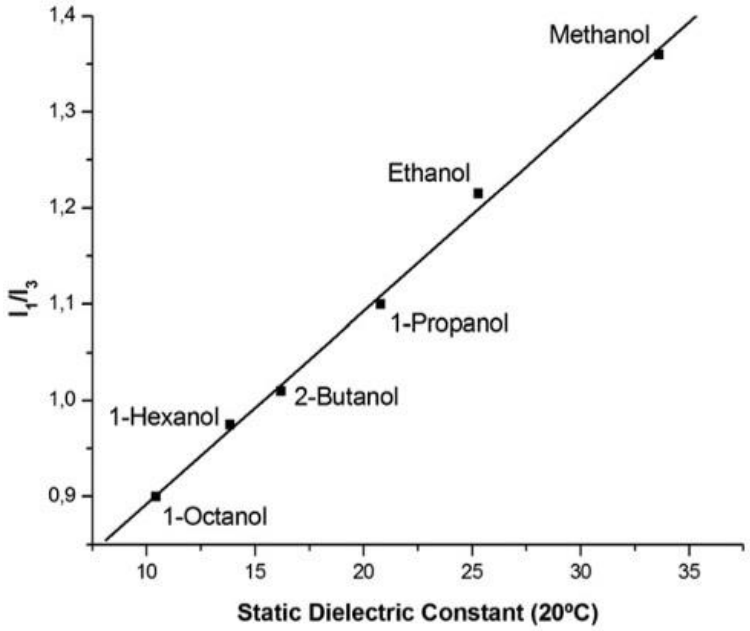

Figure 1.19 – Calibration plot for the I_1/I_3 ratio as a function of the static dielectric constant ε for different alcohols (ranging from 10.5 for 1-octanol until 33.6 for methanol), at 20 ºC; $y = 0.0201\,x + 0.6916,\ R = 0.9985$ is the fitted straight line (adapted from reference [100]).

Included in this type of study, the following sections will provide a significant and rather diverse set of equivalent polarity results, obtained in several lipid mixtures, and subsequent considerations about their consistency. By varying the chemical composition of lipid bilayers and the temperature, it was possible to characterize different lipid environments based on the (already known) phase diagrams for the chosen mixtures, thus providing some indications about the local polarity (and dielectric constant) inside model membranes.

Chapter II

MATERIALS AND METHODS

II – 1 *Chemicals and solvents*

DMPC, DPPC, POPC, DOPC, egg-SM (>99.9%) 7DHC (>95%) and DCHOL (>99%) were obtained from Avanti Polar Lipids Inc. (Alabaster, AL, USA). CHOL (>99.9%) was purchased from Sigma-Aldrich. Pyrene (≥99%, for fluorescence grade) was obtained from Fluka (Switzerland). All lipids were used without further purification. MilliQ water was produced from double distilled water, by a Millipore Integral 3 apparatus, systematically presenting an electrical conductivity of 5.6 x 10^{-6} S m^{-1} and pH around 6.5–7, at room temperature. Ethanol (EtOH), chloroform ($CHCl_3$) and methanol (MeOH) were the organic solvents used in this work and were all of PA or Chromasolv grade.

II – 2 *Stock solutions*

II – 2.1 Pyrene

Pyrene was dissolved in EtOH (molar absorption coefficient, $\varepsilon = 5.5\,x\,10^4 \mathrm{M}^{-1}\mathrm{cm}^{-1}$, at 334 nm) [122] to obtain a stock solution of 20 µM, stored at 6 ºC.

II – 2.2 Lipids

DMPC, DPPC, POPC and DOPC stock solutions were prepared by adding a chloroform:methanol ($CHCl_3$:MeOH) 2:1 (v/v) mixture to the purchased lipids. CHOL, 7DHC, DCHOL and egg-SM stock solutions were prepared only in $CHCl_3$. Their final concentration was 50 mM and they were further used to prepare working solutions of 5 mM for each lipid. These stock solutions were stored at -20 ºC.

II – 3 *Liposome preparation*

Liposomes were prepared according to the method of mechanical dispersion of a dry lipidic film in aqueous solution [123, 124]. The model membranes used in this work were MLV and the probe to lipid molar ratio was 1:5000 (unless stated otherwise).The physical and chemical stability of these vesicles is well-known [123], so that for our purposes MLV are equilibrium structures that constitute a reliable model membrane system.

II – 3.1 Pure phospholipid liposomes

Pyrene and the phospholipid solutions were mixed in an evaporating flask (total volume of 20 cm^3 with a conical shaped bottom (to facilitate the formation of a homogeneous dry lipidic film). Then the $CHCl_3$:MeOH mixture was added to obtain a volume of 5 cm^3. Initially, the solvent was evaporated under vacuum at 145 mbar until a homogeneous film was formed (10-15 min) and then the temperature was raised (above the T_m of the phospholipid) and the pressure was decreased to 5 mbar (during ~1h) to eliminate remaining traces of organic solvent. This was achieved by using a Heidolph-VV micro rotary evaporator with a Büchi V-700 vacuum pump and a liquid nitrogen trap. The pressure was controlled by a Büchi V-850 digital vaccum controller. The lipidic film deposited in the flask walls was then hydrated, using MilliQ water (previously heated above the T_m of the phospholipids). During ~1h, the lipid suspension was regular and energetically vortexed to produce MLV. The lipid suspensions were then stored at 6 ºC. The final phospholipid concentration in the liposome suspension was 0.25 mM. The use of MilliQ water discarded possible false and cumulative effects that could arise from the inorganic and/or organic ionic species abundant in buffer solutions. Additionally, it was ensured that there are no noticeable variations in the pH of MilliQ water, along all the duration of the entire spectroscopic measurements.

II – 3.2 Phospholipid/phospholipid and phospholipid/cholesterol liposomes

For liposomes prepared from binary lipidic mixtures (POPC/CHOL, egg-SM/POPC, DOPC/CHOL, egg-SM/DOPC, DPPC/CHOL, DPPC/DMPC, egg-SM/CHOL) pyrene and the two lipids were mixed with the $CHCl_3$:MeOH mixture and then dried using the same procedure as for pure phospholipid liposomes. One set of MLV was prepared for each molar proportion of the lipidic mixtures and these were chosen upon careful analysis of the phase diagrams for each mixture [37, 39, 45, 47, 62, 71] to allow the characterization of different phases. For all the mixtures involving CHOL, this sterol was added to the phospholipid in the following molar proportions: 5, 10, 15, 20, 25, 30, 35, 40 and 45 mol%. These were much lower than the maximum solubility limit calculated for CHOL in PCs (about 67 mol% [40] therefore ensuring that it was (in a great extent) incorporated in the MLV and that there were no precipitation of the sterol in the form of monohydrate crystals. The DPPC/DMPC model systems were made upon mixing of 25, 50 and 75 mol% of DMPC. For the egg-SM/POPC and egg-SM/DOPC mixtures, the unsaturated phospholipids proportions added were 5, 20, 35,

40, 45, 50, 55, 60, 65, 80 and 95 mol%. The final concentration in these lipidic suspensions was also 0.25 mM and they were stored at 6 ºC.

II – 3.3 Ternary mixtures liposomes

The liposomes prepared from ternary lipidic mixtures, were made upon mixing of POPC, egg-SM, CHOL and pyrene, to which the $CHCl_3$:MeOH mixture was added, and then dried using the same procedure as for pure phospholipid liposomes. One set of MLV was prepared for each set of molar proportions of the lipidic mixtures. As in the case of binary mixtures, these were chosen upon careful analysis of the phase diagram for the POPC/PSM/CHOL ternary mixture [62]. The lipidic mixtures were made with: 33.3 mol% of each lipid (1:1:1) for the equimolar mixture, 62.5 mol% of POPC, 12.5 mol% of egg-SM and 25 mol% of CHOL (5:1:2) for a plasma membrane resembling mixture, and 50 mol% of POPC, 37.5 mol% of egg-SM and 12.5 mol% of CHOL (4:3:1) in order to characterize a supposed three phase coexistence zone. The final concentration in these lipidic suspensions was also 0.25 mM and they were stored at 6 ºC.

II – 3.4 Sphingomyelin/Cholesterol derivatives liposomes

The liposomes were formed upon mixing pyrene (at a probe to lipid molar ratio of 1:2500), egg-SM and the respective CHOL derivative (7DHC or DCHOL) with the $CHCl_3$:MeOH mixture, and then dried using the same procedure as for pure phospholipid liposomes. One set of MLV was prepared for each molar proportion of the lipidic mixtures that were chosen in order to compare these results with the ones obtained for the egg-SM/CHOL mixtures. So, the lipidic mixtures were made upon mixing egg-SM with 5, 10, 20, 30, 35, 40 and 45 mol% of 7DHC or DCHOL. The final concentration in these lipidic suspensions was also 0.25 mM and they were stored at 6 ºC.

II – 4 *Steady-state fluorescence measurements*

Fluorescence emission spectra were performed on a Spex Fluoromax-3 spectrofluorimeter (JobinYvon – Horiba, France) using the right angle geometry. This was equipped with a thermostated cell holder with a magnetic stirring accessory coupled to a refrigerated/heated circulator Julabo F12-ED (± 0.1 ºC), with 1 cm quartz cuvettes. Using an excitation wavelength (λ_{exc}) of 334 nm, all scans were collected from 360 to 460 nm (increment of 1 nm,

integration time 1 s, using 1 nm slit widths in excitation and emission) and corrected for nonlinear instrument response (using the correction file provided by the manufacturer). The absorbance of pyrene at 334 nm ($S_0 \rightarrow S_2$ electronic transition) was always lower than 0.02 for each sample and there was no formation of excimers. In this case, the scattering resulting from the lipidic dispersion was negligible so that there was no need to subtract MLV "blanks" (MLV without pyrene). All the fluorescence and concentration features above referred were the result of careful studies to adjust experimental parameters, as the use of the empirical *Py* polarity scale requires the fluorescence spectra to be free of physical, chemical and instrumental artifacts (*e.g.* primary and secondary inner filtering, excessive light exposure, temperature) that may lead to imprecise values of dielectric constant [100, 113]. Between measurements, there was an increment of 2 ºC and respective thermal stabilization period (10 min), during which the MLV suspensions were continuously stirred.

In the particular case of egg-SM/7DHC and egg-SM/DCHOL, the slit widths of emission had to be adjusted to 2 nm, in order to obtain a better signal from pyrene. There was also the need of subtracting MLV blanks, as the scattering from the liposomes was influencing the acquirement of correct I_1/I_3 values. This subtraction was accomplished by using the spectrofluorometer software.

II – 5 *Statistical Analysis*

All the results presented are the average ± standard deviation (SD) of the I_1/I_3 ratio acquired from the emission scans of 4 independent sets of liposomes upon thermal variation, unless stated otherwise.

Chapter III

RESULTS AND DISCUSSION

Alcoholic solvents are generally used in this kind of studies as a calibration system, due to the fact that their structure emulates the phospholipids general structure. The polar (–OH) group and the hydrophobic methylenic chain provide an environment whose chemical properties are of hydrogen bonding nature similarly to the water inside the model membrane systems normally used. Though, alcohols are much simpler systems than lipid bilayer which makes the comparison between the results obtained in these two distinct media seem like an oversimplification. In fact, there will be a simplification on the view over the thermal behavior of the lipidic mixtures studied in this work. All the results presented are in the form of an "equivalent" polarity, with this arising from the fact that they are being analyzed in accordance to what was observed for homogeneous solvents, though always having in mind that lipid bilayers are highly complex environments for which polarity is not an easy property to access.

This work relies on an averaging of "polarity" near the hydrophilic/hydrophobic interface (in the more ordered zone of the methylenic chains), free from the influence of hydrogen bonds, only sensitive to the electric dipoles present in the mixtures (–PO, –CO and –OH groups for lipids).

In the cases for which the chosen temperature ranges involve results at lower temperatures, dielectric constants will be calculated (at 21 ºC) by intersecting the I_1/I_3 values obtained for pure phospholipid bilayers and for mixtures in the presence of 20 and 40 mol% of a second lipid with the calibration plot represented in Figure 1.19 (Section I – 2.3.2). This allows the characterization of significantly different chemical compositions therefore providing a "quantification" of the polarity inside lipid bilayers, for the experimental conditions used in this work.

The lines plotted in the graphics are merely guidelines to facilitate the correct analysis of the results and to allow the differentiation of chemical compositions for the lipid bilayers studied. They are not to be seen as linear dependencies.

III – 1 *Equivalent polarity for binary mixtures involving unsaturated phospholipids*

III – 1.1 POPC/Cholesterol mixtures

The already known phase diagrams for the POPC/CHOL mixture [47, 62, 71, 125] (*e.g.* Figure 1.12 – B, Section I – 1.2.2.3) are only partial and/or rather incomplete. Still, they are said to have the same general shape as the well-studied phase diagram proposed for the DPPC/CHOL mixture (Section 1.2.2.2, Figure 1.11) [44, 45, 46, 47]. The T_m for POPC is -2.6 ºC (Section I – 1.2.1, Table 1.1), so the results for pure POPC and all the POPC/CHOL mixtures are the outcome of pyrene experiencing a fluid environment. The indications from previous studies are that for this type of mixtures (unsaturated PC and CHOL) in the hydrophobic/hydrophilic region, CHOL and the phospholipids interact mainly through the formation of hydrogen bonds [24, 126]. Therefore, it is expected that the polarity reported by pyrene depends in a great extent on the water dipoles present in its surroundings.

Figure 3.1 represents the I_1/I_3 variation with temperature for pure POPC bilayers and POPC/CHOL mixtures with different chemical composition (Appendix – Table I). Through this view the impact of the addition of CHOL may not be clear, so the I_1/I_3 variation as a function of the sterol amount is represented in Figure 3.2, as a supplement.

The observation of these two graphics indicate that, for the experimental conditions used in this work, the addition of low amounts of CHOL (≈5 mol%) does not seem to lead to significant changes in the pyrene surroundings: the I_1/I_3 values are similar to those for pure POPC bilayers. These findings are in accordance with previous studies that state that, for temperatures between 15 ºC and 45 ºC, the bilayer is in the l_d phase and that it may behave like pure POPC bilayers [16, 127]. In fact, the equivalent polarity values do not differ significantly between 5 and 35 mol% of sterol in the mixture. This is interesting because, by looking at the phase diagram for this mixture [47, 62, 71], from ≈10 mol % to ≈35 mol % of CHOL in the mixture, one would expect to be in a $l_\mathrm{d} + l_\mathrm{o}$ phase coexistence zone. The use of fluorescence microscopy [67] and ^{2}H-NMR [48, 67, 72, 47, 128] showed that, for temperatures above the T_m for POPC bilayers (which is the case in this work), there is no evidence of phase separation for these CHOL proportions, *i.e.* the bilayer profile is similar to pure POPC bilayers [127].

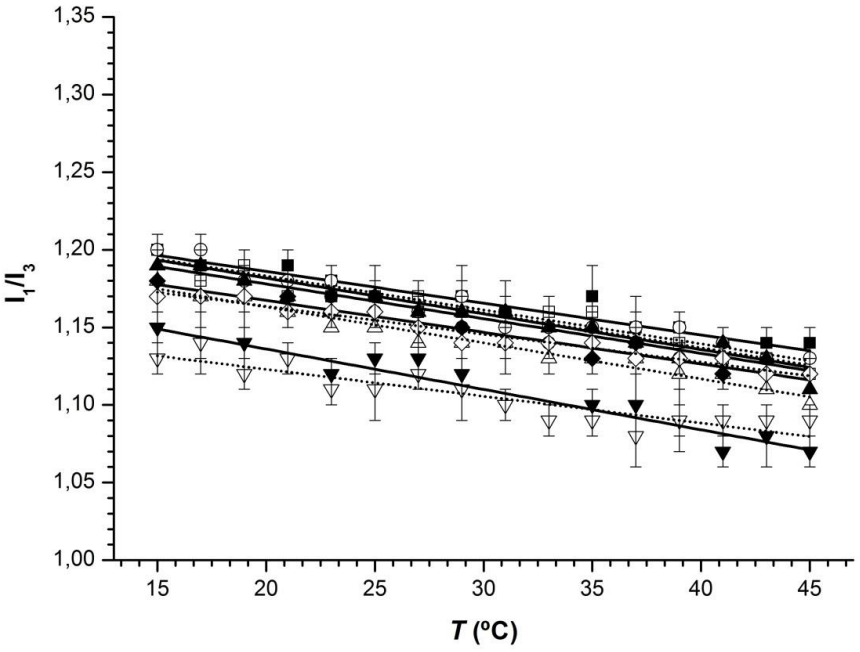

Figure 3.1 – Thermal variation of equivalent polarity values (I_1/I_3) for POPC/CHOL mixtures with different molar compositions (mol%/mol%): (■) 100/00; (□) 95/05; (●) 90/10; (○) 85/15; (▲) 80/20; (Δ) 75/25; (♦) 70/30; (◊) 65/35; (▼) 60/40; (▽) 55/45. The lines plotted match the filled (—) and the outlined symbols (.....).

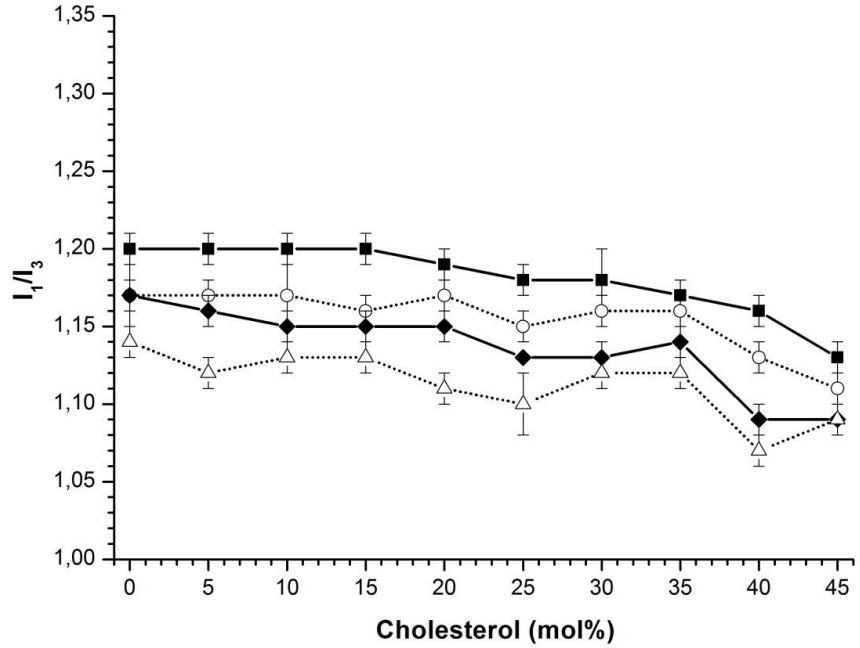

Figure 3.2 – Variation of equivalent polarity values (I_1/I_3) with CHOL content for POPC/CHOL mixtures: (■) 15 ºC; (○) 25 ºC; (♦) 35 ºC; (Δ) 45 ºC. The lines match the filled (—) and the outlined symbols (.....).

This can be explained by the fact that the sterol molecules may be incapable to induce the closer packing of the POPC acyl chains, not being able to exert its condensing effect, due to the existence of the kink introduced by the *cis*-double bond in one of the methylenic chains. On the other hand, some studies refer that this zone of heterogeneous lateral organization ($l_d + l_o$ phase coexistence) exists upon a range of ≈10 to 40 mol% of CHOL, for temperatures between 5 ºC and 25 ºC [16, 129, 130, 131]. If this is the case, there may be subtle variations in the pyrene surroundings which are not being detected within our experimental conditions. Another possible explanation to this, is the fact that pyrene, being a rigid molecule (like CHOL), may have a preference for the more disordered phase (with less CHOL) for nonideal mixtures, like this one. For nearly ideal mixtures (DMPC/DPPC), the probe does not seem have a marked preference for the fluid phase, though its distribution seems to indicate that it is located in a greater extent in the fluid phase than it would be expected (further considerations about DMPC/DPPC mixture results are presented in Section III – 2.1), therefore indicating that this may be a correct insight.

Figure 3.1 and Figure 3.2 also indicate that the presence of 40 mol% of CHOL leads to a slight decrease on the I_1/I_3 values, with these being similar to those for the addition of 45 mol % of this sterol. This is in accordance with studies that refer that that for POPC bilayers the addition of 30 mol % of CHOL or more, leads to some ordering of the hydrophobic chains of the phospholipids [67] which may cause significant effect in lipids diffusion [7, 125]. Additionally, studies of chemical stability of lipids to oxidative damage and hydrolysis [10] indicate that CHOL "dries" the lipid/water interface which will lead to the enhancement of the van der Waals interactions between the phospholipids and, therefore, to the decrease of the bilayer permeability (and consequently) the extent of water penetration. The difference between these and the results for the lower CHOL concentrations may rely in the increasing bilayer ordering and decreasing of the free volume (and water amounts) and for 40 and 45 mol % of CHOL one should probably be in the presence of a l_o phase [16, 129].

If this is the case, the differences in the dielectric constants between these and the results for the fluid phases may be of significance, therefore representing different phases.

III – 1.2 POPC/egg-Sphingomyelin mixtures

The phase diagram for this mixture is represented in Figure 1.12 – C (Section I – 1.2.2.3) and it has the same general shape as the POPC/CHOL mixture [62]. The equivalent polarity

variation with temperature obtained for the POPC/egg-SM mixtures is represented in Figure 3.3 (these values are represented in Appendix – Table II).

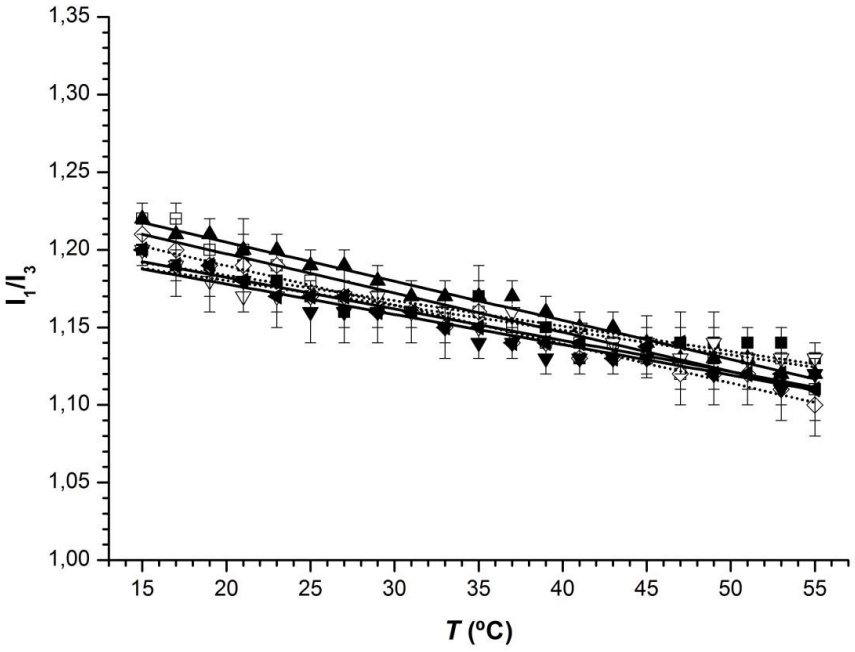

Figure 3.3 – Thermal variation of equivalent polarity values (I_1/I_3) for POPC/egg-SM mixtures with different molar compositions (mol%/mol%): (■) 100/00; (□) 95/05; (▲) 80/20; (◊) 65/35; (▼) 60/40; (∇) 55/45; (◄) 50/50. The lines plotted match the filled (—) and the outlined symbols (.....).

At 21 ºC, I_1/I_3 = 1.20 for 20 mol% of egg-SM and I_1/I_3 = 1.18 in the case of 40 mol% of egg-SM in the mixture. These represent dielectric constants of ε = 25.3 and ε = 24.3, respectively (similar to ethanol and to pure POPC bilayers), indicating that these environments may not be significantly different in terms of polarity. In fact, the analysis of Figure 3.3 shows that there is no significant difference between the I_1/I_3 results for all the different chemical compositions and that these are similar to those obtained for the POPC/CHOL mixture (from 5 to 35 mol% of CHOL), therefore also resembling homogeneous polar solvents [100]. This may indicate that pyrene is reporting a polarity environment of a fluid phase. In fact, this is accordance with the phase diagram [62] for the temperature range used in this work. Similar water amounts and similar influence from the dipoles in the hydrophilic/hydrophobic interface would explain the analogous results for

mixing egg-SM or CHOL with POPC, as the former also provides a more ordered environment which can influence the unsaturated phospholipid molecules.

The variation of the equivalent polarity values as a function of the egg-SM molar proportion is depicted in Figure 3.4.

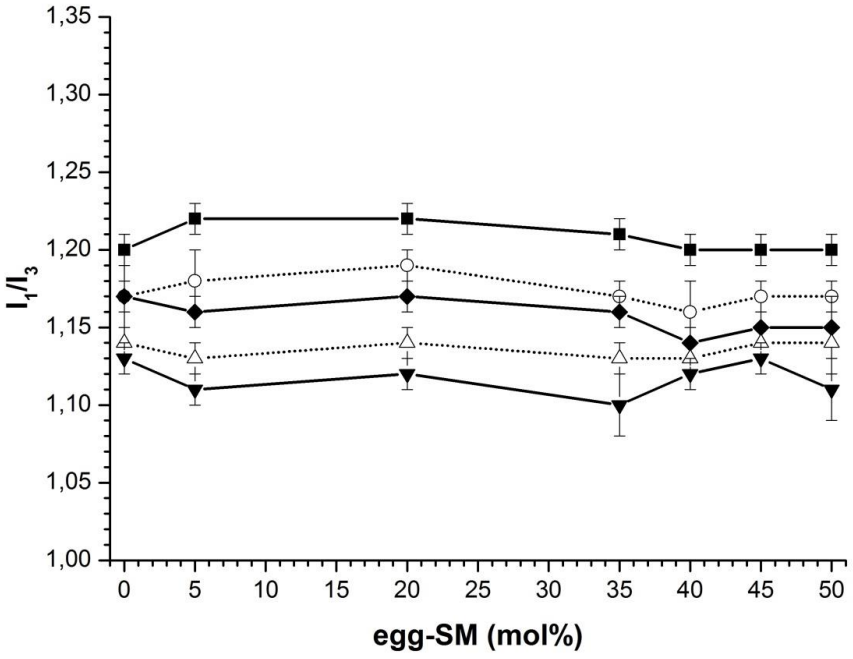

Figure 3.4 – Variation of equivalent polarity values (I_1/I_3) with CHOL content for POPC/egg-SM mixtures: (■) 15 ºC; (○) 25 ºC; (♦) 35 ºC; (Δ) 45 ºC; (▼) 55 ºC. The lines match the filled (—) and the outlined symbols (.....).

The analysis of the phase diagram for the POPC/egg-SM mixture also shows that the presence of higher egg-SM amounts (*i.e.* 35, 40, 45 and 50 mol%) would originate different phases, at different temperatures: for lower temperatures (≈ 15 ºC – 25 ºC), a coexistence of gel phase rich in egg-SM (So_2) and a l_d phase; for higher temperatures (≈ 25 ºC – 55 ºC), a l_d phase. Furthermore, the equivalent polarity seems to be higher than that for POPC/CHOL with a higher CHOL content (in the supposed l_o phase).

In terms of equivalent polarity, it was not possible to observe the supposed phase coexistence (So_2 + l_d). There are experimental evidences that indicate that the interaction between POPC and egg-SM is unfavorable (ordered SM, disordered POPC) [67] and weakly

repulsive [132]. If so, it is possible that, similarly to what seems to happen in the POPC/CHOL mixtures, the probe may "prefer" the l_d phase (richer in POPC), as there would be more conformational freedom and a favorable inclusion of this rigid molecule in the ordered "section" of the lipid bilayer. Earlier studies reveal that the addition of SM to phospholipids reduces the bilayer permeability to water [82], so the increase egg-SM content in the mixture may be responsible for subtle differences in lipid-lipid interactions and water content in the membrane. Though, this was not detected within the experimental approach adopted in the present work.

The dissimilarity between the I_1/I_3 values for the presence of higher amounts of egg-SM or CHOL mixed with POPC seems more difficult to explain, as earlier findings are contradictory in this matter. There are indications that the POPC/CHOL mixtures provide a less ordered and less "dry" lipid/water interface [50], when compared to SM/POPC mixtures. In this case, there would be a higher electrostatic component and higher water shielding [24] resulting in higher I_1/I_3 values, though this does not relate with the former observation. On the other hand, there is experimental evidence that the POPC *cis*-double bond chain seems to pack favorably with the methylated side of the ring system of CHOL, and the saturated chain packs well with the smooth side of the sterol (with no lateral groups) [129], leading to a gradually more favorable interaction as the CHOL concentration in the mixture increases. This would result into stronger lipid-lipid interactions and less permeability to water, which may be the most reasonable explanation for the lower I_1/I_3 values observed for this mixture.

III – 1.3 DOPC/Cholesterol mixtures

The phase diagram for this mixture is not known. The results obtained for the DOPC/CHOL mixtures are represented in Figure 3.5 (available in Appendix – Table III). As in the case of the POPC/CHOL mixtures, these also correspond to fluid environments as the T_m for this phospholipid is also negative, *i.e.* -20 ºC (Section I – 1.2.1, Table 1.1).

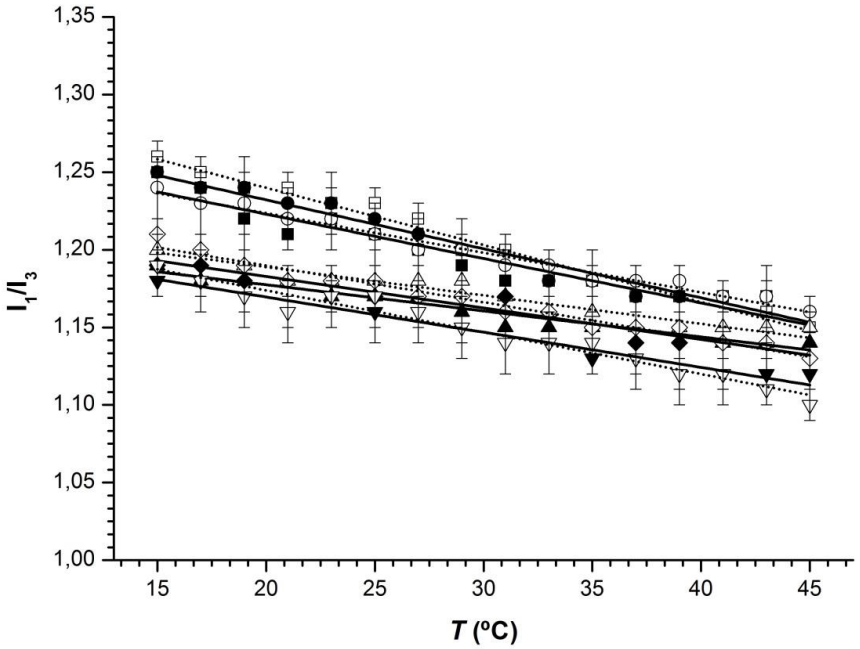

Figure 3.5 – Thermal variation of equivalent polarity values (I_1/I_3) for DOPC/CHOL mixtures with different molar compositions (mol%/mol%): (■) 100/00; (□) 95/05; (●) 90/10; (○) 85/15; (▲) 80/20; (Δ) 75/25; (♦) 70/30; (◊) 65/35; (▼) 60/40; (▽) 55/45. The lines plotted match the filled (—) and the outlined symbols (.....).

The thermal behavior of this mixture also resembles homogeneous polar solvents. At 21 ºC, for pure DOPC, I_1/I_3 = 1.21 which corresponds to ε = 25.8 (similar to ethanol). The addition of 20 mol% of CHOL leads to I_1/I_3 = 1.18 and ε = 24.3 (between ethanol and 1-propanol). For 40 mol% of CHOL, I_1/I_3 = 1.16 and ε = 23.3 (which also stands between ethanol and 1-propanol, but closer to the latter). There is a gradual decrease of the dielectric constant with increasing CHOL, though it is not as accentuated as the observed for POPC/CHOL mixtures, indicating that the influence of the sterol may be smaller than in the latter case. Indeed, the analysis of Figure 3.5 indicates that the polarity values and its variation with increasing temperature are relatively identical for the presence of 5, 10 and 15 mol% of CHOL in the mixture. When the sterol content is increased to 20 mol %, the I_1/I_3 values decrease. Though previous studies indicate that there is no evidence of $l_d + l_o$ phase coexistence, as fluid-phase immiscibility may not occur [72, 133, 134], the results obtained in this work indicate that the addition of this CHOL amount has some influence on the polarity reported by the probe. This may be a consequence of the sterol's condensing effect, leading to

a slightly more packed bilayer and, as a consequence, to the reduction of the free volume (affecting the permeability and decreasing the water penetration). For a hybrid lipid such as POPC [58, 59] an equivalent effect is detected at higher CHOL content (above 40 mol %), as the organization effect of CHOL will eventually affect more extensively the lipid with both oleoyl chains. This is also reflected in the experimental error for both mixtures: it is higher for DOPC/CHOL (Appendix – Table III) than for the mixture of POPC with this sterol (Appendix – Table I). This leads into thinking that DOPC and CHOL may interact poorly due to the existence of a *cis*-double bond in each methylenic chain of the phospholipid. It would also result in a less packed environment in which pyrene would have more free volume available for its lateral and transversal movements and for water penetration into the lipid bilayers, therefore explaining the higher I_1/I_3 values obtained for the DOPC/CHOL mixture.

Figure 3.6 represents the polarity variation as a function of the CHOL concentration.

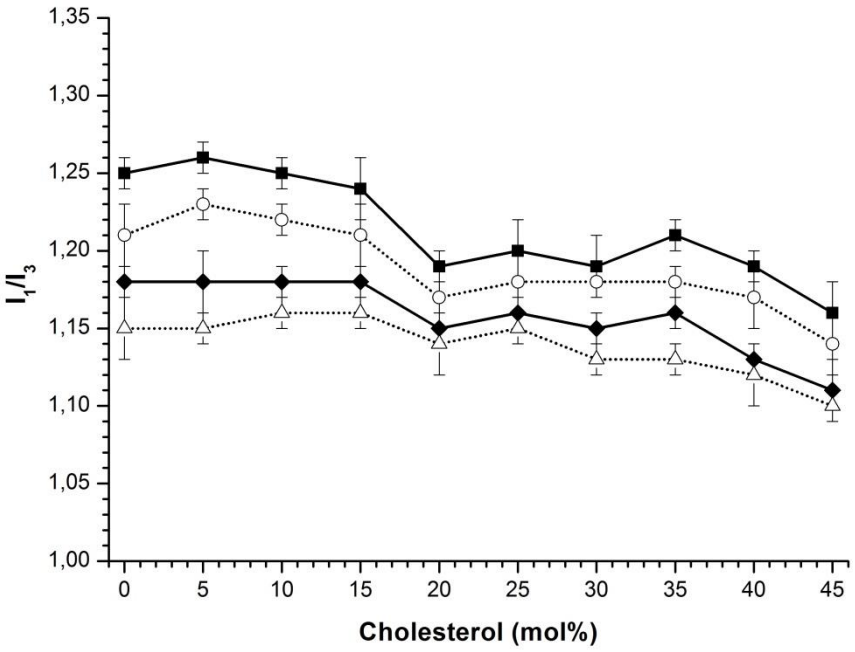

Figure 3.6 – Variation of equivalent polarity values (I_1/I_3) with CHOL content for DOPC/CHOL mixtures: (■) 15 ºC; (○) 25 ºC; (♦) 35 ºC; (Δ) 45 ºC. The lines match the filled (—) and the outlined symbols (.....).

On the other side, the addition of higher CHOL amounts to DOPC, show equivalent polarity values similar to those for the mixture with 20 mol% of this sterol. Some studies have been performed in order to understand the effects of the presence of high CHOL amounts (30-50 mol%) in a DOPC bilayer. By using different sets of parameters, techniques and CHOL concentrations (up to 50 mol%), these works demonstrated that there is a net reduction of the total lipid bilayer area, which would give rise to a more "compact" environment (probably due to the CHOL condensing effect) [48], therefore explaining the lower polarity values. Studies of lateral diffusion indicate that it is possible that lipidic systems with this composition are in a fluid phase, for temperatures between 25 ºC and 50 ºC [133], and that a l_o phase may exist (though, being slightly different from the typical l_o phase) [39, 134]. If this is true, for these experimental conditions, there can be the existence of a homogeneous phase in terms of polarity, because there were no substantial differences detected. It is also interesting to notice that for these sterol amounts, the equivalent polarities resemble the majority of the results obtained for the POPC/CHOL mixture (with the exception being the mixtures with 40 and 45 mol % of CHOL), so that in terms of polarity there may be no significant difference in having POPC or DOPC mixed with the sterol.

III – 1.4 DOPC/egg-Sphingomyelin mixtures

There is a phase diagram suggestion for the mixtures between these two phospholipids [39], represented in Figure 1.10 – B (Section I – 1.2.2.1). In order to evaluate the effects of the addition of egg-SM to DOPC, analogous studies to the POPC/egg-SM mixtures were performed. The variation of the I_1/I_3 values with temperature is represented in Figure 3.7. The results are presented in Appendix – Table IV.

For all the egg-SM concentrations added, the thermal behavior is similar to those observed for homogeneous polar solvents. In this case, at 21 ºC, for the addition of 20 mol% of egg-SM, I_1/I_3 = 1.20 so that ε = 25.3 (comparable to ethanol and slightly lower than pure DOPC bilayers) and for 40 mol% of egg-SM, I_1/I_3 = 1.15, resulting in ε = 22.8 (between ethanol and 1-propanol). This leads to a more accentuated decrease than in the case of POPC/egg-SM (Figure 3.3 and Figure 3.4) and DOPC/CHOL mixtures (Figure 3.5 and Figure 3.6).

The similarity between the results for pure DOPC bilayers and for the mixtures with 5 and 20 mol% of egg-SM is evident if one observes Figure 3.7 and Figure 3.8, which is the representation of the equivalent polarity values with varying egg-SM molar proportions.

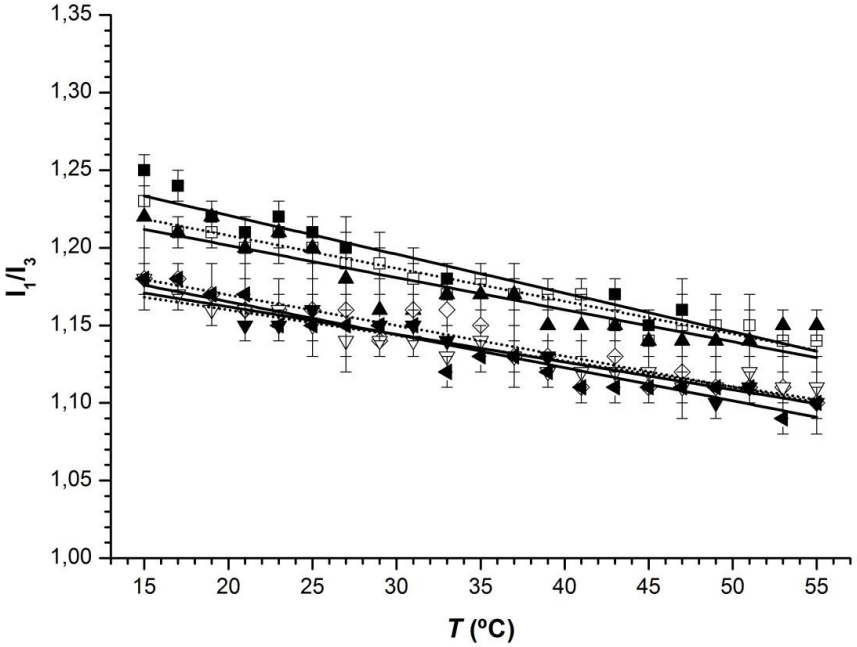

Figure 3.7 – Thermal variation of equivalent polarity values (I_1/I_3) for DOPC/egg-SM mixtures with different molar compositions (mol%/mol%): (■) 100/00; (□) 95/05; (▲) 80/20; (◊) 65/35; (▼) 60/40; (∇) 55/45; (◄) 50/50. The lines plotted match the filled (—) and the outlined symbols (.....).

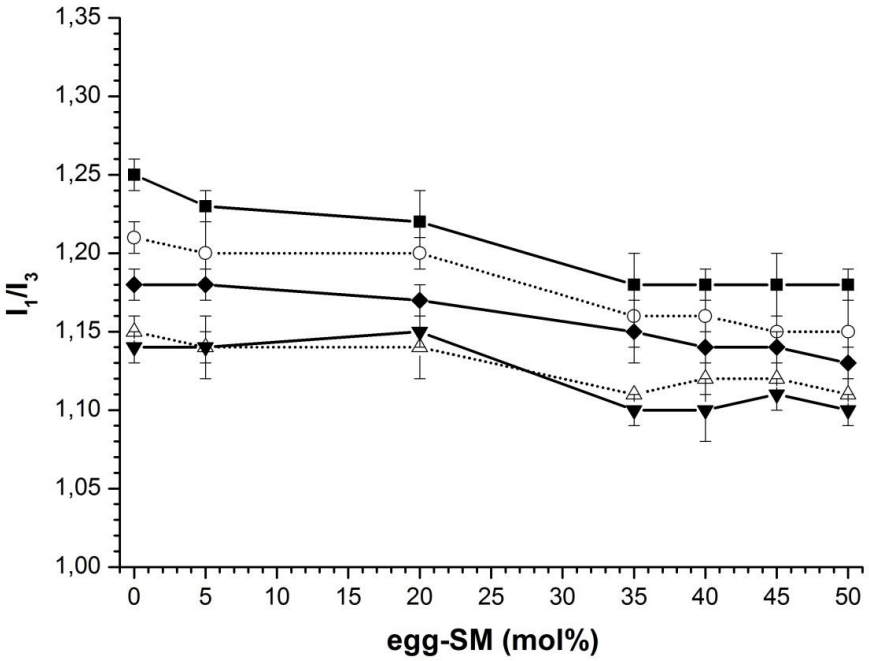

Figure 3.8 – Variation of equivalent polarity values (I_1/I_3) with egg-SM concentration for DOPC/egg-SM mixtures for specific temperature values: (■) 15 ºC; (□) 25 ºC; (♦) 35 ºC; (Δ) 45 ºC; (▼) 55 ºC. The lines match the filled (—) and the outlined symbols (.....).

Besides the unfavorable interactions between DOPC and egg-SM, it is possible that at this egg-SM content, the natural "disorder" of the DOPC is not being influenced by the presence of more ordered egg-SM molecules, or at least if there are slight differences, they were not detectable within the experimental parameters. These results are in accordance with the phase diagram suggested for this mixture [39] that indicates that for approximately 80 mol% DOPC and 20 mol% of egg-SM, a gel phase starts to form. The addition of 35, 40, 45 and 50 mol% of egg-SM in the mixture is indicated as having a two phase-like behavior with increasing temperature: hypothetical phase coexistence between a gel phase and a fluid phase for lower temperatures and a fluid phase for higher temperatures. Other studies [128] mention that there is no evidence of this phase coexistence within the experimental resolution of their work, but that there is the indication of the existence of a fluid phase for temperatures between 30 and 60 ºC. The results presented in this work also point to the existence of a fluid phase, but it is not possible to speculate about the coexistence of gel and liquid phases for lower temperature values. There are differences in the I_1/I_3 values for lower (5 and 20 mol%) and higher (35, 40, 45 and 50 mol%) of egg-SM. These are lower in the latter case creating dissimilarities between DOPC/egg-SM and POPC/egg-SM mixtures (Figure 3.3). It is possible that in this particular case, the probe is also partitioning to the fluid phase of DOPC, but that this naturally disordered phospholipid is being forced to slightly order itself as the gel "domains" formed by egg-SM are becoming larger. So, when mixing POPC or DOPC with egg-SM, the equivalent polarity profiles are similar in terms of thermal variation (Figure 3.3 and Figure 3.7, respectively), but dissimilar when analyzing the I_1/I_3 changes with increasing egg-SM concentration.

By comparing the DOPC/CHOL mixtures (Figure 3.5) with the DOPC/egg-SM mixtures (Figure 3.7), it is possible to see that the I_1/I_3 values are higher in the former case. There is also a higher experimental error associated with these results (Appendix – Table III) which may indicate that the interactions between CHOL and DOPC are more unfavorable than the interactions between egg-SM and DOPC. On the other hand, there are some similarities for the addition of 20 mol% of CHOL or egg-SM to DOPC bilayers. For the experimental conditions of this work, this seems to be a specific concentration after which the DOPC bilayer properties may change in terms of polarity.

III – 2 *Equivalent polarity for binary mixtures involving saturated phospholipids*

III – 2.1 DMPC/DPPC mixtures

In order to understand if pyrene does "prefer" the fluid phase, for these experimental conditions, similar studies were performed with the DMPC/DPPC binary mixture and are represented in Figure 3.9. The phase diagram for this mixture [37, 38] is represented in Figure 1.10 – A (Section I – 1.2.2.1) and all the I_1/I_3 values are presented in Appendix – Table V. As it has already been referred the mixture between these two lipids seems to be nearly ideal, so one is considering a random distribution of the lipids in each phase.

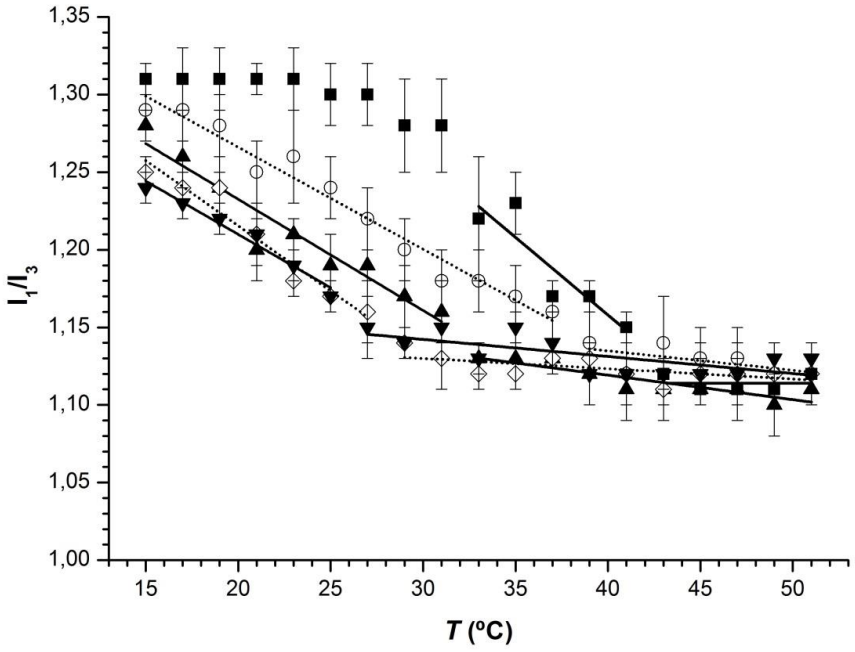

Figure 3.9 – Thermal variation of equivalent polarity values (I_1/I_3) for DMPC/DPPC mixtures with different molar proportions (mol%/mol%): (■) 00/100; (○) 25/75 (▲) 50/50; (◊) 75/25; (▼) 100/00. The lines plotted match the filled (—) and the outlined symbols (.....).

The results show a similar behavior for all the mixtures that is comparable to those for pure phospholipid bilayers: at lower temperatures, there is a more accentuated variation in the

I_1/I_3 values, and for higher temperatures, the thermal variation is not significant within the experimental error (further considerations about this particular behavior to be seen in Section III – 2.2). The observation of Figure 3.9 also shows that the main transition temperature indicated by pyrene is progressively lowering as the DMPC concentration in the mixture is higher. It is interesting to notice that these temperature values seem to correspond to the line that separates the phase coexistence zone from the liquid crystalline phase in the phase diagram. In the case of pure DMPC and DPPC, pyrene reported gel-to-fluid transitions for ≈25 and ≈41 ºC, respectively, which are very close to the T_m indicated for these phospholipids in (Table 1.1 in Section I – 1.2.1), proving that this is not be an artifact. If pyrene had a marked preference for the fluid phase, it would be reporting the transition between gel phase and the phase coexistence zone, which does not seem to happen. In order to investigate this, two temperature values were chosen with the purpose of using the I_1/I_3 values (different within the experimental error) representing a $L_{\beta'}$ phase (100 mol% DPPC), a L_α phase (100 mol% DMPC) and the supposed phase coexistence between these two phases, in order to perform a simple calculus that may be indicative of the preference of pyrene. If the probe had no preference at all, in the phase coexistence zone, for a mixture of 75 mol% of DPPC with 25 mol% of DMPC at 29 ºC, the theoretical I_1/I_3 value would be given by equation 6:

$$(I_1/I_3)^{75/25\ \text{mixture},\ 29\,^\circ\text{C}}_{\text{theoretical}} = 0.75\ (I_1/I_3)^{\text{pure DPPC},\ 29\,^\circ\text{C}} + 0.25\ (I_1/I_3)^{\text{pure DMPC},\ 29\,^\circ\text{C}} \qquad (6)$$

which would roughly represent 75 % of the contribution of the presence of the probe in the gel phase (rich in DPPC) and 25 % of the contribution of the results for the fluid phase (rich in DMPC) for this temperature. In this case, $(I_1/I_3)^{\text{pure DPPC},\ 29\,^\circ\text{C}}$ = 1.28 and $(I_1/I_3)^{\text{pure DMPC},\ 29\,^\circ\text{C}}$ = 1.14 and one would obtain $(I_1/I_3)^{75/25\ \text{mixture},\ 29\,^\circ\text{C}}_{\text{theoretical}}$ = 1.25 (for 31 ºC, the theoretical I_1/I_3 is almost identical). This value is higher than the experimental value obtained for this temperature (1.20), thus demonstrating that the probe may not be evenly distributed. The *Py* parameter is actually reporting a greater contribution from the more disordered phase (richer in DMPC) than what would be expected from an assumed equivalent distribution of pyrene between both phases.

Therefore, in the case of nonideal lipidic mixing (for more dissimilar lipids than these two), it is likely that pyrene prefers to interact with the more disordered phase, as it would be

unfavorable for the molecule to be located in the liquid ordered domains, where the bilayer cohesion is higher due to the presence of CHOL or egg-SM. This confirms the results presented in Section III – 1, for the equivalent polarity values in lipidic mixtures involving unsaturated phospholipids.

III – 2.2 DPPC/Cholesterol mixtures

The phase diagram for these mixtures [44, 45, 46, 47] is represented in Figure 1.11 (Section I – 1.2.2.2) while the I_1/I_3 values are available in Appendix – Table VI. This gives rise to a more complex set of results, so in order to get a correct and more detailed analysis they were grouped based on the CHOL content in the mixture being presented in terms of low (0, 5, 10 and 15 mol%), intermediate (20, 25 and 30 mol%) and high (35, 40 and 45 mol%) CHOL molar proportions.

Previous results for the DMPC/DPPC mixtures (Figure 3.9) indicate that for pure DPPC bilayers, the polarity variation is different when comparing the gel and the liquid crystalline phases. One would expect higher polarity values for the L_α phase as there is a more water penetrating the bilayer due to the increase in the disorder of the lipidic system (higher permeability and higher free volume). Though, this indicated in Figure 3.10, which represents the equivalent polarity thermal variation for the DPPC/CHOL mixture with low sterol amounts. Pyrene is reporting higher equivalent polarity values for the $L_{\beta'}$ phase when compared to the L_α phase. Below the T_m, the I_1/I_3 values decrease with increasing temperature, resembling a homogeneous polar solvent. Above 41 ºC, the equivalent polarity values are comparable to a less polar environment (almost no variation).

This can be explained in terms of water molecular motion throughout the thermal variation range. These molecules are in constant movement from the bilayer interface to the bulk water and *vice versa*, but the lower temperatures are problematical when it comes to any reorientation process inside lipid bilayers. The water molecules seem to progressively reach a "locked-in" state in the gel phases with a less randomized orientation of its dipoles due to the drastic lowering of the rotational movements [101]. This restriction of the water molecules movements leads to the increase in the dipolarity reported by pyrene within the lipid bilayer and to the consequent report of higher equivalent polarity values even with the bilayer in the gel phase containing lesser water amounts. As the temperature increases, the molecular

motion becomes higher, thus decreasing the dipolar nature of the water interactions with pyrene therefore decreasing the I_1/I_3 values reported for its immediate surroundings.

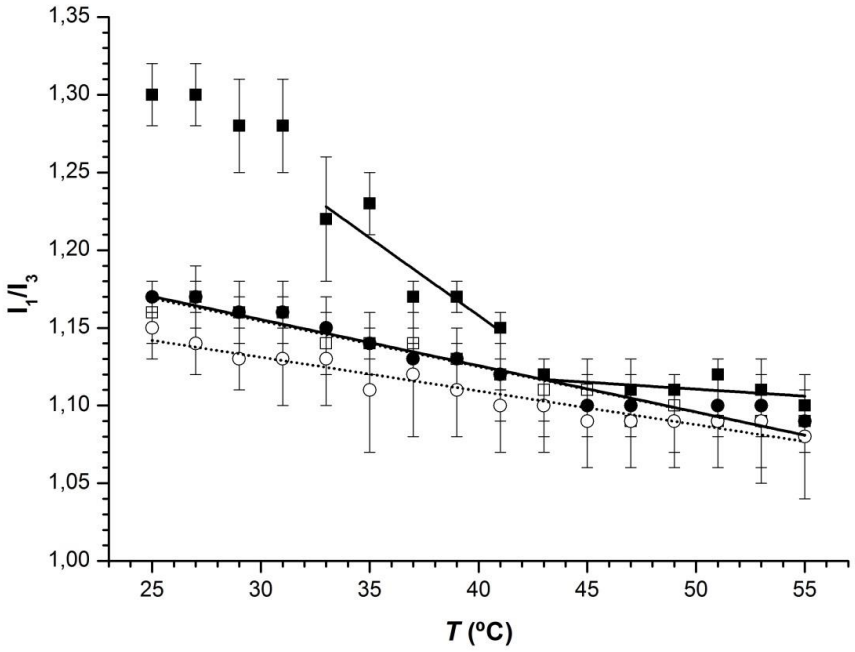

Figure 3.10 – Thermal variation of the equivalent polarity values (I_1/I_3) for DPPC/CHOL mixtures with low CHOL content (mol%/mol%): (■) 100/00; (□) 95/05; (●) 90/10; (○) 85/15. The lines plotted match the filled (—) and the outlined symbols (.....).

The mixing of CHOL into these lipidic systems accounts for an increase in the complexity of overall interactions. These are in part controlled by the position and orientation of its polarized ring system, its side chain and –OH group which will affect the bilayer electrostatics. The addition of 5 mol % of CHOL seems to "abolish" the dissimilar behavior above and below the T_m observed for the pure DPPC bilayers (Figure 3.10), but it does not seem to significantly affect the equivalent polarity in the bilayer for the fluid phases. In fact, the addition of 5, 10 and 15 mol% of CHOL gives rise to similar results. These are in accordance with studies that state that, for saturated phospholipids, the addition of low CHOL concentrations may not produce significant results in equivalent polarity, water penetration in the membrane and/or lipid-CHOL interactions [22, 42] correlating with DSC [135] and MD studies [42] that indicate that in these cases, the general bilayer properties are analogous to the

pure phospholipid bilayers features. The addition of small amounts of CHOL may contribute to a minor reduction of the free volume and to the slight increase of the distance between the phospholipid head groups, thus weakening the hydrogen bonding network and its electrostatic interactions. Nevertheless, pyrene does not seem to be sensitive to these subtle changes. The effects of the addition of CHOL at lower temperatures leads to a more accentuated decrease, but as the gel phases are not biologically relevant this will not be extensively analyzed.

Figure 3.11 represents the I_1/I_3 variation with temperature for mixtures with intermediate CHOL content. The overall behavior is similar to that obtained for low sterol amounts, as the polarity values decrease with increasing temperature. The phase diagram for this mixture shows that, at these sterol concentrations, there is a supposed phase coexistence zone, where a phospholipid-rich phase (l_d) coexists with a CHOL-rich phase (l_o). For these CHOL amounts there are evidences of phase separation [18, 52, 67, 136] and the indication that CHOL interacts preferentially with the l_o phase [67] leading to a lower sterol amount in the l_d phase.

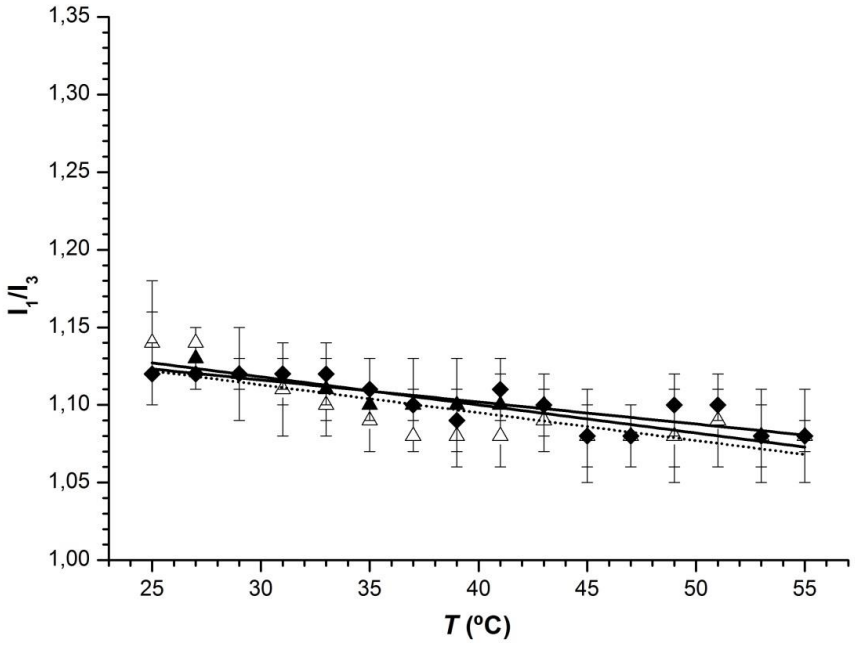

Figure 3.11 – Thermal variation of equivalent polarity values (I_1/I_3) for DPPC/CHOL mixtures with intermediate CHOL content (mol%/mol%): (▲) 80/20; (Δ) 75/25; (♦) 70/30. The lines plotted match the filled (—) and the outlined symbols (.....).

The results presented in this work indicate that, until the 30 mol % of CHOL is reached, pyrene is reporting I_1/I_3 values similar to those for the L_α phase. This would be possible, if the probe demonstrated some preference for more disordered environments, as in the case of the binary mixtures involving unsaturated phospholipids presented earlier (Section III – 1).

The effects of the presence of higher CHOL amounts in the polarity averaged by pyrene are depicted in Figure 3.12. It shows that the addition of 35 mol% of this sterol seems to be responsible for a decrease in the polarity values, when compared to the previously referred CHOL concentrations, yet still reporting a polarity environment similar to the one of homogeneous polar solvents.

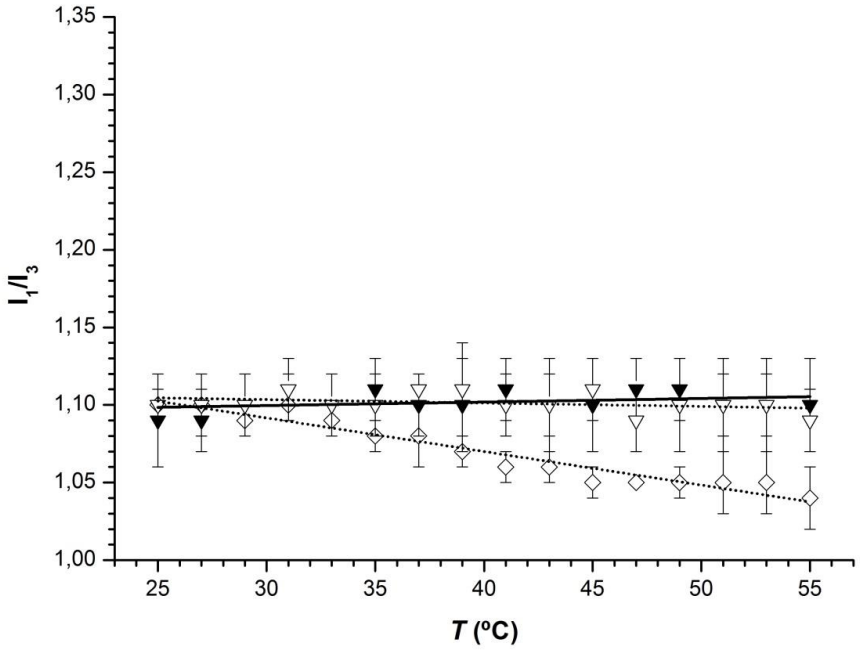

Figure 3.12 – Thermal variation of equivalent polarity values (I_1/I_3) for DPPC/CHOL mixtures with high CHOL content (mol%/mol%): (◊) 65/35, (▼) 60/40, (▽) 55/45. The lines plotted match the filled (──) and the outlined symbols (.....).

The stronger lipid-lipid interactions and consequent less water penetration may explain these results, as there are evidences that when the CHOL content is high, the membrane permeability is affected (less water penetrating the lipid bilayer, lower polarity values) [137]. Following this line of thought, it would be acceptable if one expected that this would occur gradually with increasing CHOL content, but that is not what Figure 3.12 is showing. In fact,

35 mol% of this sterol seems to be a "critical" composition after which there is the increase in the I_1/I_3 values and the clear observation of a thermal behavior that resembles a homogeneous apolar solvent.

The presence of 40 and 45 mol% of CHOL in the mixture, gives rise to similar results. At this sterol content, there is almost one phospholipid to one CHOL molecule, which may alter the expected bilayer physical properties: this can be responsible for an increase in the distance between the phospholipid head groups, leading to a slight disruption in the lipid-water and in the lipid-lipid interactions (if we analyze this through the view presented by the Umbrella Model, referred in Section I – 1.2.2.2). As a consequence, there would be more free volume and the water molecules would be penetrating deeper in the bilayer. Additionally, a molecule like CHOL (with polarizable π orbitals) may also produce changes in the solvent dielectric constant by affecting the solvent structure while accounting for an electrostatic contribution increasing the distortional polarizability and, therefore, the I_1/I_3 values reported by pyrene [100, 138].

The observation of these effects is reinforced when observing the graphical representation of the variation of equivalent polarity with CHOL concentration, depicted in Figure 3.13.

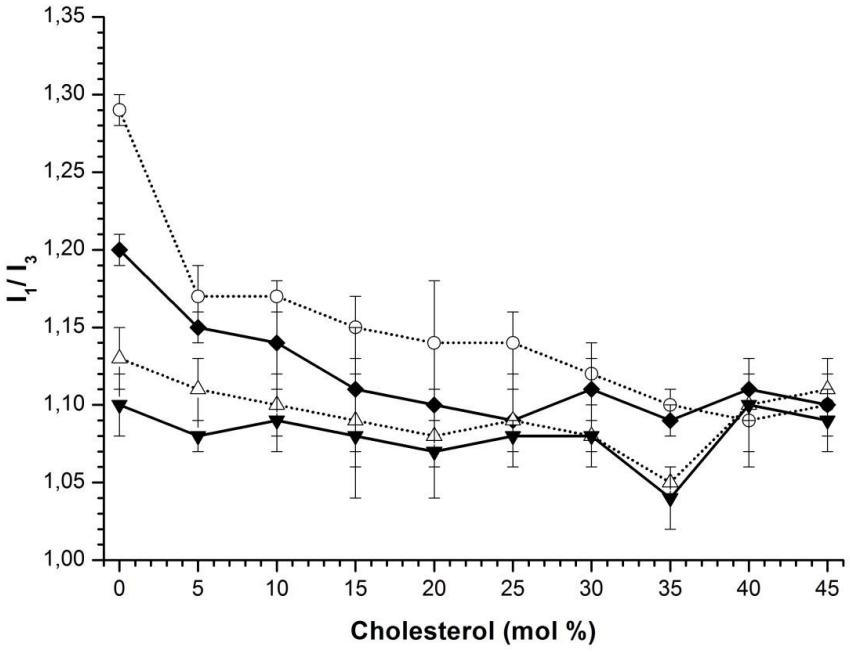

Figure 3.13 – Variation of equivalent polarity values (I_1/I_3) with CHOL concentration for DPPC/CHOL mixtures for specific temperature values (○) 25 ºC; (♦) 35 ºC; (Δ) 45 ºC; (▼) 55 ºC. The lines match the filled (—) and the outlined symbols (.....).

The difference between the results for the fluid phases of these mixtures when compared to those of unsaturated phospholipids (higher in the latter case), confirms what has already been said in Section III – 1 about the extent of water penetration being greater in the case of unsaturated phospholipid based bilayers [47].

III – 2.3 Egg-Sphingomyelin/Cholesterol mixtures

Egg-SM is mainly composed by 16:0 SM (18:0, 22:0 and 24:1 are present at very low amounts) so the resulting lipidic bilayer properties are similar to the ones attributed to pure PSM bilayers [139]. That is being considered from now on. The phase diagram suggested [62] for PSM/CHOL is represented in Figure 1.12 – A (Section I – 1.2.2.3). All the I_1/I_3 results are available in Appendix – Table VII and its analysis is based on the same criteria used for the DPPC/CHOL mixtures.

For lower sterol amounts, the variation of the I_1/I_3 values as a function of temperature is represented in Figure 3.14.

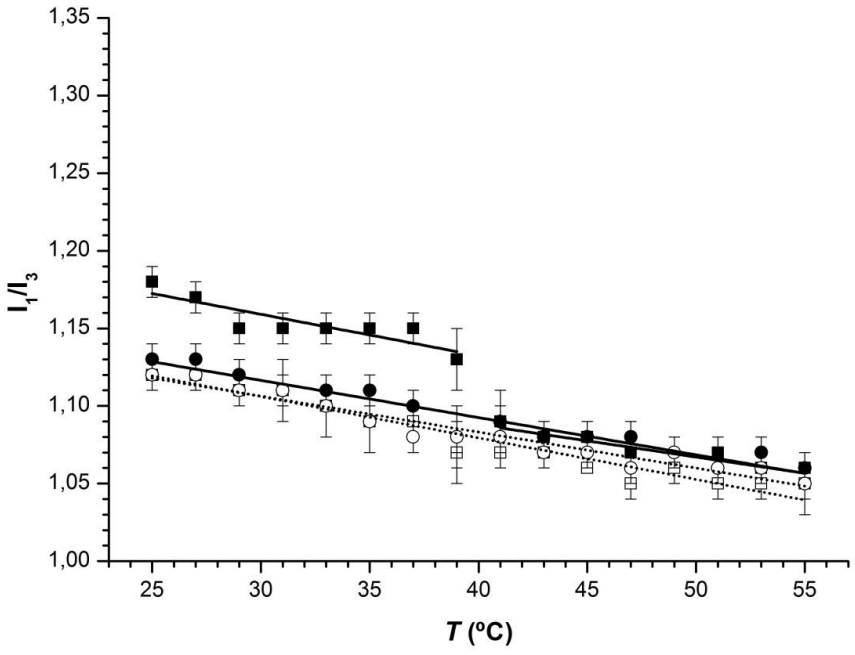

Figure 3.14 – Thermal variation of equivalent polarity values (I_1/I_3) for egg-SM/CHOL mixtures with low CHOL content (mol%/mol%): (■) 100/00; (□) 95/05; (●) 90/10; (○) 85/15. The lines plotted match the filled (—) and the outlined symbols (.....).

It is possible to observe that the behavior for the pure phospholipid bilayers of egg-SM resembles the DPPC/CHOL mixture (though for the gel phase, the behavior is slightly different, probably due to the fact that there is a pretransition in the case of DPPC [3]).

There is also the indication of slightly lower polarity values in the case of pure egg-SM. In general, SM provide a more ordered environment than PC: the SM bilayers display slower fluctuations in the area per molecule, suppressed hydrocarbon rotations and slower lateral diffusion, when compared to a DPPC bilayer, resulting in more rigidity and lower in-plane elasticity [140]. Also, the intramolecular hydrogen bonding and the presence of a *trans*-double bond (in the sphingosine group) leads to a tight and very stable environment where the lipids are closely packed. As a consequence, less water enters the interfacial and hydrocarbon regions [141]. This explains the lower polarity results obtained for the egg-SM bilayers when compared to the DPPC bilayers.

As it was observed in DPPC/CHOL mixtures, but with slightly lower I_1/I_3 values, the addition of 5 mol % of CHOL to egg-SM seems to eliminate the difference between the results for the gel and fluid phases, having a thermal variation similar to homogeneous polar solvents. Moreover, the addition of 5, 10 or 15 mol % of CHOL does not seem to produce significant differences in the I_1/I_3 values. This is in accordance with DSC studies [135] that indicate that until ≈12 mol % of CHOL in the mixture is reached, the bilayer properties are alike those for pure PSM bilayers. Nevertheless, the known phase diagrams [47, 62] point out to the fact that there is evidence of a zone with phase separation [47, 126, 135, 136] that leads to the coexistence of CHOL-rich regions and SM-rich regions from ≈10 - 25 mol% of CHOL in the mixture.

Data for the addition of 20 and 25 mol% of CHOL are represented in Figure 3.15 that represents the thermal variation of I_1/I_3 for intermediate CHOL amounts. It is clear that these resemble the DPPC/CHOL mixtures with the referred sterol content and are not significantly different from the results for lower CHOL. DSC and ESR studies indicate that in these cases there are gradual changes in the bilayer properties *i.e.* lipid-lipid interactions, lipid-water interactions, surface density, bilayer thickness [135, 142]. It also seems that the phase coexistence zone for SM/CHOL is the region for which the lateral diffusion coefficient decreases more abruptly [133], though data presented in this work is not representative of these changes.

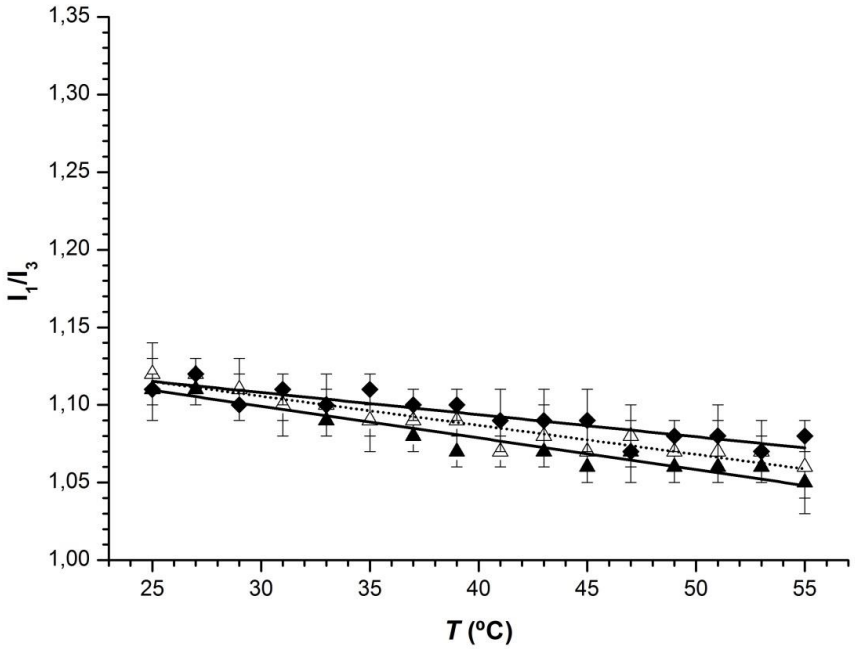

Figure 3.15 – Thermal variation of equivalent polarity values (I_1/I_3) egg-SM/CHOL mixtures with intermediate CHOL content (mol%/mol%): (▲) 80/20; (Δ) 75/25; (♦) 70/30. The lines plotted match the filled (—) and the outlined symbols (.....).

Pyrene reports equivalent polarity values and thermal behavior similar to the L_α and/or l_d phases, therefore correlating with previous observations that indicate a preferential location of the probe in these environments.

The higher amounts of CHOL in egg-SM bilayers give rise to significant changes and these are represented in Figure 3.16. Earlier studies [126] [142] show that, for these CHOL content, there are evidences of the existence of a l_o phase characterized by a significantly lower diffusion coefficient compared to the fluid phase and phase coexistence regions. There is also the indication that the existence of this phase does not seem to depend on the CHOL proportion in the mixture [62]. However, Figure 3.16 shows that the equivalent polarity for this supposed l_o phase may depend on the CHOL content in the mixture. The results with 35 mol% of CHOL are slightly different from the previously referred intermediate sterol amounts, as the I_1/I_3 values are slightly higher and its thermal behavior resembles homogeneous apolar solvents. At this point, CHOL may already be sufficient to dry the lipid bilayer at a large extent (what would explain the apolar profile) with the higher polarity values being determined by the remaining quantity of water trapped within the bilayer.

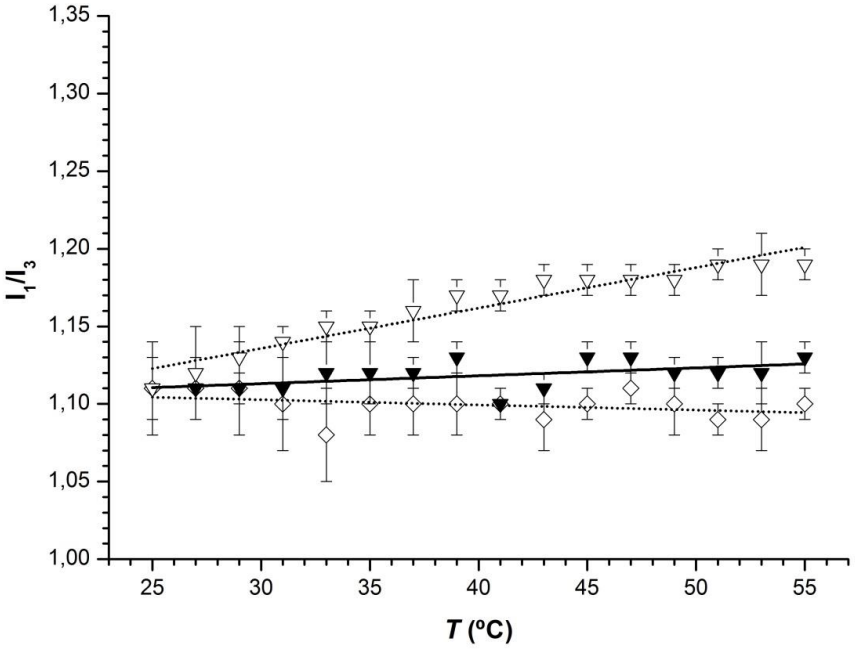

Figure 3.16 – Thermal variation of equivalent polarity values (I_1/I_3) egg-SM/CHOL for mixtures with high CHOL content (mol%/mol%): (◊) 65/35; (▼) 60/40; (▽) 55/45. The lines plotted match the filled (──) and the outlined symbols (.....).

With the egg-SM/CHOL mixtures representing more cohesive bilayers, one might think that CHOL would induce the separation of the methylenic chains and of the egg-SM head groups, leading to a deeper water penetration. Yet, this does not seem to be the case. The results for 40 and 45 mol % of CHOL show that there is a tendency for the equivalent polarity to increase as the temperature is raised, which is much more pronounced for the higher CHOL proportion in the mixture. The solvent thermal behavior is therefore ranging between a similarity to homogeneous polar solvent (for low and intermediate CHOL amounts), and the resemblance of a dielectric material (like rubbers or plastics), as the I_1/I_3 values increase when the temperature is raised. The polarizability rises as a function of the increase in the thermal movements of the composing polymeric molecules. [143]. More likely, the bilayer is highly dehydrated so that the probe is only sensing the polarizability of its immediate environment. In fact, some studies indicate that, in the interfacial region of a lipid bilayer,

charge pairing between PSM and CHOL (electrostatic interactions between the positively charged methyl groups of the hydrocarbon chains and the negatively charged phosphate oxygens in the polar head group and –OH group from CHOL [21] is more frequent than the typical hydrogen bonding preference between PC and CHOL [24, 126]. This may account for a higher polarizability component (distortional polarity), so that in this case the polarity may depend less on the water content (orientational polarity, due to the water dipole) than in the case of PCs.

The representation of the I_1/I_3 variation as a function of CHOL content in Figure 3.17, allows the observation of these changes in a more detailed view.

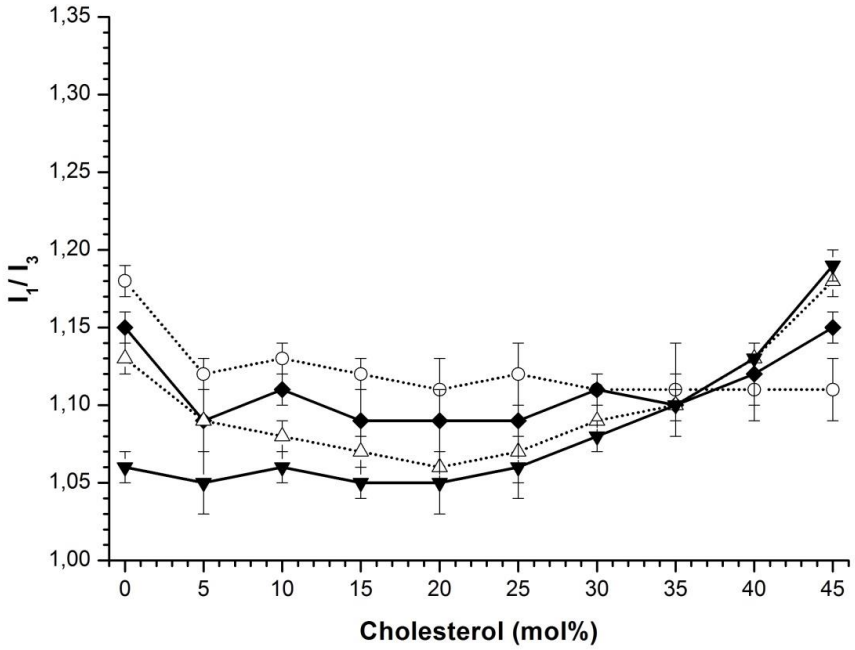

Figure 3.17 – Variation of equivalent polarity values (I_1/I_3) with CHOL concentration for egg-SM/CHOL mixtures for specific temperature values: (○) 25 ºC; (♦) 35 ºC; (Δ) 45 ºC; (▼) 55 ºC. The lines match the filled (—) and the outlined symbols (.....).

This is comparable to Figure 3.13 for DPPC/CHOL mixtures, but with more accentuated differences in the polarity variation for the supposed l_o phase.

III – 2.4 Egg-Sphingomyelin/POPC mixtures

The results for this mixture are present in Appendix – Table VIII. They were analyzed grouped in terms of low CHOL (0, 5 and 20 mol %) and high CHOL content (35, 40 and 45 mol %).

The mixtures with low POPC content are represented in Figure 3.18. Their thermal variation is different as the POPC molar proportion in the mixture is raised. The mixing of 5 and 20 mol% of POPC gives rise to equivalent polarity values that are similar within the experimental error and show the existence of two different behaviors alike pure phospholipid bilayers.

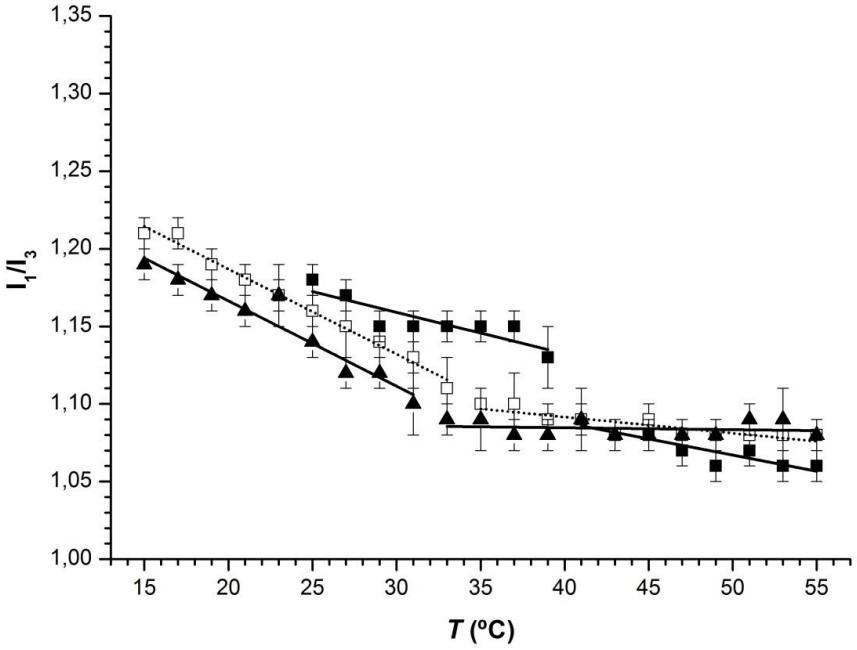

Figure 3.18 – Thermal variation of equivalent polarity values (I_1/I_3) for egg-SM/POPC mixtures with low POPC content (mol%/mol%): (■) 100/00; (□) 95/05; (▲) 80/20. The lines plotted match the filled (—) and the outlined symbols (.....).

Figure 3.19 represents the variation of I_1/I_3 with higher POPC molar proportions. The addition of 35 mol% of POPC still indicates the same behavior as observed for the mixtures with lower POPC amount. Also, the polarity values are also similar. The addition of 40, 45 and 50 mol% of POPC, which is also responsible for similar results within the experimental

error, seems to eliminate the differences between the results at lower and higher temperatures values, leading to a behavior alike homogeneous polar solvents along the temperature range.

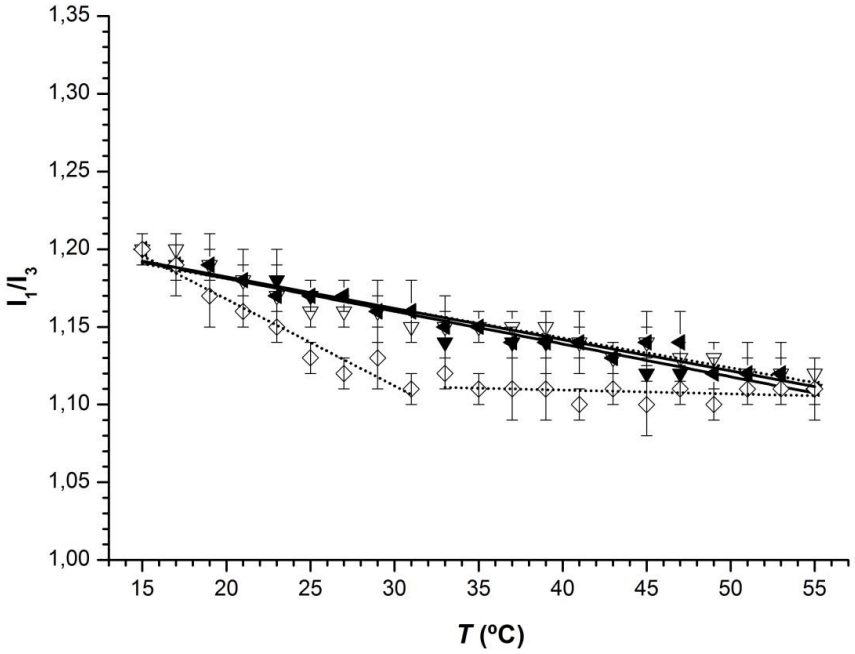

Figure 3.19 – Thermal variation of equivalent polarity values (I_1/I_3) for egg-SM/POPC mixtures with high POPC content (mol%/mol%): (◊) 65/35; (▼) 60/40; (∇) 55/45; (◄) 50/50. The lines plotted match the filled (—) and the outlined symbols (.....).

Figure 3.20 shows the variation of the I_1/I_3 values as a function of the POPC amount in the mixture. The weakly repulsive interactions between these phospholipids may lead to their non-ideal mixing [67] and formation of small SM domains (but not to phase separation), though the phase diagram [62] indicates a supposed phase coexistence of L_α + So_2. In general, these I_1/I_3 values are higher than the results for lower POPC molar proportions. These observations indicate that pyrene is likely to be located in a zone strongly influence by the presence of egg-SM (either in a gel-phase like or a phase coexistence surrounding), until there is sufficient POPC in the mixture for the probe to partition to a more fluid phase.

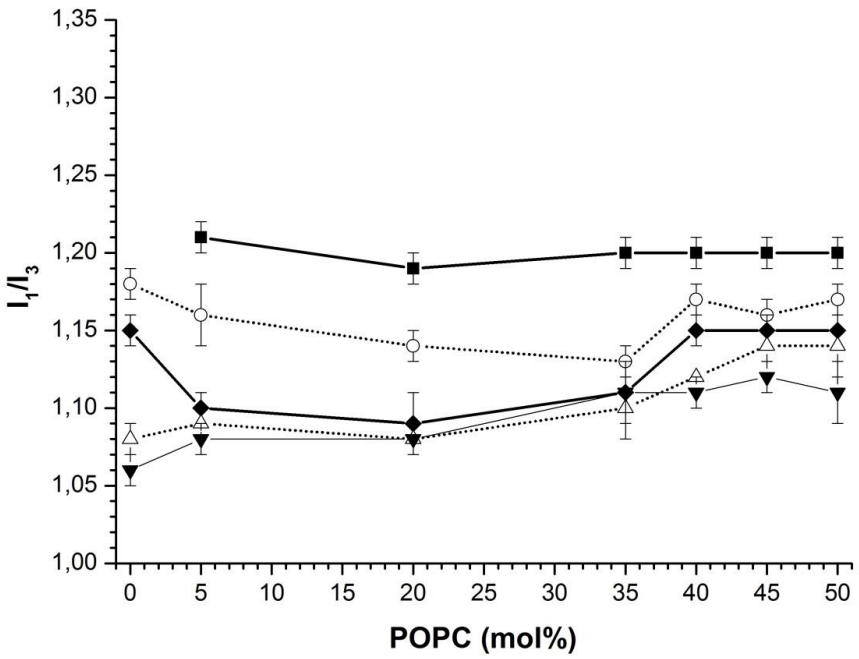

Figure 3.20 – Variation of equivalent polarity values (I_1/I_3) with POPC concentration for egg-SM/POPC mixtures for specific temperature values: (■) 15 ºC; (○) 25 ºC; (♦) 35 ºC; (Δ) 45 ºC; (▼) 55 ºC. The lines match the filled (—) and the outlined symbols (.....).

III – 2.5 Egg-Sphingomyelin/DOPC mixtures

Figure 3.21 represents the I_1/I_3 variation with temperature for low DOPC content (also see Appendix – Table IX). Similarly to what was observed in the egg-SM/POPC mixtures, the results are significantly different as the DOPC content is raised and resemble pure egg-SM bilayers. For the presence of 20 mol% of DOPC in the mixture, the temperature value at which pyrene seem to stop reporting a more polar environment and start detecting an apolar environment (indicated in the phase diagram as a transition from a L_α + L_β at ≈35 ºC) [39] does not match the one indicated in this work (≈45 ºC). Nevertheless, results from previous sections demonstrate that pyrene is able to report phase transitions with some accuracy so that this discrepancy may be the result of the different experimental parameters used in both works. The addition of higher DOPC amounts to egg-SM is represented in Figure 3.22.

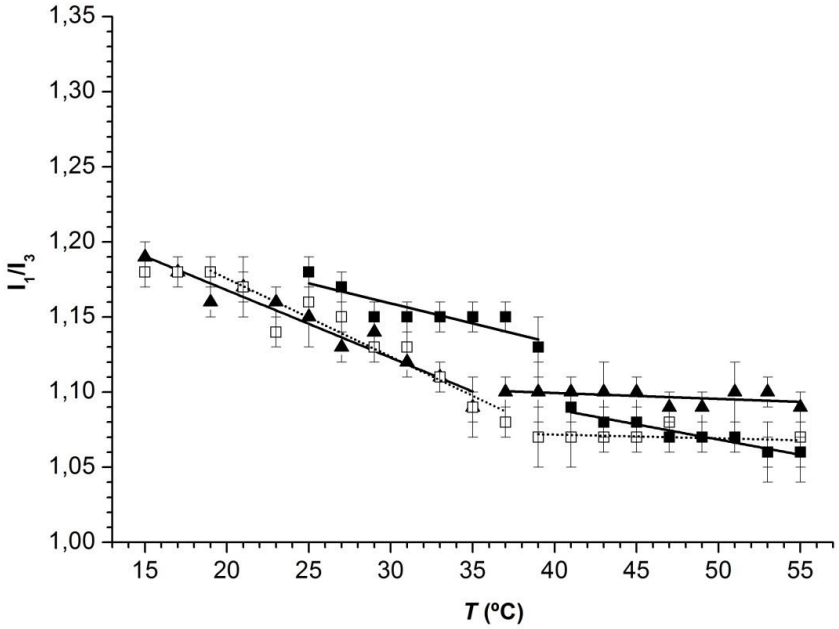

Figure 3.21 – Thermal variation of equivalent polarity values (I_1/I_3) for egg-SM/DOPC mixtures with low DOPC content (mol%/mol%): (■) 100/00; (□) 95/05; (▲) 80/20. The lines plotted match the filled (—) and the outlined symbols (.....).

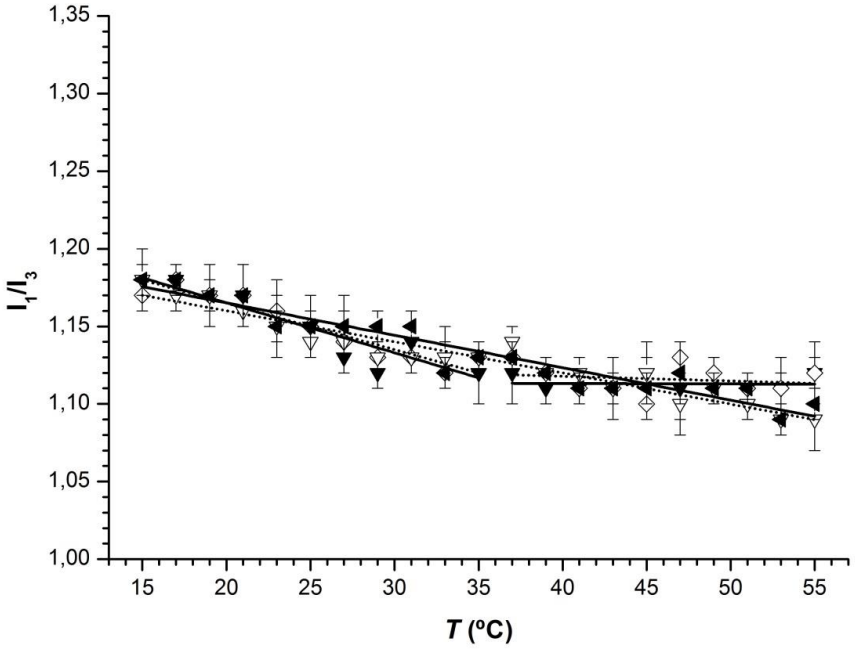

Figure 3.22 – Thermal variation of equivalent polarity values (I_1/I_3) for egg-SM/DOPC mixtures with high DOPC content (mol%/mol%): (◊) 65/35; (▼) 60/40; (▽) 55/45; (◄) 50/50. The lines plotted match the filled (—) and the outlined symbols (.....).

The addition of 35 and 40 mol% is still compared lower DOPC amounts, while the addition of 45 and 50 mol% of DOPC, leads to similar results within the experimental error, and seems to eliminate the referred differences between the I_1/I_3 values at lower and higher temperatures values (homogeneous polar solvents-like). For these DOPC amounts, the I_1/I_3 values are higher in the fluid phase when compared to the mixtures with lower DOPC concentrations. This is easier to access by observing Figure 3.23 which corresponds to the variation of I_1/I_3 with DOPC content.

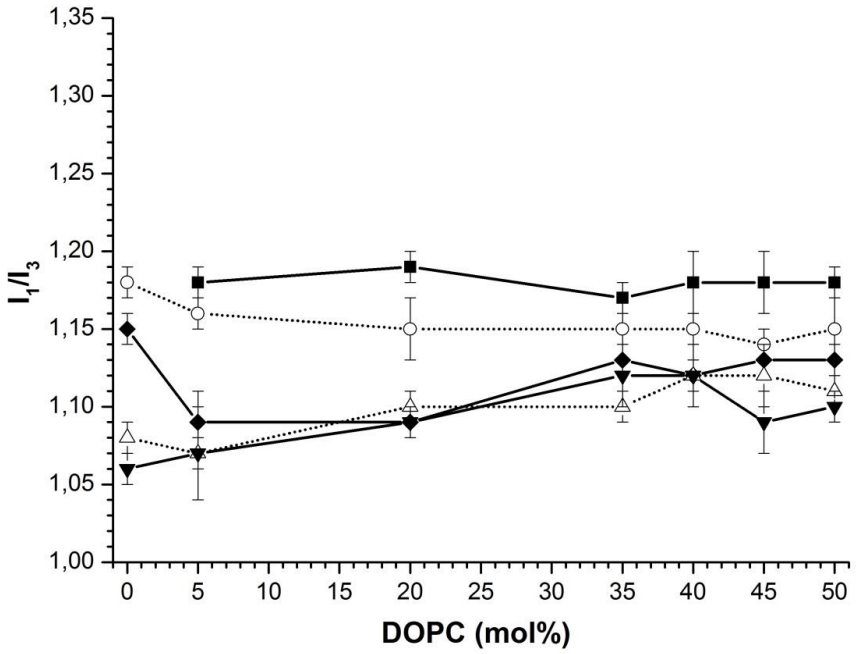

Figure 3.23 – Variation of equivalent polarity values (I_1/I_3) with DOPC concentration for egg-SM/DOPC mixtures for specific temperature values: (■) 15 ºC; (○) 25 ºC; (♦) 35 ºC; (Δ) 45 ºC; (▼) 55 ºC. The lines match the filled (—) and the outlined symbols (.....).

As in the case of the egg-SM/POPC mixtures, it seems like pyrene may partition to the fluid phase, or that the addition of higher DOPC concentrations is weakening the egg-SM interactions therefore, disordering the bilayer and increasing the amount of water penetration in the bilayer.

III – 3 *Equivalent polarity for ternary mixtures of POPC, egg-Sphingomyelin and cholesterol*

The phase diagrams known for these mixtures [62] (represented in Section I – 1.2.2.3, Figure 1.12 – D and 1.12 – E) indicate that the compositions studied in this work, for 23 ºC and 37 ºC would represent different zones. Figure 3.24 describes the thermal variation of the equivalent polarity for three different mixtures (see Appendix – Table X). At 23 ºC, both equimolar (1:1:1) and plasmatic membrane resembling (5:2:1) mixtures may represent a l_d + l_o phase coexistence, while the other mixture (4:3:1) would be in a three phase coexistence zone (l_d + l_o + S_o). At physiological temperature (37 ºC), only the first two mixtures appear to correspond to the same zone.

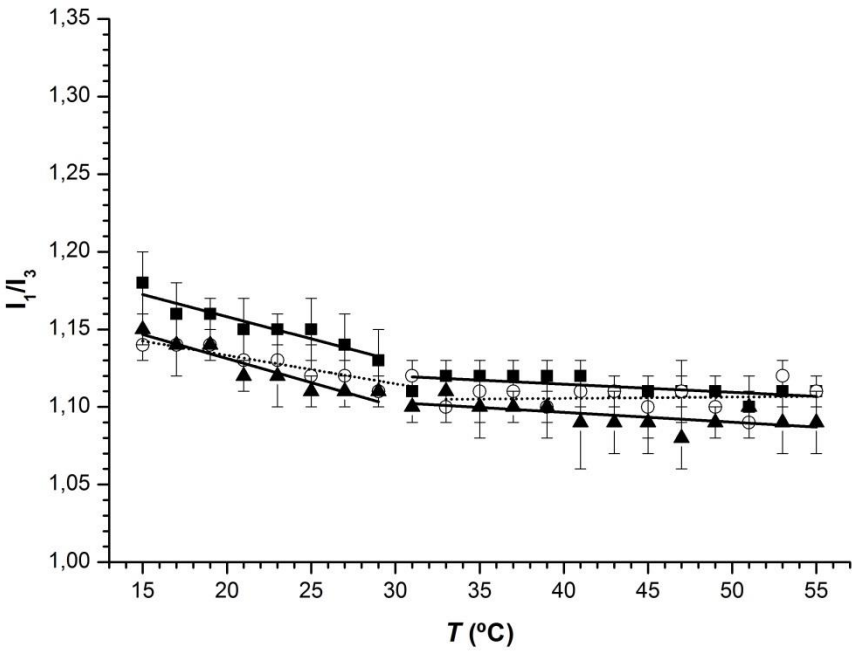

Figure 3.24 – Thermal variation of equivalent polarity values (I_1/I_3) for POPC/egg-SM/CHOL mixtures of different lipidic proportions: (■) 1:1:1; (□) 4:3:1; (▲) 5:1:2. The lines plotted match the filled (—) and the outlined symbols (.....).

According to the phase diagram [62], when the temperature is raised, the three-phase coexistence zone seems to be shifted to the right side of the phase diagram. The results presented here indicate that, for these experimental conditions, the I_1/I_3 values are not significantly different for these three mixtures, with the exception being the results for the 5:1:2 mixture (at 23 ºC) that seem to be slightly higher. As there are no significant differences between the three mixtures and generally is the nearly equimolar POPC/egg-SM/CHOL mixture that is considered the canonical raft mixture, the discussion will now be centered in the equivalent polarity results for this lipidic composition.

Using the same approach as for the binary mixtures analysis, this ternary mixture seem to present two different sets of results with increasing temperature: there is a slightly more accentuated variation of the I_1/I_3 values for lower temperatures (until the temperature reaches ≈ 30 ºC) and almost no variation for higher temperatures. Pyrene seems to be reporting two different polarity environments: a behavior that resembles polar homogeneous solvents and at higher temperatures the thermal behavior is more alike less polar homogeneous solvents. Yet, this behavior is not as accentuated as in the case of the studied binary mixtures. According to previous studies [128, 144] above ≈ 40 ºC, there is an overall fluid phase (l_d). In fact, this supports the results obtained in this section. There are evidences that POPC/egg-SM/CHOL bilayers containing 20-50 mol % of CHOL seem to range from either a single l_o phase or a l_d + l_o phase coexistence, for which l_o phase is the major component [78]. Taking this into account, it is possible that there is a l_d + l_o phase coexistence below ≈ 30 ºC and a l_d phase above this temperature value. In this matter, one might try to evaluate the possible distribution of the probe in fluid or more ordered phases. Early studies indicate that at 23 ºC we would be in the presence of phase coexistence between a l_d phase POPC-rich with 4-6 mol % of CHOL and a l_o phase (SM and CHOL-rich) with ≈ 25 mol % of POPC [68, 77]. If pyrene would show the same preference for fluid environments as in the case of binary mixtures, it may be located in a more disordered environment (with less CHOL and more POPC) in the case of phase coexistence. If this is the case, the l_d phase would resemble the POPC/CHOL mixture with 5 mol % of CHOL. At 25 ºC, the POPC/egg-SM/CHOL equimolar mixture, presents I_1/I_3 = 1.12 and the POPC bilayers with 5 mol % of CHOL present I_1/I_3 = 1.18, which are significantly different results. On the other hand, if the probe would be located in a more ordered environment (dominated by SM/CHOL domains) the equivalent polarity reported may be the result of an almost even distribution of POPC, egg-SM and CHOL. For egg-

SM/CHOL mixtures with 45 mol % of CHOL at 25 ºC (because there is no data available for 23 ºC), I_1/I_3 = 1.11 (see Appendix, Table VII) which is alike the value obtained for the equimolar mixture. This is not in accordance with the previous referred pyrene preference for fluid phases, though one has to consider the differences in the interactions between the lipids in a ternary mixture. In this matter, some studies indicate that PSM in PSM/CHOL may have higher order parameters than when in a ternary mixture, while POPC is expected to be more "disordered" in the POPC/CHOL binary mixture [132], so it is likely that the influence of one of the three lipids cannot be discarded.

Another scenario is brought by when thinking about the significance attributed to the I_1/I_3 values which represent the polarity for the l_d and l_o phases. It has been seen that for mixtures involving the presence of CHOL, these are likely to be minor than in the case of phospholipid-phospholipid mixtures. So, if these are significantly different it is possible that the polarity and associated dielectric constants would represent an additional contribution to the phase separation. It is possible to consider two different CHOL distributions. If each component constitutes approximately one third of the mixture, one can look at a situation where CHOL has an equal distribution *i.e.* one half of the sterol would be shared between the l_d phase (richer in POPC) and to the l_o (richer in egg-SM) in the same amount. The mixtures for which it is assumed that CHOL constitutes nearly one third of the amount of lipids are those with 65 mol% of phospholipid and 35 mol% of sterol. At 25 ºC (supposing that the ternary phase diagram would not change significantly for this temperature value), for POPC/CHOL, I_1/I_3 = 1.11 (Appendix – Table I) and for egg-SM/CHOL, I_1/I_3 =1.16 (Appendix – Table VII). On the other hand, if CHOL showed a preference for interacting with egg-SM, thus being present at very low amounts in the POPC-rich phase, it would be possible to compare the results between the same binary mixtures but with 55 mol% egg-SM mixed with 45 mol% of CHOL (I_1/I_3 = 1.11) and 95 mol% of POPC mixed with 5 mol% of CHOL (I_1/I_3 = 1.17), at the same temperature value. Either way, the difference seems to be significant for mixtures where CHOL is present, indicating that the equivalent polarity may indeed constitute an additional parameter driving to phase separation.

III – 4 *Equivalent polarity for binary mixtures of egg-Sphingomyelin and cholesterol derivatives*

The results obtained for the egg-SM/CHOL mixtures with high sterol amounts, lead to a simple question: is the CHOL double bond of the steroid ring system contributing to the increase of the I_1/I_3 values when the temperature is raised? To clarify this, one proceeded with the mixing of specific CHOL derivatives and egg-SM: 7DHC (with an extra double bond when compared to CHOL) and DCHOL (with no double bond).

III – 4.1 Egg-Sphingomyelin/7DHC mixtures

In order to obtain reliable I_1/I_3 values, the mixing of 7DHC with egg-SM brought the need to adjust the experimental conditions to obtain a better probe signal as well as the need of 7DHC blank (7DHC/egg-SM, without pyrene) subtraction for each spectrum. The preparation of MLV, using the same method for the other lipidic mixtures presented along this work, revealed itself a harder task. The lipidic film was not easily "removed" from the flask due to the problems in the hydration step of MLV production. The results reflect these experimental difficulties. Figure 3.25 represents the thermal variation of equivalent polarity for binary mixtures of egg-SM and low amounts of 7DHC. The addition of 5 mol % of 7DHC leads to different behaviors above and below 37 ºC: a slightly more polar environment for lower temperatures and an apolar solvent-like environment for higher temperature values. When compared to mixtures with different chemical composition (10 and 20 mol% of 7DHC in the mixture) the thermal behavior seems to be irregular, with a higher experimental error, revealing itself problematic for the analysis of the results through the same approach used for the other mixtures. This may be a consequence of the fact that 7DHC may not interact specifically with SM [145] as there are evidences that at physiological temperature the SM/7DHC association may be unstable [146]. The lower purity of 7DHC (when compared to all the other lipids used in this work) may also contribute to this through the loss of spectral resolution. Figure 3.26 represents the thermal variation of equivalent polarity for binary mixtures with higher 7DHC content. The overall tendency for the egg-SM/7DHC mixtures to display an irregular behavior (and higher experimental error) with increasing temperature is also observed at higher sterol content, revealing that the already mentioned unfavorable interaction between SM and 7DHC may be even more accentuated in this case.

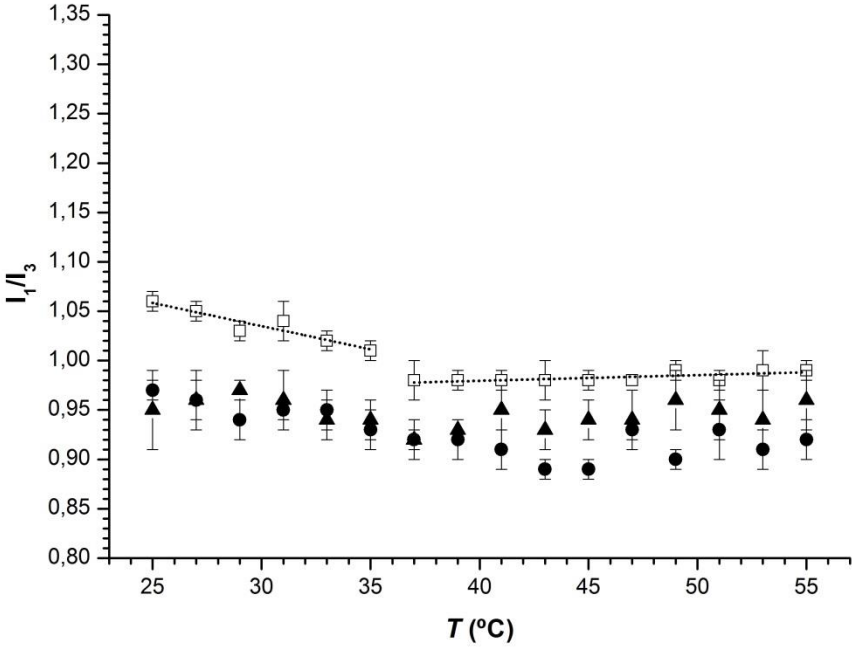

Figure 3.25 – Thermal variation of the equivalent polarity values (I_1/I_3) for egg-SM/7DHC mixtures with low 7DHC content. The symbols represent the different molar proportions (mol% / mol%): (□) 95/05; (●) 90/10; (▲) 80/20. The lines plotted match the outlined symbols (.....).

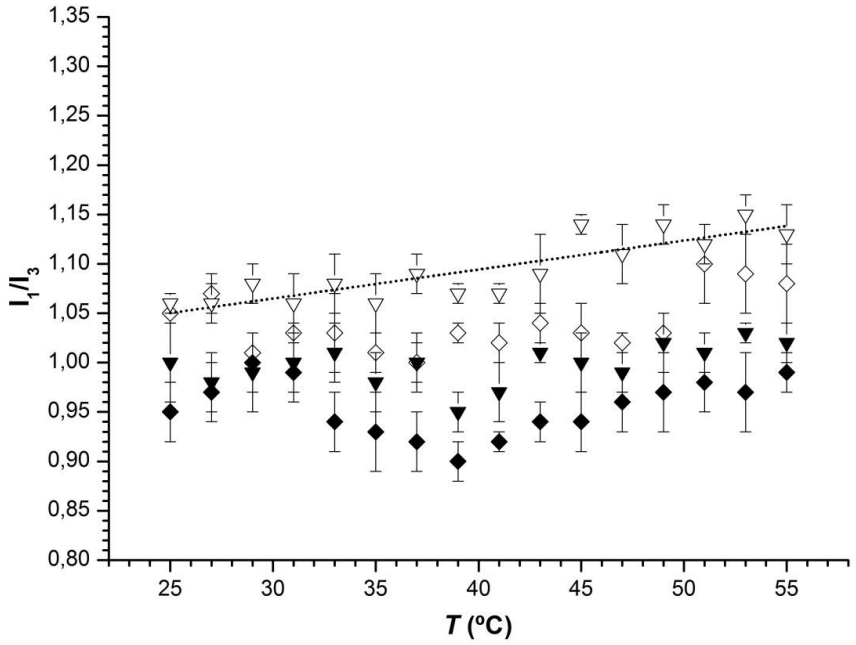

Figure 3.26 – Thermal variation of the equivalent polarity values (I_1/I_3) for egg-SM/7DHC mixtures with high 7DHC content. The symbols represent the different molar proportions (mol% / mol%): (♦) 70/30; (◊) 65/35; (▼) 60/40; (∇) 55/45. The line plotted matches the outlined symbols (.....).

The results for the addition of 30 mol% are similar those obtained for 10 and 20 mol%. From then, there seems to be a tendency for a gradual increase of the I_1/I_3 values until 45 mol% of sterol in the mixture, for which the equivalent polarity seems to increase with increasing temperature. The plot for the mixture with 45 mol% of 7DHC represents this tendency. The interactions between egg-SM and 7DHC do not seem very specific and the fact that 7DHC has an additional double bond in the B-ring that contributes to the loss of planarity [26, 27], may be an additional issue in this matter, as the presence of this sterol will probably give rise to some extra structural constraints.

III – 4.2 Egg-Sphingomyelin/Cholestanol mixtures

Figure 3.27 represents the I_1/I_3 variation with temperature for egg-SM/DCHOL for lower DCHOL amounts. There is a thermal behavior and I_1/I_3 values similar to the ones obtained for the addition of 5 mol% of 7DHC and for pure egg-SM bilayers.

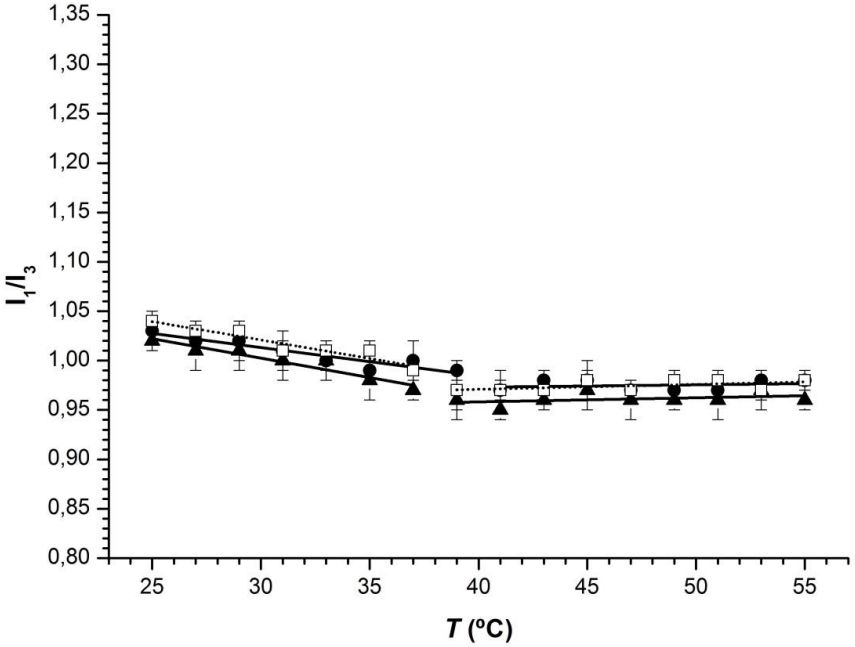

Figure 3.27 – Thermal variation of the equivalent polarity values (I_1/I_3) for egg-SM/DCHOL mixtures with low DCHOL content. The symbols represent the different molar proportions (mol%/mol%): (□) 95/05; (●) 90/10; (▲) 80/20. The lines plotted match the filled (—) and the outlined symbols (.....).

Figure 3.28 represents the results for the addition of higher DCHOL amounts. The I_1/I_3 values and their thermal variation are similar for the addition of 30 and 35 mol% (but slightly lower than those obtained for lower sterol amounts), resembling homogeneous polar solvents, which is a markedly different behavior when compared to 7DHC. These values are also a bit lower when compared to those for 7DHC, which may be an effect of the electrostatic contribution of its additional double bond. There is a tendency for the I_1/I_3 values to raise as the temperature increases for 40 and 45 mol% of DCHOL as in the case of egg-SM/CHOL mixtures (Figure 3.16).

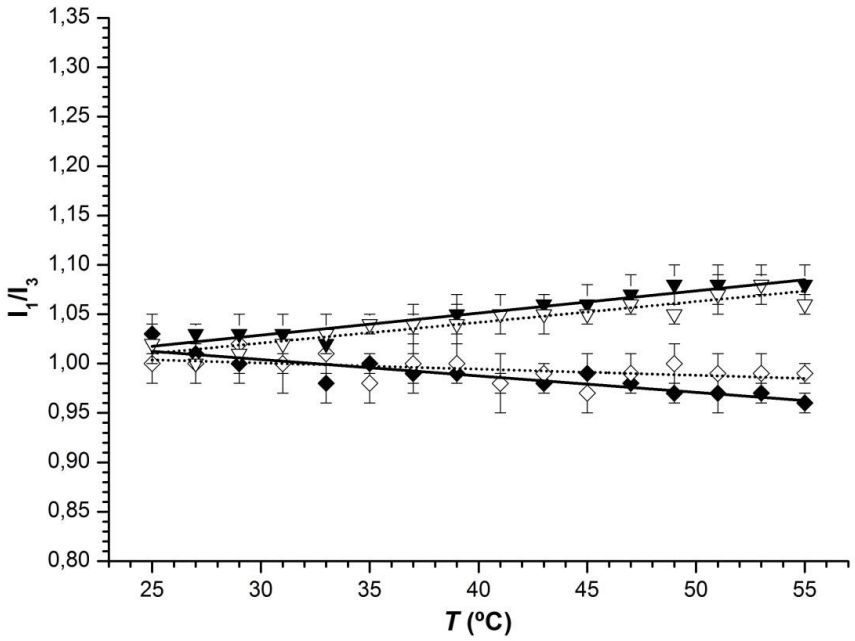

Figure 3.28 – Thermal variation of the equivalent polarity values (I_1/I_3) for egg-SM/DCHOL mixtures with high DCHOL content. The symbols represent the different molar proportions (mol% / mol%): (♦) 70/30; (◊) 65/35; (▼) 60/40; (▽) 55/45. The lines plotted match the filled (—) and the outlined symbols (.....).

III – 4.3 Egg-Sphingomyelin/Cholesterol derivatives vs. egg-Sphingomyelin/ Cholesterol

As the results for the egg-SM/CHOL mixture (Section III – 2.3) were obtained under different experimental conditions, it is not correct to quantitatively compare these with the I_1/I_3 values for the CHOL derivatives, only to look at overall tendencies and behaviors.

In fact, when looking at the egg-SM/CHOL mixtures with low sterol concentration (Figure 3.14), it is clear that, for 5, 10 and 20 mol% of sterol in the mixture, the thermal variation is not the same as a bilayer containing low amounts of 7DHC or DCHOL: it is irregular for 7DHC and shows dissimilar thermal behavior for lower and higher temperatures in the case of DCHOL. However, this is not as accentuated as in the case of pure bilayers. It can be merely a slight effect combining the presence of these particular sterols and the increase of temperature, giving rise to minor differences on the water content in the bilayer (because this is not verified with CHOL).

For higher 7DHC content, there seems to be a tendency for a gradual increase of the I_1/I_3 values until 45 mol% of sterol in the mixture for which the equivalent polarity seems to increase with increasing temperature, as in the case of egg-SM/CHOL (Figure 3.16). Apparently, DCHOL affects the lipid bilayers in a similar extent to CHOL, as it also seem to promote phase separation due to its condensation ability [28]. Even though the behavior for egg-SM/DCHOL with 40 and 45 mol% of sterol resembles the one obtained for the egg-SM/CHOL mixtures with 45 mol% of sterol, they "spread" into different directions as the temperature rises, meaning an abrupt change on the thermal behavior.

All these observations may be an indication that this is likely to be a specific effect brought on by the interaction between egg-SM and sterols, in general. This is supported by the fact that this unusual behavior is maintained even in the absence of a double bond in the steroid ring system (all the other structural features are common to the three sterols). The unusual thermal behavior of the bilayers containing egg-SM mixed sterols (increasing of the polarity with temperature, at high sterol content) may suggest that this observation might be likely due to the increased polarizability as a function of temperature, arising from the more ordered state of SM based lipid bilayers.

Chapter IV

CONCLUDING REMARKS

IV – 1 *Binary mixtures involving unsaturated phospholipids*

This work showed that, in terms of polarity, the mixing of CHOL or egg-SM in POPC bilayers seems to give rise to some differences. The POPC/cholesterol mixtures, are quite similar to pure POPC bilayers, within the experimental error, until the 40 mol% of sterol is reached, so that it was not possible to detect any phase coexistence. In addition, according to the phase diagrams, the presence of high CHOL amounts leads to the formation of a l_o phase: lower lipid diffusion and decrease in membrane permeability, free volume and polarity. For the mixtures of unsaturated lipids and CHOL, the polarity seems to depend mostly on the lipid-lipid interactions and hydrogen bonds as there is a consequent lowering of the I_1/I_3 values with the decrease in the water content. The mixing of egg-SM into POPC bilayers does not seem to have a significant effect in the equivalent polarity: all the results resemble those obtained for the pure POPC bilayers. In polarity terms, having POPC mixed with egg-SM or with CHOL (below 40 mol%) is practically the same.

The DOPC based mixtures show that adding either CHOL or egg-SM is similar: 20 mol% of the second lipid seems to be a concentration which leads to some changes in the equivalent polarity reported by pyrene. There is no evidence of phase coexistence and this particular lipid concentration seems to be the one for which the pyrene surroundings are starting to be affected by the CHOL condensing effect or the presence of a saturated and rigid phospholipid with the slight lowering of the I_1/I_3 values as a consequence of the lesser molecular freedom, lower free volume and membrane permeability to water. So, in terms of polarity, it may be equivalent to have egg-SM or CHOL mixed with DOPC.

The POPC/CHOL and DOPC/CHOL profiles of I_1/I_3 variation with temperature are quite similar, as they not change substantially until the addition of a considerable amount of CHOL to the mixture, even though this specific sterol concentration is different for both mixtures (40 mol% for POPC/CHOL and 20 mol% for DOPC/CHOL). If analyzed in terms of CHOL concentration, the equivalent polarity results show us that pyrene is reporting a slightly less polar environment for the DOPC/CHOL mixture after we reached the 20 mol% of the sterol is reached and that these values resemble the ones obtained for POPC/CHOL at lower CHOL content.

The POPC/egg-SM and DOPC/egg-SM present a slight different behavior, as the addition of egg-SM does not seem to affect the polarity reported by pyrene in the former case, but seems to lead to lowering of the I_1/I_3 values from 20 mol% to higher values. The overall

results suggest that DOPC bilayers, being more disordered than the POPC counterpart, are more susceptible to the ordering effects of CHOL or egg-SM and start to be influenced at lower proportion (20 mol %) of these lipids than POPC (only above 40 mol%).

The calculated dielectric constants provide a quantification method, showing that indeed one is in the presence of different environments that depend mostly on the temperature and chemical composition. This can be important for the transport across the membrane, as well as for the insertion, stabilization and function of membrane proteins. For example, the Ca^{2+}–ATPase and Na^{+},K^{+}–ATPase maximum function is known to depend on the CHOL proportion in its lipidic membranous environment. It is known that protein sorting along the secretory pathway may be performed through the existence of a gradient in the hydrophobic thickness of the membrane systems that the proteins pass in order to achieve their target. Indeed, the existence of CHOL and SM in the membranes (that is gradually higher passing from the ER, Golgi and plasma membrane), may contribute to the enlargement of their thickness [9]. The results obtained in this section show that the polarity may be an additional contribution to this issue, as this work points out in the direction that there may be significant differences in the polarity for POPC containing bilayers at higher CHOL concentrations.

IV – 2 *Binary mixtures involving saturated phospholipids*

The binary mixtures involving saturated phospholipids are usually more studied than those involving unsaturated phospholipids, so that there is more information available (especially in the case of the DMPC/DPPC and DPPC/CHOL mixtures).

The studies with the former indicate that pyrene may not have a marked preference for fluid phases though its distribution does not seem equal in fluid and more ordered phases.

For the DPPC/CHOL mixtures, one of the most important contributions to improve the knowledge about lipid bilayers is the indication that, in terms of polarity, the l_o phase may depend on temperature and CHOL content. This tendency is even more accentuated in the case of the egg-SM/CHOL (for which the thermal variation of the polarity results obtained may be compared with the one from a rubber or plastic). Other than that, through these studies it has been shown that even though both mixtures involve the interaction between CHOL and a saturated phospholipid and there are many similarities, there are also some important differences. In general terms, the behavior is similar for both mixtures (with exception for the higher CHOL content), but the egg-SM/CHOL mixture polarity tends to be lower, when

compared with the DPPC/CHOL mixtures. The tendency for the experimental error to increase as the cholesterol content is raised does not seem to occur in the case of the egg-SM/CHOL mixtures.

The mixtures of egg-SM with POPC or DOPC show similar behaviors, but confirm that the polarity variation in mixtures with this composition may depend on which lipid is present in a higher molar proportion.

The polarity for mixtures involving unsaturated phospholipids (*i.e.* POPC/CHOL and DOPC/CHOL), for these experimental conditions, is generally higher than in the case of saturated mixtures (DPPC/CHOL and egg-SM/CHOL), as it was indicated in early studies [89].

IV – 3 *Ternary mixtures of POPC, egg-Sphingomyelin and cholesterol*

The results for the ternary mixtures analyzed show that in terms of polarity, there are no significant differences between the three compositions used. In fact, by analyzing these results using the same procedure as in the case of the binary mixtures, it is possible to detect a behavior similar to what was obtained for pure phospholipid bilayer (though less accentuated). This may indicate that for ternary mixtures, there may also be different polarity environments depending on temperature (as for binary mixtures). This is a more complex case, because it involves the mixing of three different lipids and the supposed formation of lipidic domains of different composition. Still, if these results are compared with the outcomes for the binary mixtures, at higher temperatures (including physiological temperature), there is the indication of the existence of an "overall" phase for all the compositions studied with the characteristics of a fluid phase, in contrast with the different polarity reported by the probe for lower temperature values (including room temperature), which indicates a more ordered environment. In this case, the differences in the I_1/I_3 values for some particular compositions indicate that this may also be a contribution to phase separation (and phase coexistence).

IV – 4 *Binary mixtures of egg-Sphingomyelin and cholesterol derivatives*

The use of these specific CHOL derivatives brought us some enlightenment about the possible contribution of the double bond present in the CHOL steroid ring to the polarity reported by pyrene, in the case of egg-SM/CHOL mixtures with high CHOL content. This preliminary analysis showed us that, for the experimental conditions used in this work, 7DHC

does not seem to mix well with egg-SM and that the presence of higher DCHOL molar proportions seems to have a similar effect to the presence of a higher CHOL content in the mixture. This indicates that this may be an effect of specific egg-SM/sterol interactions.

IV – 5 *Perspectives*

The results discussed in the previous sections indicate that the use of pyrene provides a sensitive tool to report changes in the molecular composition in lipidic mixtures and its effects on the local polarity. As this provides results for the more ordered zone of the lipid bilayer, the use of a pyrene probe linked to an acyl chain (thus maintaining the molecule's symmetry in its long axis) would be helpful in order to obtain polarity results for the deeper hydrocarbon core (which is many times assumed to be hexadecane-like).

It is known that these results can be deeply affected by the fluidity/viscosity of the bilayers. This is not only a consequence of the solvent (water) dipole reorientation around the solute molecules, but also an effect of molecular motion, as the results obtained for the gel phases are significantly different from those obtained for the fluid phases. It would be interesting to study the lipidic mixtures used in this work in order to access the effects of thermal and molecular composition variation in bilayer fluidity/viscosity.

Throughout the work, the main focus was the major components of the outer leaflet of the mammalian plasmatic membrane, so the study of lipid mixtures with different compositions may also be of great value. The application of this method to lipid mixtures composed by anionic phospholipids, which are one of the main components of the inner leaflet of the plasmatic membrane (*e.g.* 1-palmitoyl-2-oleoyl-*sn*-glycero-3-phospho-L-serine (POPS)) would also be an interesting point of study to observe the effect of the "charged" polar headgroup in the local polarity sensed by pyrene and what would be the consequences of changing the molar proportions of the mixtures, therefore comparing the equivalent polarity for mixtures with higher proportions of POPS with the one obtained for lower proportions of POPS. In this matter, a good path to follow is the report the effect of a counterion (*e.g.* Ca^{2+}), as this would result in a stabilization of the negative charge of the POPS head groups.

The studies with the CHOL derivatives can be useful in order to understand the effect of sterols in the local polarity. As this work indicates that the effects of the addition of high sterol amounts is likely to be a consequence of specific sterol-SM interactions, the analysis of the variation of the polarity profiles in mixtures of DPPC (a PC similar to SM) and 7DHC or DCHOL may be a helpful addition to the obtained results. The common features between

CHOL, 7DHC and DCHOL are the hydrocarbon chain, the steroid ring and the –OH group, with the difference being exclusively in the number of existing double bonds, so effects of other kinds of derivatives, like 4β-hydroxycholesterol (similar to CHOL, but with two hydroxyl groups), may be a useful perspective.

REFERENCES

[1] Gennis R.B., *Biomembranes: Molecular Structure and Function*, Springer-Verlag New York, 1989.
[2] Vance D.E. and Vance J.E., *Biochemistry of Lipids, Lipoproteins and Membranes*, 5th Ed., Elsevier, 2008.
[3] Heimburg T., *Thermal Biophysics of Membranes*, Wiley-VCH, 2007.
[4] Singer S.J. and Nicolson G.L. (1972) The fluid mosaic model, *Science*, 172:720-731
[5] Mouritsen O.G. and Bloom M. (1984) Mattress model of lipid-protein interactions in membranes, *Biophys. J.*, 46:141-153.
[6] Yeagle P.L., *The Structure of Biological Membranes*, 2nd Ed., CRC Press, 2005.
[7] Róg T., Pasenkiewicz-Gierula M., Vattulainen I. and Karttunen M. (2009) Ordering effects of cholesterol and its analogues, *Biochim. Biphys. Acta*, 1788:97-121
[8] Vaz W.L.C., *Lipid Bilayer Properties*, in Wiley Encyclopedia of Chemical Biology, Wiley & Sons, Inc., 2008.
[9] Mouritsen O.G., *Life - As a Matter of Fat, The emerging science of lipidomics*, Springer-Verlag, Berlin, 2005.
[10] Barenholz Y. (2002) Cholesterol and other membrane active sterols: from membrane evolution to "rafts", *Prog. Lipid Res.*, 41:1-5.
[11] Deveaux P. and Hermann A., *Transmembrane Dynamics of Lipids*, Wiley & Sons, Inc., 2012.
[12] Ohvo-Rekilä H., Ramstedt B., Leppimäki P. and Slotte J.P. (2002) Cholesterol interactions with phospholipids and membranes, *Prog. Lipid Res.*, 41:66-97.
[13] Maxfield F.R.and Tabas I. (2005) Role of cholesterol and lipid organization in disease, *Nature*, 438:612-621.
[14] Li Y., Ge M., Ciani L., Kuriakose G., Westover E.J., Dura M., Covey D.F., Freed J.H., Maxfield F.R., Lytton J. and Tabas I. (2004) Enrichment of Endoplasmic Reticulum with Cholesterol Inhibits Sarcoplasmic-Endoplasmic Reticulum Calcium ATPase-2b Activity in Parallel with Increased Order of Membrane Lipids: Implications for Depletion of Endoplasmic Reticulum Calcium Stores and Apoptosis In Cholesterol-Loaded Macrophages, *J. Biol. Chem.*, 279:37030-37039.
[15] Epand R.M.; Hughes D.W., Sayer B.G., Borochov N., Bach D. and Wachtel E. (2003) Novel properties of cholesterol-dioleoylphosphatidylcholine mixtures, *Biochim. Biophys. Acta*, 1616:196-208.
[16] Plesnar E., Subczynski W.K. and Pasenkiewicz-Gierula M. (2012) Saturation with cholesterol increases vertical order and smoothes the surface of the phosphatidylcholines bilayer: a molecular simulation study, *Biochim. Biophys. Acta*, 1818:520-529.
[17] Wolozin B. (2004) Cholesterol, statins and dementia, *Current Opinion in Lipidology*, 15:667-672.
[18] Kessel A., Ben-Tal N. and May S. (2001) Interactions of Cholesterol with Lipid Bilayers: The Preferred Configuration and Fluctuations, *Biophys. J.*, 81:643-658.
[19] Mouritsen O.G and Zuckermann M.J (2004) What's so special about cholesterol?, *Lipids*, 39:1101-1112.
[20] Mannock D.A., Lewis R.N.A.H., McMullen T.P.W. and McElhaney R.N. (2010) The effect of variations in the phospholipid and sterol structure on the nature of lipid-sterol interactions in lipid bilayer model membranes, *Chem. Phys. Lipids*, 163:403-448.

[21] Martinez-Seara H., Róg T., Pasenkiewicz-Gierula M., Vattulainen I., Karttunen M. and Reigada R. (2008) Interplay of Unsaturated Phospholipids and Cholesterol in Membranes: Effect of the Double-Bond Position, *Biophys. J.*, 95:3295-3305.

[22] Smondyrev A.M. and Berkowitz M.L. (1999) Structure of Dipalmitoylphophatidylcholine/cholesterol bilayer at Low and High Cholesterol Concentrations: Molecular Dynamics Simulation, *Biophys. J.*, 77:2075-2089.

[23] Aittoniemi J., Róg T., Niemelä P., Pasenkiewicz-Gierula M., Karttunen M. and Vattulainen I. (2006) Tilt: Major Factor in Sterols' Ordering Capability in Membranes, *J. Phys. Chem. B Letters*, 110:25562-25564.

[24] Aittoniemi J., Niemelä P., Hyvönen M.T., Karttunen M. and Vattulainen I. (2007) Insight into the Putative Specific Interactions between Cholesterol, Sphingomielyn, and Palmitoyl-Oleoyl Phosphatidylcholine, *Biophys. J.*, 92:1125-1137

[25] Róg T., Pasenkiewicz-Gierula M., Vattulainen I. and Karttunen M. (2007) What Happens if Cholesterol Is Made Smoother: Importance of Methyl Substituents in Cholesterol Ring Structure on Phosphatidylcholine-Sterol Interaction, *Biophys. J.*, 92:3346-3357.

[26] Valencia A., Rajadurai A., Carle A.B. and Kochevar I.E. (2006) 7-Dehydrocholesterol enhances ultravioleta A-induced oxidative stress in keratinocytes: Roles of NADPH oxidase, mitochondria, and lipid rafts, *Free Radical Biology & Medicine*, 41:1704-1718.

[27] Serfis A.B., Brancato S. and Fliesler S.J. (2001) Comparative behavior of sterols in phosphatidylcholine-sterol monolayer films, *Biochim. Biophys. Acta*, 1511:341-348.

[28] Lintker K.B., Kpere-Daibo P., Fliesler S.J. and Serfis A.B. (2009) A comparison of the packing behavior of egg phosphatidylcholine with cholesterol and biogenically related sterols in Langmuir monolayer films, *Chem. Phys. Lipids*, 161:22-31.

[29] Porter F.D. (2006) Cholesterol precursors and facial clefting, *The Journal of Clinical Investigation*, 116:2322-2325.

[30] Ollila O.H.S, Róg T., Karttunen M. and Vattulainen I. (2007) Role of sterol type on lateral pressure profiles of lipid membranes affecting membrane protein functionality: comparison between cholesterol, desmosterol, 7-dehydrocholesterol and ketosterol, *J. Structural Biology.*, 159:311-323.

[31] Keller R.K, Arnold T.P. and Fliesler S.J. (2004) Formation of 7-dehydrocholesterol-containing membrane rafts in vitro and in vivo with relevance to the Smith-Lemli-Opitz Syndrome, *J. Lipid Res.*, 45:347-355.

[32] Lomize A.L., Pogozheva I.D. and Mosberg H.I. (2011) Anisotropic Solvent Model of the Lipid Bilayer. 2. Energetics of Insertion of Small Molecules, Peptides, and Proteins in Membranes, *J. Chem. Inf. Model.*, 51:930–946.

[33] Peróchon E., Lopéz A. and Tocanne J.F. (1992) Polarity of Lipid Bilayers. A Fluorescence Investigation, *Biochemistry*, 31:7672-7682.

[34] Seelig J. and Seelig A. (1980) Lipid conformation in model membranes and biological membranes, *Quart. Rev. Biophys.*, 13:19-61.

[35] Atkins P.W., *Physical Chemistry*, 6th Ed., Oxford University Press, 1998.

[36] Avanti Polar Lipids: www.avantilipids.com

[37] Mabrey S. and Sturtevant J.M. (1976) Investigation of phase transitions of lipids and lipid mixtures by high sensitivity differential scanning calorimetry (lipid bilayers/membranes/phase diagrams/transition heat capacity curves), *PNAS*, 73:3862-3866.
[38] Wu S.H.W. and McConnell H.M. (1975) Phase separations in phospholipid membranes, *Biochemistry*, 14:847–854.
[39] Nyholm T.K.M., Lindroos D., Westerlund B. and Slotte J.P. (2011) Construction of a DOPC/PSM/Cholesterol Phase Diagram Based on the Fluorescence Properties of *trans*-Parinaric Acid, *Langmuir*, 27:8339–8350.
[40] Huang J., Buboltz J. T. and Feigenson G. W. (1999) Maximum solubility of cholesterol in phosphatidylcholine and phosphatidylethanolamine bilayers, *Biochim. Biophys. Acta*, 1417:89 –100.
[41] Kessel A., Ben-Tal N. and May S. (2001) Interactions of Cholesterol with Lipid Bilayers: The Preferred Configuration and Fluctuations, *Biophys. J.*, 81:643-658.
[42] Tu K., Klein M.L. and Tobias D.J. (1998) Constant-Pressure Molecular Dynamics Investigation of Cholesterol Effects in a Dipalmitoylphosphatidylcholine Bilayer, *Biophys. J.*, 75:2147-2156.
[43] Lide D.R., *Handbook of Chemistry and Physics*, 86th Ed., CRC Press, 2008.
[44] Ipsen J.H., Mouritsen O.G. and Zuckermann M.J. (1989) Theory of thermal anomalies in the specific heat of lipid bilayers containing cholesterol, *Biophys. J.*, 56:661-667.
[45] Vist M.R. and Davis J.H. (1990) Phase Equilibria of Cholesterol/Dipalmitoylphosphatidylcholine Mixtures: ^{2}H-Nuclear Magnetic Resonance and Differential Scanning Calorimetry Biochemistry, 29:451-464.
[46] Sankaram M.B. and Thompson T.E. (1991) Cholesterol-induced fluid-phase immiscibility in membranes, *PNAS*, 88:8686-8690.
[47] Marsh D. (2010) Liquid-ordered phases induced by cholesterol: A compendium of binary phase diagrams, *Biochim. Biophys. Acta*, 1798:688-699.
[48] Alwarawrah M., Dai J. and Huang J. (2010) A Molecular View of the Cholesterol Condensing Effect in DOPC Lipid Bilayers, *J. Phys. Chem. B*, 114:7516-7523.
[49] Ipsen J.H., Karlström G., Mourtisen O.G., Wennerström H. and Zuckermann M.J. (1987) Phase equilibria in the phosphatidylcholine-cholesterol system, *Biochim. Biophys. Acta*, 905:162-172.
[50] Silvius J.R. (2003) Role of cholesterol in lipid raft formation: lessons from lipid model systems, *Biochim. Biophys. Acta*, 1610:174-183.
[51] Anderson T.G. and McConnell H.M. (2001) Condensed Complexes and the Calorimetry of Cholesterol-Phospholipid Bilayers, *Biophys. J.*, 81: 2774-2785.
[52] McConnell H.M. and Radhakrishnan A. (2003) Condensed complexes of cholesterol and phospholipids, *Biochim. Biophys. Acta*, 1610:159-173.
[53] McConnell H.M. and Vrljic M. (2003) Liquid-liquid immiscibility in membranes, *Annu. Rev. Biophys. Biomol. Struct.*, 32: 469-492.
[54] Chong P. L.-G., Zhu W. and Venegas B. (2009) On the lateral structure of model membranes containing cholesterol, *Biochim. Biophys. Acta*, 1788:2-11.
[55] Huang, J. and Feigenson G.W. (1999) A microscopic interaction model of maximum solubility of cholesterol in lipid bilayers, *Biophys. J.*, 76:2142–2157.
[56] Barenholz Y. and Thompson T.E. (1999) Sphingomyelin: biophysical aspects, *Chem. Phys. Lipids*, 102:29:34.
[57] Brown R.E. (1998) Sphingolipid organization in biomembranes: what physical studies of model membrane reveals, *J. Cell. Science*, 111:1-9.

[58] Brewster R., Pincus P.A. and Safran S.A. (2009) Hybrid Lipids as a Biological Surface-Active Component, *Biophys. J.*, 97:1087-1094.
[59] Brewster R. and Safran S.A. (2010) Line Active Hybrid Lipids Determine Domain Size in Phase Separation of Saturated and Unsaturated Lipids, *Biophys. J.*, 98:L21-L23.
[60] Berkowitz M.L. (2009) Detailed molecular dynamics simulations of model biological membranes containing cholesterol, *Biochim. Biophys. Acta*, 1788:86-96.
[61] Travesset A. (2006) Effect of dipolar moments in domain sizes of lipid bilayers and monolayers, *J. Chem. Phys.*, 125: 084905.
[62] de Almeida R., Fedorov A. and Prieto M. (2003) Sphingomyelin/phosphatidylcholines/cholesterol phase diagram: boundaries and composition of lipid rafts, *Biophys. J.*, 85:2406-2416.
[63] Mattjus P. and Slotte J.P. (1996) Does cholesterol discriminate between sphingomyelin and phosphatidylcholines in mixed monolayers containing both phospholipids?, *Chem. Phys. Lipids*, 81:69-80.
[64] Veatch S.L. , Soubias O., Keller S.L. and Gawrisch K. (2007) Critical fluctuations in domain-forming lipid mixtures, *PNAS*, 104:17650-17655.
[65] Simons K. and Vaz W.L.C. (2004) Model Systems, Lipid Rafts and Cell Membranes, *Annu. Rev. Biophys. Biomol. Struct.*, 33:269-295.
[66] Sprong H., van der Sluijs P. and van Meer G. (2001) How proteins move lipids and lipids move proteins**,** Nature Reviews Molecular Cell Biology, 2:504-513.
[67] Almeida P.F.F. (2008) Thermodynamics of lipid interactions in complex bilayers, *Biochim. Biophys. Acta*, 1788:72-85.
[68] Slotte J.P. and Ramstedt B. (2007) The functional role of sphingomyelin in cell membrane, *Eur. J. Lipid Sci. Technol.*,109:977-981.
[69] Edidin M. (2003) The State of Lipid Rafts: From Model Membranes to Cells, *Annu. Rev. Biomol. Struct.*, 32:257-283.
[70] Martinez-Seara H., Róg T., Karttunen M., Reigada R. and Vattulainen I. (2008) Infuence of the cis double-bond parametrization on lipid membrane properties: how seemingly insignificant details in force-field change even qualitative trends, *J. Chem. Phys*., 129: 105103.
[71] Reyes-Mateo C., Acuña A.U.and Brochon J.C. (1995) Liquid-crystalline phases of cholesterol/lipid bilayers as revealed by the fluorescence of *trans*-parinaric acid, *Biophys. J.*, 68:978-987.
[72] Marsh D. (2009) Cholesterol-induced fluid membrane domains: a compendium of lipid-raft ternary phase diagrams, *Biochim. Biophys. Acta*, 1788:2114-2123.
[73] Tauc P., Mateo C.R. and Brochon J.-C. (1998) Pressure effects of the lateral distribution of cholesterol in lipid bilayers: a time-resolved spectroscopy study, *Biophys. J.*, 74:1864-1870.
[74] Pokorny A., Yandek L.E., Elegbede A.I., Hinderliter A. and Almeida P.F.F. (2006) Temperature and Composition Dependence of the Interaction of δ-Lysin with Ternary Mixtures of Sphingomyelin/Cholesterol/POPC, *Biophys. J.*, 91:2184-2197.
[75] Heerklotz H (2002) Triton promotes domain formation in lipid raft mixtures, *Biophys J.*, 83:2693-701.
[76] Pike L.J. (2004) Lipid rafts: heterogeneity on the high seas, *Biophys. J.*, 378:281-292.

[77] Brown D.A. and London E. (1998) Functions of lipid rafts in biological membranes, *Annu. Rev. Cell Dev. Biol.*, 14:111-136.
[78] Almeida P.F.F., Pokorny A. and Hinderliter A. (2005) Thermodynamics of membrane domains, *Biochim. Biophys. Acta*, 1720:1-13.
[79] Simons K. and Ikonen E. (1997) Functional rafts in cell membranes, *Nature*, 387:569-72.
[80] McIntosh T.J. and Simon S.A. (2006) Roles of bilayer material properties in function and distribution of membrane proteins, *Annu. Rev. Biophys. Biomol. Struct.*, 35:177-198.
[81] Ikonen E. (2001) Roles of lipid rafts in membrane transport, *Curr. Opin. Cell Biol.*, 13:470-477.
[82] Munro S. (2003) Lipid Rafts: Elusive or Illusive?, *Cell*, 115:377-388.
[83] Pike L.J. (2003) Lipid Rafts: bringing order to chaos, *J. Lipid. Res.*, 44:655-667.
[84] Schroeder R.J., Ahmed S.N., Zhu Y., London E. and Brown D.A. (1998) Cholesterol and Sphingolipid Enhance the Triton X-100 Insolubility of Glycosylphosphatidylinositol-anchored Proteins by Promoting the Formation of Detergent-insoluble Ordered Membrane Domains, *J. Biol. Chem.*, 273: 1150-1157.
[85] Resh M.D. (2004) Membrane targeting of lipid modified signal transduction proteins, *Subcell. Biochem.*, 37:217-32.
[86] White S.H. and Wimley W.C. (1998) Hydrophobic interactions of peptides with membrane interfaces, *Biochim. Biophys. Acta*, 1376:339-352.
[87] Ho C., Slater J.S. and Stubbs C.D. (1995) Hydration and Order in Lipid Bilayers, *Biochemistry*, 34:6188-6195.
[88] Subczynski W.K., Wisniewska A., Yin J-J., Hyde S. and A. Kusumi (1994) Hydrophobic Barriers of Lipid Bilayer Membranes Formed by the Reduction of Water Penetration by Alkyl Chain Unsaturation and Cholesterol, *Biochemistry*, 33:7670-7681.
[89] Marsh D. (2001) Polarity and permeation profiles in lipid membranes, *PNAS*, 98: 7777-7782
[90] Marsh D. (2002) Membrane water-penetration profiles from spin labels, *Eur. Biophys. J.*, 31:559-562.
[91] Erilov D.A., Bartucci R., Guzzi R., Shubin A.A., Maryasov A.G., Marsh D., Dzuba S.A. and Sportelli L. (2005) Water concentration profiles in membranes measured by ESEEM of spin-labeled lipids, *J. Phys. Chem. B*, 109:12003-12013.
[92] Disalvo E.A., Larion F., Martini F., Tymczyszyn E., Frias M., Almaleck H. and Gordillo G.J. (2008) Structural and functional properties of hydration and confined water in membrane interfaces, *Biochim. Biophys Acta*, 1778:2655-2670.
[93] Jendrasiak G.L., Smith R.L. and Shaw W. (1996) The water adsorption characteristics of charged phospholipids, *Biochim Biophys Acta*, 1279:63-9.
[94] Rasaiah J.C., Garde S. and Hummer G. (2008) Water in Nonpolar Confinement: From Nanotubes to Proteins and Beyond, *Annu. Rev. Phys. Chem.*, 59:713-40.
[95] Valeur B., *Molecular Fluorescence: Principles and Applications*, Wiley-VCH, 2001.
[96] Kirkwood J.G. (1939) The Dielectric Polarization of Polar Liquids, *J. Chem. Phys.*, 7:911-919.
[97] Gawrisch K., Ruston D., Zimmerberg J., Parsegian V.A., Rand R.P. and Fuller N. (1992) Membrane dipole potentials, hydration forces, and the ordering of water at membrane surfaces, *Biophys. J.*, 61:1213 – 1223.

[98] Brockman H. (1994) Dipole potential of lipid membranes, Chem. Phys. Lipids, 73:57-79.

[99] Smorodin V. and Melo E. (2001) Shape and Dimensions of Gel-Domains in Phospholipid Bilayers: A Theoretical Study, J. Phys. Chem. B, 105:6010–6016.

[100] Arrais D. and Martins J. (2007) Bilayer polarity and its thermal dependency in the ℓ_o and ℓ_d phases of binary phosphatidylcholine/cholesterol mixtures, *Biochim. Biophys. Acta*, 1768:2914-2922.

[101] Bublitz G.U. and Boxer S.G. (1998) Effective Polarity of Frozen Solvent Glasses in the Vicinity of Dipolar Solutes, *J. Am. Chem. Soc.*, 120:3988–3992.

[102] Wang P. and Anderko A., (2001) Computation of Dielectric Constants of Solvent Mixtures and Electrolyte Solutions, *Fluid Phase Equilibria*, 186:103-122.

[103] Lakowicz J.R., *Principles of Fluorescence Spectroscopy*, 3rd Ed., Springer, 2006.

[104] Vaz W.L.C. and Melo E. (2001) Fluorescence spectroscopic studies on phase heterogeneity in lipid bilayer membranes, *J. Fluorescence*, 11:255-271.

[105] Kamlet M.J, Abboud J.-L. and Taft R.W. (1977) The Solvatochromic Comparison Method. 6. The π^* Scale of Solvent Polarities, *J. Am. Chem. Soc.*, 99:6027-6038.

[106] Ham, J.S. (1953), A New Electronic State in Benzene, *J. Chem. Phys.*, 21:756-758.

[107] A. Nakajima (1971), Solvent effect on the vibrational structure of the fluorescence and absorption spectra of pyrene, *Bull. Chem. Soc. Jpn.*, 44:3272-3277.

[108] Kalyanasundaram K. and Thomas J.K. (1977) The Environmental Effects on Vibronic Band Intensities in Pyrene Monomer Fluorescence and their Application in Studies of Micellar Systems, *J. Am. Chem. Soc.*, 99:2039-2044.

[109] Dong D.C. and Winnik M.A. (1984) The Py scale of solvent polarities, *Can. J. Chem*., 62:2560-2665.

[110] Karpovich D.S. and Blanchard G.J (1995) Relating the Polarity-Dependent Fluorescence Response of Pyrene to Vibronic Coupling. Achieving a Fundamental Understanding of the Py Polarity Scale, *J. Phys. Chem.*, 99:3951-3958.

[111] Chen S. and McGuffin V.L. (1994) Temperature Effect on Pyrene as a Polarity probe for Supercritical Fluid and Liquid Solutions, *Appl. Spectr.*, 48:596-603.

[112] Lianos P., Mukhopadhyay K. and Georghiou S. (1980) Microenvironment of aromatic hydrocarbons employed as fluorescence probes of liposomes, *Photochem. Photobiol.*, 32:415-419.

[113] Street K.W. and Acree W.E. (1986) Experimental Artifacts and Determination of Accurate Py Values", *The Analyst*, 3:1197-1201.

[114] Arrais D., Manuel M. and J. Martins (2012) Can pyrene be localized inside lipid bilayers by simultaneously measuring Py values, and fulfilling the excimer formation conditions?, *Chemistry and Physics of Lipids*, 165:866-869.

[115] Sun Y., Ma B., Lawson G.E., Bunker C.E. and Rollins H.W. (1996) Effects of photochemical reactions of pyrene in alcohol and aqueous solvent systems on spectroscopic analysis, *Anal. Chim. Acta*, 319:379-386.

[116] Parasassi T., Krasnowska E. K., Bagatolli L. and Gratton E. (1998) Laurdan and Prodan as Polarity-Sensitive Fluorescent Membrane Probes, *J. Fluorescence*, 8:365-373.

[117] Krishna M. M. G. (1999) Excited-State Kinetics of the Hydrophobic Probe Nile Red in Membranes and Micelles, *J. Phys. Chem. A*, 103:3589–3595.
[118] Klymchenko A.S., Mély Y., Demchenko A.P. and Duportail G. (2004) Simultaneous probing of hydration and polarity of lipid bilayers with 3-hydroxyflavone fluorescent dyes, *Biochim. Biophys. Acta*, 1665: 6-19.
[119] Marsh D. (2010) Spin-Label EPR for Determining Polarity and Proticity in Biomolecular Assemblies: Transmembrane Profiles, *Appl. Magn. Reson.*, 37:435–454.
[120] Hoff B., Strandberg E., Ulrich A.S., Tieleman D.P. and Posten C. (2005) ^{2}H-NMR study and molecular dynamics simulation of the location, alignment, and mobility of pyrene in POPC bilayers, *Biophys. J.*, 88:1818-1827.
[121] Loura L.M.S., do Canto A.M.T. M. and Martins J. (2013) Sensing hydration and behavior of pyrene in POPC and POPC/cholesterol bilayers: A molecular dynamics study, *Biochim. Biophys. Acta*, 1828: 1094-1101.
[122] Birks J.B., *Photophysics of Aromatic Molecules*, Wiley-Interscience, London, 1970.
[123] Skoza Jr., F. and Papahadjopoulos D. (1980) Comparative properties and methods of preparation of lipid vesicles (liposomes), *Annu. Rev. Biophys. Bioeng.*, 9:467-508.
[124] Woodle M.C. and Papahadjopoulos D. (1989) Liposome preparation and size characterization, *Method Enzymol.*, 171:193-217.
[125] Thewalt J.L. and Bloom M. (1992) Phosphatidylcholine:cholesterol phase diagrams, *Biophys. J.*, 63:1176-1181.
[126] Quinn P.J. and Wolf C. (2009) The liquid-ordered phase in membranes, *Biochim. Biophys. Acta*, 1788:33-46.
[127] Chiu S.W., Jacobsson E. and Scott H.L. (2001) Combined Monte Carlo and Molecular Dynamics Simulation of Hydrated Lipid-Cholesterol Lipid Bilayers at Low Cholesterol Concentration, *Biophys. J.*, 80:1104-1114.
[128] Goñi F.M., Alonso A., Bagatolli L.A., Brown R.E., Marsh D., Prieto M. and Thewalt J.L. (2008) Phase diagrams of lipid mixtures relevant to the study of membrane rafts, *Biochim. Biophys. Acta*, 1781:665-684.
[129] Pandit S.A., Chiu S.W., Jakobsson E., Grama A. and Scott H.L. (2008) Cholesterol Packing around Lipids with Saturated and Unsaturated Chains: A Simulation Study, Langmuir, 24:6858-6865.
[130] Henriksen J., Rowat A.C., Brief E., Hsueh Y.W., Thewalt J.L., Zuckermann M.J. and Ipsen J.H. (2006) Universal behavior of membranes with sterols, *Biophys. J.*, 90:1639-1649.
[131] Ahmed S.N., Brown D.A. and London E. (1997) On the Origin of Sphingolipid/Cholesterol-Rich Detergent-Insoluble Cell Membranes: Physiological Concentrations of Cholesterol and Sphingolipid Induce Formation of a Detergente-Insoluble, Liquid-Ordered Lipid Phase in Model Membranes, *Biochemistry*, 36:10944-10953.
[132] Bunge A., Müller P., Stöck M., Herrmann A. and Huster D. (2008) Characterization of the Ternary Misture of Sphingomyelin, POPC and Cholesterol: Support for an Inhomogenous Lipid Distribution at High Temperatures, *Biophys. J.*, 94:2680-2690.
[133] Filippov A., Orädd G. and Lindblom G. (2003) The Effect of Cholesterol on the Lateral Diffusion of Phospholipids in Oriented Bilayers, *Biophys. J.*, 84:3079-3086.

[134] Warschawski D.E. and Devaux P.F. (2005) Order parameters of unsaturated phospholipids in membranes and the effect of cholesterol: a ^{1}H–^{13}C solid-state NMR study at natural abundance**,** ***Eur. Biophys. J.*****,** 34:987-996**.**

[135] Estep T.N., Mountcastle D.B., Barenholz Y., Biltonen R.L. and Thompson T.E. (1979) Thermal Behavior of Synthetic Sphingomyelin-Cholesterol Dispersions, *Biochemistry*, 18 2113-2117.

[136] Snyder B. and Freire E. (1980) Compositional domain structure in phosphatidylcholine-cholesterol and sphingomyelin-cholesterol bilayers, *PNAS*, 77:4055-4059.

[137] Raffy S. and Teissié J. (1999) Control of Lipid Membrane Stability by Cholesterol Content, *Biophys. J.*, 76:2072-2080.

[138] Le Goff G., Vitha M.F. and Clarke R.J. (2007) Orientational polarizability of lipid membrane surfaces, *Biochim. Biophys. Acta*, 1768:562-570.

[139] Tsamaloukas A., Szadkowska H. and Heerklotz H. (2006) Thermodynamic comparison of the interactions of cholesterol with unsaturated phospholipid and sphingomyelins, *Biophys. J.*, 90:4479-4487.

[140] Niemelä P., Hyvönen M.T. and Vaittulainen I. (2004) Structure and Dynamics of Sphingomyelin Bilayer: Insight Gained through Systematic Comparison to Phosphatidylcholine, *Biophys. J.*, 87:2976-2989.

[141] Janosi L. and Gorfe A. (2010) Importance of the Sphingosine Base Double-Bond Geometry for the Structural and Thermodynamic Properties of Sphingomyelin Bilayers, *Biophys. J.*, 99 :2957-2966.

[142] Mannock D.A., McIntosh T.J., Jiang X., Covey D.F. and McElhaney R.N. (2003) Effects of Natural and Enantiomeric Cholesterol on Thermotropic Phase Behavior and Structure of Egg-Sphingomyelin Bilayer Membranes, *Biophys. J.*, 84:1038-1046.

[143] Scaife B.K.P., *Principles of Dielectrics*, Clarendon Press, 1998.

[144] Nicolini C., Kraineva J., Khurana M., Periasamy N., Funari S.S. and Winter R. (2006) Temperature and pressure effects on structural and conformational properties of POPC/SM/Cholesterol model raft mixtures – a FT-IR, SAXS, DSC, PPC and Laurdan fluorescence spectroscopy study, *Biophys. Biochim. Acta*, 1758:248-258.

[145] Wolf C., Koumanov K., Tenchov B. and Quinn P.J. (2001) Cholesterol favors phase separation of sphingomyelin, *Biophys. Chem.*, 89:163-172.

[146] Wolf C. and Chachaty C. (2000) Compared effects of cholesterol and 7-dehydrocholesterol on sphingomyelin-glycerophospholipid bilayers studied by ESR, *Biophys. Chem*, 84:269-279.

APPENDIX

Equivalent polarity results (I_1/I_3 values)

Table I – Thermal variation of equivalent polarity values (I_1/I_3) for 1-palmitoyl-2-oleoyl-*sn*-glycero-3-phosphocholine (POPC)/Cholesterol (CHOL) mixtures with different chemical compositions (represented in terms of average ± standard deviation).

	POPC / CHOL (mol% / mol%)									
T **(ºC)**	**100/00**	**95/05**	**90/10**	**85/15**	**80/20**	**75/25**	**70/30**	**65/35**	**60/40**	**55/45**
15	1,20 ± 0,01	1,20 ± 0,01	1,20 ± 0,01	1,20 ± 0,01	1,19 ± 0,01	1,18 ± 0,01	1,18 ± 0,02	1,17 ± 0,01	1,15 ± 0,01	1,13 ± 0,01
17	1,19 ± 0,01	1,18 ± 0,01	1,20 ± 0,01	1,20 ± 0,01	1,19 ± 0,01	1,17 ± 0,01	1,17 ± 0,01	1,17 ± 0,01	1,14 ± 0,01	1,14 ± 0,02
19	1,19 ± 0,02	1,19 ± 0,01	1,18 ± 0,02	1,18 ± 0,01	1,18 ± 0,01	1,17 ± 0,01	1,17 ± 0,02	1,17 ± 0,01	1,14 ± 0,01	1,12 ± 0,01
21	1,19 ± 0,01	1,17 ± 0,01	1,18 ± 0,02	1,18 ± 0,01	1,17 ± 0,01	1,16 ± 0,01	1,17 ± 0,02	1,16 ± 0,01	1,13 ± 0,01	1,13 ± 0,01
23	1,18 ± 0,00	1,17 ± 0,01	1,17 ± 0,01	1,18 ± 0,01	1,16 ± 0,01	1,15 ± 0,01	1,16 ± 0,01	1,16 ± 0,01	1,12 ± 0,01	1,11 ± 0,01
25	1,17 ± 0,01	1,17 ± 0,01	1,17 ± 0,02	1,16 ± 0,01	1,17 ± 0,01	1,15 ± 0,01	1,16 ± 0,01	1,16 ± 0,01	1,13 ± 0,01	1,11 ± 0,02
27	1,16 ± 0,01	1,17 ± 0,01	1,16 ± 0,02	1,16 ± 0,01	1,16 ± 0,01	1,14 ± 0,01	1,15 ± 0,01	1,15 ± 0,01	1,13 ± 0,01	1,12 ± 0,01
29	1,17 ± 0,01	1,16 ± 0,01	1,15 ± 0,02	1,17 ± 0,02	1,16 ± 0,01	1,14 ± 0,01	1,15 ± 0,01	1,14 ± 0,00	1,12 ± 0,01	1,11 ± 0,02
31	1,16 ± 0,01	1,16 ± 0,02	1,16 ± 0,01	1,15 ± 0,01	1,16 ± 0,01	1,14 ± 0,01	1,14 ± 0,02	1,14 ± 0,01	1,10 ± 0,01	1,10 ± 0,01
33	1,16 ± 0,01	1,16 ± 0,01	1,14 ± 0,02	1,15 ± 0,01	1,15 ± 0,01	1,13 ± 0,01	1,14 ± 0,01	1,14 ± 0,01	1,09 ± 0,01	1,09 ± 0,01
35	1,17 ± 0,02	1,16 ± 0,01	1,15 ± 0,01	1,15 ± 0,01	1,15 ± 0,01	1,13 ± 0,00	1,13 ± 0,01	1,14 ± 0,01	1,10 ± 0,01	1,09 ± 0,01
37	1,15 ± 0,01	1,14 ± 0,01	1,15 ± 0,02	1,15 ± 0,01	1,14 ± 0,02	1,13 ± 0,01	1,14 ± 0,01	1,13 ± 0,00	1,10 ± 0,02	1,08 ± 0,02
39	1,15 ± 0,01	1,14 ± 0,01	1,13 ± 0,02	1,15 ± 0,01	1,13 ± 0,01	1,12 ± 0,01	1,13 ± 0,01	1,13 ± 0,01	1,09 ± 0,02	1,09 ± 0,01
41	1,13 ± 0,01	1,13 ± 0,01	1,14 ± 0,01	1,14 ± 0,01	1,14 ± 0,01	1,12 ± 0,01	1,12 ± 0,01	1,13 ± 0,01	1,07 ± 0,01	1,09 ± 0,01
43	1,14 ± 0,01	1,13 ± 0,01	1,13 ± 0,01	1,13 ± 0,01	1,13 ± 0,01	1,11 ± 0,01	1,12 ± 0,01	1,12 ± 0,01	1,08 ± 0,02	1,09 ± 0,01
45	1,14 ± 0,01	1,12 ± 0,01	1,13 ± 0,01	1,13 ± 0,01	1,11 ± 0,01	1,10 ± 0,02	1,12 ± 0,01	1,12 ± 0,01	1,07 ± 0,01	1,09 ± 0,01

Table II – Thermal variation of equivalent polarity values (I_1/I_3) for 1-palmitoyl-2-oleoyl-*sn*-glycero-3-phosphocholine (POPC)/egg-Sphingomyelin (egg-SM) mixtures with different chemical compositions (represented in terms of average ± standard deviation).

	POPC / egg-SM (mol% / mol%)						
T **(ºC)**	**100/00**	**95/05**	**80/20**	**65/35**	**60/40**	**55/45**	**50/50**
15	1,20 ± 0,01	1,22 ± 0,01	1,22 ± 0,01	1,21 ± 0,01	1,20 ± 0,01	1,20 ± 0,01	1,20 ± 0,01
17	1,19 ± 0,01	1,22 ± 0,01	1,21 ± 0,01	1,20 ± 0,01	1,19 ± 0,02	1,19 ± 0,01	1,19 ± 0,02
19	1,19 ± 0,02	1,20 ± 0,02	1,21 ± 0,01	1,19 ± 0,02	1,18 ± 0,02	1,18 ± 0,01	1,19 ± 0,02
21	1,19 ± 0,01	1,20 ± 0,02	1,20 ± 0,01	1,19 ± 0,01	1,18 ± 0,02	1,17 ± 0,01	1,18 ± 0,02
23	1,18 ± 0,00	1,19 ± 0,01	1,20 ± 0,01	1,19 ± 0,01	1,17 ± 0,01	1,17 ± 0,01	1,17 ± 0,02
25	1,17 ± 0,01	1,18 ± 0,02	1,19 ± 0,00	1,17 ± 0,01	1,16 ± 0,02	1,17 ± 0,01	1,17 ± 0,01
27	1,16 ± 0,01	1,17 ± 0,02	1,19 ± 0,01	1,17 ± 0,01	1,16 ± 0,02	1,17 ± 0,01	1,17 ± 0,02
29	1,17 ± 0,01	1,17 ± 0,01	1,18 ± 0,01	1,16 ± 0,01	1,16 ± 0,01	1,17 ± 0,01	1,16 ± 0,02
31	1,16 ± 0,01	1,17 ± 0,01	1,17 ± 0,01	1,16 ± 0,02	1,16 ± 0,02	1,16 ± 0,01	1,16 ± 0,02
33	1,16 ± 0,01	1,16 ± 0,02	1,17 ± 0,01	1,15 ± 0,01	1,15 ± 0,01	1,16 ± 0,01	1,15 ± 0,02
35	1,17 ± 0,02	1,16 ± 0,01	1,17 ± 0,01	1,16 ± 0,01	1,14 ± 0,01	1,15 ± 0,01	1,15 ± 0,02
37	1,15 ± 0,01	1,15 ± 0,01	1,17 ± 0,01	1,14 ± 0,01	1,14 ± 0,01	1,16 ± 0,01	1,14 ± 0,01
39	1,15 ± 0,01	1,14 ± 0,01	1,16 ± 0,01	1,14 ± 0,01	1,13 ± 0,00	1,14 ± 0,01	1,14 ± 0,02
41	1,13 ± 0,01	1,14 ± 0,01	1,15 ± 0,01	1,13 ± 0,01	1,13 ± 0,01	1,15 ± 0,01	1,14 ± 0,02
43	1,14 ± 0,01	1,14 ± 0,01	1,15 ± 0,01	1,13 ± 0,01	1,13 ± 0,01	1,14 ± 0,01	1,13 ± 0,01
45	1,14 ± 0,01	1,13 ± 0,01	1,14 ± 0,01	1,13 ± 0,01	1,13 ± 0,01	1,14 ± 0,01	1,14 ± 0,02
47	1,14 ± 0,01	1,12 ± 0,01	1,13 ± 0,01	1,12 ± 0,02	1,13 ± 0,01	1,13 ± 0,01	1,14 ± 0,02
49	1,14 ± 0,01	1,13 ± 0,01	1,13 ± 0,01	1,12 ± 0,02	1,12 ± 0,01	1,14 ± 0,01	1,12 ± 0,01
51	1,14 ± 0,01	1,13 ± 0,01	1,13 ± 0,01	1,12 ± 0,02	1,13 ± 0,01	1,13 ± 0,02	1,12 ± 0,02
53	1,14 ± 0,01	1,13 ± 0,01	1,12 ± 0,01	1,11 ± 0,02	1,11 ± 0,01	1,13 ± 0,02	1,12 ± 0,02
55	1,13 ± 0,01	1,11 ± 0,00	1,12 ± 0,01	1,10 ± 0,02	1,12 ± 0,01	1,13 ± 0,01	1,11 ± 0,02

Table III – Thermal variation of equivalent polarity values (I_1/I_3) for 1,2-dioleoyl-*sn*-glycero-3-phosphocholine (DOPC)/Cholesterol (CHOL) mixtures with different chemical compositions (represented in terms of average ± standard deviation).

	DOPC / CHOL (mol% / mol%)									
***T* (ºC)**	**100/00**	**95/05**	**90/10**	**85/15**	**80/20**	**75/25**	**70/30**	**65/35**	**60/40**	**55/45**
15	1,25 ± 0,01	1,26 ± 0,01	1,25 ± 0,01	1,24 ± 0,02	1,19 ± 0,01	1,20 ± 0,02	1,19 ± 0,02	1,21 ± 0,01	1,18 ± 0,01	1,19 ± 0,02
17	1,24 ± 0,01	1,25 ± 0,01	1,24 ± 0,01	1,23 ± 0,02	1,18 ± 0,01	1,20 ± 0,01	1,19 ± 0,01	1,19 ± 0,01	1,18 ± 0,01	1,18 ± 0,02
19	1,22 ± 0,01	1,24 ± 0,01	1,24 ± 0,02	1,23 ± 0,02	1,18 ± 0,01	1,19 ± 0,02	1,18 ± 0,01	1,20 ± 0,01	1,17 ± 0,02	1,17 ± 0,01
21	1,21 ± 0,01	1,24 ± 0,01	1,23 ± 0,01	1,22 ± 0,01	1,18 ± 0,01	1,18 ± 0,01	1,18 ± 0,01	1,19 ± 0,01	1,16 ± 0,01	1,16 ± 0,02
23	1,22 ± 0,01	1,23 ± 0,02	1,23 ± 0,00	1,22 ± 0,02	1,17 ± 0,01	1,18 ± 0,01	1,18 ± 0,01	1,18 ± 0,01	1,17 ± 0,01	1,17 ± 0,02
25	1,21 ± 0,01	1,23 ± 0,01	1,22 ± 0,01	1,21 ± 0,02	1,17 ± 0,01	1,18 ± 0,02	1,17 ± 0,01	1,18 ± 0,01	1,16 ± 0,02	1,17 ± 0,02
27	1,20 ± 0,02	1,22 ± 0,01	1,21 ± 0,02	1,20 ± 0,02	1,17 ± 0,01	1,18 ± 0,01	1,17 ± 0,01	1,18 ± 0,01	1,16 ± 0,01	1,16 ± 0,02
29	1,19 ± 0,02	1,20 ± 0,01	1,20 ± 0,02	1,20 ± 0,02	1,16 ± 0,01	1,18 ± 0,01	1,17 ± 0,01	1,17 ± 0,01	1,15 ± 0,01	1,15 ± 0,02
31	1,18 ± 0,01	1,20 ± 0,01	1,19 ± 0,02	1,19 ± 0,01	1,15 ± 0,01	1,17 ± 0,01	1,17 ± 0,01	1,17 ± 0,01	1,14 ± 0,02	1,14 ± 0,02
33	1,18 ± 0,01	1,18 ± 0,02	1,18 ± 0,02	1,19 ± 0,01	1,15 ± 0,01	1,16 ± 0,01	1,16 ± 0,01	1,16 ± 0,01	1,14 ± 0,02	1,14 ± 0,02
35	1,18 ± 0,01	1,18 ± 0,02	1,18 ± 0,01	1,18 ± 0,01	1,15 ± 0,01	1,16 ± 0,01	1,15 ± 0,01	1,16 ± 0,01	1,13 ± 0,01	1,14 ± 0,02
37	1,17 ± 0,01	1,17 ± 0,01	1,17 ± 0,01	1,18 ± 0,01	1,15 ± 0,01	1,15 ± 0,01	1,14 ± 0,01	1,15 ± 0,01	1,13 ± 0,01	1,13 ± 0,02
39	1,17 ± 0,01	1,17 ± 0,01	1,17 ± 0,01	1,18 ± 0,01	1,15 ± 0,01	1,15 ± 0,01	1,14 ± 0,01	1,15 ± 0,01	1,12 ± 0,01	1,12 ± 0,02
41	1,17 ± 0,01	1,17 ± 0,01	1,17 ± 0,01	1,17 ± 0,01	1,14 ± 0,01	1,15 ± 0,01	1,14 ± 0,02	1,15 ± 0,01	1,12 ± 0,01	1,12 ± 0,02
43	1,17 ± 0,01	1,16 ± 0,02	1,17 ± 0,02	1,17 ± 0,01	1,14 ± 0,02	1,15 ± 0,01	1,14 ± 0,01	1,14 ± 0,01	1,12 ± 0,02	1,11 ± 0,01
45	1,15 ± 0,01	1,15 ± 0,01	1,16 ± 0,01	1,16 ± 0,01	1,14 ± 0,02	1,15 ± 0,01	1,13 ± 0,01	1,13 ± 0,01	1,12 ± 0,02	1,10 ± 0,01

Table IV – Thermal variation of equivalent polarity values (I_1/I_3) for 1,2-dioleoyl-*sn*-glycero-3-phosphocholine (DOPC)/egg-SM mixtures with different chemical compositions (represented in terms of average ± standard deviation).

	DOPC / egg-SM (mol% / mol%)						
T **(ºC)**	**100/00**	**95/05**	**80/20**	**65/35**	**60/40**	**55/45**	**50/50**
15	1,25 ± 0,01	1,23 ± 0,01	1,22 ± 0,02	1,18 ± 0,02	1,18 ± 0,01	1,18 ± 0,02	1,18 ± 0,01
17	1,24 ± 0,01	1,21 ± 0,01	1,21 ± 0,01	1,18 ± 0,01	1,17 ± 0,01	1,17 ± 0,01	1,18 ± 0,01
19	1,22 ± 0,01	1,21 ± 0,01	1,22 ± 0,01	1,17 ± 0,02	1,16 ± 0,01	1,16 ± 0,01	1,17 ± 0,02
21	1,21 ± 0,01	1,20 ± 0,01	1,20 ± 0,01	1,16 ± 0,02	1,15 ± 0,01	1,16 ± 0,01	1,17 ± 0,02
23	1,22 ± 0,01	1,21 ± 0,02	1,21 ± 0,01	1,16 ± 0,02	1,15 ± 0,01	1,16 ± 0,01	1,15 ± 0,01
25	1,21 ± 0,01	1,20 ± 0,02	1,20 ± 0,01	1,16 ± 0,02	1,16 ± 0,02	1,15 ± 0,01	1,15 ± 0,02
27	1,20 ± 0,02	1,19 ± 0,02	1,18 ± 0,02	1,16 ± 0,01	1,14 ± 0,01	1,14 ± 0,02	1,15 ± 0,02
29	1,19 ± 0,02	1,19 ± 0,01	1,16 ± 0,02	1,14 ± 0,01	1,15 ± 0,01	1,14 ± 0,01	1,15 ± 0,01
31	1,18 ± 0,01	1,18 ± 0,02	1,16 ± 0,01	1,16 ± 0,01	1,15 ± 0,02	1,14 ± 0,01	1,15 ± 0,01
33	1,18 ± 0,01	1,17 ± 0,01	1,17 ± 0,01	1,16 ± 0,01	1,14 ± 0,01	1,13 ± 0,01	1,12 ± 0,01
35	1,18 ± 0,01	1,18 ± 0,01	1,17 ± 0,01	1,15 ± 0,02	1,14 ± 0,01	1,14 ± 0,01	1,13 ± 0,01
37	1,17 ± 0,01	1,17 ± 0,01	1,17 ± 0,02	1,13 ± 0,01	1,13 ± 0,01	1,13 ± 0,02	1,13 ± 0,01
39	1,17 ± 0,01	1,17 ± 0,01	1,15 ± 0,02	1,13 ± 0,01	1,13 ± 0,01	1,12 ± 0,01	1,12 ± 0,01
41	1,17 ± 0,01	1,17 ± 0,01	1,15 ± 0,02	1,11 ± 0,01	1,12 ± 0,01	1,12 ± 0,02	1,11 ± 0,01
43	1,17 ± 0,01	1,15 ± 0,02	1,15 ± 0,02	1,13 ± 0,01	1,12 ± 0,01	1,12 ± 0,01	1,11 ± 0,01
45	1,15 ± 0,01	1,14 ± 0,01	1,14 ± 0,02	1,11 ± 0,00	1,12 ± 0,01	1,12 ± 0,02	1,11 ± 0,01
47	1,16 ± 0,02	1,15 ± 0,02	1,14 ± 0,01	1,12 ± 0,01	1,11 ± 0,01	1,11 ± 0,01	1,12 ± 0,02
49	1,15 ± 0,02	1,15 ± 0,01	1,14 ± 0,02	1,11 ± 0,01	1,10 ± 0,01	1,11 ± 0,01	1,11 ± 0,01
51	1,15 ± 0,01	1,15 ± 0,02	1,14 ± 0,02	1,11 ± 0,01	1,11 ± 0,01	1,12 ± 0,01	1,11 ± 0,01
53	1,14 ± 0,01	1,14 ± 0,02	1,15 ± 0,01	1,11 ± 0,02	1,11 ± 0,01	1,11 ± 0,01	1,09 ± 0,01
55	1,14 ± 0,01	1,14 ± 0,02	1,15 ± 0,01	1,10 ± 0,01	1,10 ± 0,02	1,11 ± 0,01	1,10 ± 0,01

Table V – Thermal variation of equivalent polarity values (I_1/I_3) for 1,2-dipalmitoyl-*sn*-glycero-3-phosphocholine (DPPC)/ 1,2-dimyristoyl-*sn*-glycero-3-phosphocholine (DMPC) mixtures with different chemical compositions (represented in terms of average ± standard deviation).

	DPPC/DMPC (mol% / mol%)				
***T* (ºC)**	**100/00**	**75/25**	**50/50**	**25/75**	**00/100**
15	1,31 ± 0,01	1,29 ± 0,02	1,28 ± 0,01	1,25 ± 0,01	1,24 ± 0,01
17	1,31 ± 0,02	1,29 ± 0,02	1,26 ± 0,01	1,24 ± 0,01	1,23 ± 0,01
19	1,31 ± 0,02	1,28 ± 0,02	1,24 ± 0,02	1,24 ± 0,01	1,22 ± 0,01
21	1,31 ± 0,01	1,25 ± 0,02	1,20 ± 0,02	1,21 ± 0,02	1,21 ± 0,01
23	1,30 ± 0,02	1,26 ± 0,03	1,21 ± 0,01	1,18 ± 0,01	1,19 ± 0,01
25	1,30 ± 0,02	1,24 ± 0,02	1,19 ± 0,02	1,17 ± 0,02	1,17 ± 0,01
27	1,30 ± 0,02	1,22 ± 0,02	1,19 ± 0,01	1,16 ± 0,02	1,15 ± 0,02
29	1,28 ± 0,03	1,20 ± 0,01	1,17 ± 0,02	1,14 ± 0,01	1,14 ± 0,01
31	1,28 ± 0,03	1,18 ± 0,02	1,16 ± 0,02	1,13 ± 0,02	1,15 ± 0,01
33	1,22 ± 0,04	1,17 ± 0,02	1,13 ± 0,01	1,12 ± 0,01	1,13 ± 0,01
35	1,23 ± 0,02	1,16 ± 0,02	1,13 ± 0,01	1,12 ± 0,01	1,15 ± 0,01
37	1,17 ± 0,01	1,14 ± 0,02	1,13 ± 0,01	1,13 ± 0,01	1,15 ± 0,02
39	1,17 ± 0,01	1,12 ± 0,01	1,12 ± 0,01	1,13 ± 0,01	1,12 ± 0,02
41	1,15 ± 0,01	1,14 ± 0,01	1,11 ± 0,01	1,12 ± 0,01	1,12 ± 0,02
43	1,12 ± 0,01	1,13 ± 0,03	1,11 ± 0,01	1,11 ± 0,01	1,12 ± 0,01
45	1,11 ± 0,01	1,13 ± 0,02	1,11 ± 0,01	1,12 ± 0,01	1,12 ± 0,01
47	1,11 ± 0,02	1,13 ± 0,02	1,11 ± 0,00	1,12 ± 0,01	1,12 ± 0,02
49	1,11 ± 0,01	1,12 ± 0,01	1,10 ± 0,02	1,12 ± 0,01	1,13 ± 0,01
51	1,12 ± 0,01	1,12 ± 0,00	1,11 ± 0,01	1,12 ± 0,01	1,13 ± 0,01

Table VI – Thermal variation of equivalent polarity values (I_1/I_3) for 1,2-dipalmitoyl-*sn*-glycero-3-phosphocholine (DPPC)/Cholesterol (CHOL) mixtures with different chemical compositions (represented in terms of average ± standard deviation).

	DPPC / CHOL (mol% / mol%)									
T **(ºC)**	**100/00**	**95/05**	**90/10**	**85/15**	**80/20**	**75/25**	**70/30**	**65/35**	**60/40**	**55/45**
25	1,30 ± 0,02	1,16 ± 0,02	1,17 ± 0,01	1,15 ± 0,02	1,14 ± 0,04	1,14 ± 0,02	1,12 ± 0,02	1,10 ± 0,01	1,09 ± 0,03	1,10 ± 0,01
27	1,30 ± 0,02	1,17 ± 0,02	1,17 ± 0,01	1,14 ± 0,02	1,13 ± 0,02	1,14 ± 0,01	1,12 ± 0,03	1,10 ± 0,01	1,09 ± 0,02	1,10 ± 0,02
29	1,28 ± 0,03	1,16 ± 0,01	1,16 ± 0,02	1,13 ± 0,02	1,12 ± 0,03	1,12 ± 0,01	1,12 ± 0,04	1,09 ± 0,01	1,10 ± 0,02	1,10 ± 0,02
31	1,28 ± 0,03	1,16 ± 0,02	1,16 ± 0,01	1,13 ± 0,03	1,11 ± 0,03	1,11 ± 0,01	1,12 ± 0,02	1,10 ± 0,01	1,11 ± 0,02	1,11 ± 0,01
33	1,22 ± 0,04	1,14 ± 0,02	1,15 ± 0,02	1,13 ± 0,03	1,11 ± 0,02	1,10 ± 0,02	1,12 ± 0,03	1,09 ± 0,01	1,10 ± 0,02	1,10 ± 0,02
35	1,23 ± 0,02	1,14 ± 0,01	1,14 ± 0,02	1,11 ± 0,04	1,10 ± 0,01	1,09 ± 0,02	1,11 ± 0,02	1,08 ± 0,01	1,11 ± 0,02	1,10 ± 0,02
37	1,17 ± 0,01	1,14 ± 0,01	1,13 ± 0,01	1,12 ± 0,04	1,10 ± 0,03	1,08 ± 0,01	1,10 ± 0,03	1,08 ± 0,02	1,10 ± 0,02	1,11 ± 0,01
39	1,17 ± 0,01	1,13 ± 0,02	1,13 ± 0,02	1,11 ± 0,03	1,10 ± 0,03	1,08 ± 0,02	1,09 ± 0,03	1,07 ± 0,01	1,10 ± 0,03	1,11 ± 0,03
41	1,15 ± 0,01	1,12 ± 0,03	1,12 ± 0,01	1,10 ± 0,03	1,10 ± 0,02	1,08 ± 0,02	1,11 ± 0,02	1,06 ± 0,01	1,11 ± 0,02	1,10 ± 0,02
43	1,12 ± 0,01	1,11 ± 0,02	1,10 ± 0,02	1,09 ± 0,03	1,10 ± 0,02	1,09 ± 0,02	1,10 ± 0,01	1,06 ± 0,01	1,10 ± 0,03	1,10 ± 0,02
45	1,11 ± 0,01	1,11 ± 0,02	1,10 ± 0,02	1,09 ± 0,03	1,08 ± 0,02	1,08 ± 0,03	1,08 ± 0,02	1,05 ± 0,01	1,10 ± 0,03	1,11 ± 0,02
47	1,11 ± 0,02	1,09 ± 0,01	1,10 ± 0,02	1,08 ± 0,03	1,08 ± 0,02	1,08 ± 0,02	1,08 ± 0,02	1,05 ± 0,00	1,11 ± 0,02	1,09 ± 0,02
49	1,11 ± 0,01	1,10 ± 0,01	1,09 ± 0,02	1,09 ± 0,03	1,08 ± 0,03	1,08 ± 0,02	1,10 ± 0,03	1,05 ± 0,01	1,11 ± 0,02	1,10 ± 0,03
51	1,12 ± 0,01	1,09 ± 0,01	1,10 ± 0,02	1,08 ± 0,03	1,09 ± 0,03	1,09 ± 0,01	1,10 ± 0,02	1,05 ± 0,02	1,10 ± 0,03	1,10 ± 0,02
53	1,11 ± 0,02	1,09 ± 0,03	1,10 ± 0,02	1,08 ± 0,04	1,08 ± 0,03	1,08 ± 0,02	1,08 ± 0,01	1,05 ± 0,02	1,10 ± 0,03	1,10 ± 0,02
55	1,10 ± 0,02	1,09 ± 0,01	1,09 ± 0,02	1,08 ± 0,04	1,07 ± 0,03	1,08 ± 0,01	1,08 ± 0,01	1,04 ± 0,02	1,10 ± 0,03	1,09 ± 0,02

Table VII – Thermal variation of equivalent polarity values (I_1/I_3) for egg-Sphingomyelin (egg-SM)/Cholesterol (CHOL) mixtures with different chemical compositions (represented in terms of average ± standard deviation).

	egg-SM / CHOL (mol% / mol%)									
T **(ºC)**	**100/00**	**95/05**	**90/10**	**85/15**	**80/20**	**75/25**	**70/30**	**65/35**	**60/40**	**55/45**
25	1,18 ± 0,01	1,12 ± 0,01	1,13 ± 0,01	1,12 ± 0,01	1,11 ± 0,02	1,12 ± 0,02	1,11 ± 0,01	1,11 ± 0,03	1,11 ± 0,02	1,11 ± 0,02
27	1,17 ± 0,01	1,12 ± 0,01	1,13 ± 0,01	1,12 ± 0,01	1,11 ± 0,01	1,12 ± 0,01	1,12 ± 0,01	1,11 ± 0,02	1,11 ± 0,02	1,12 ± 0,03
29	1,15 ± 0,01	1,11 ± 0,01	1,12 ± 0,01	1,11 ± 0,01	1,11 ± 0,01	1,11 ± 0,02	1,10 ± 0,01	1,11 ± 0,03	1,11 ± 0,01	1,13 ± 0,02
31	1,15 ± 0,01	1,11 ± 0,02	1,11 ± 0,01	1,11 ± 0,01	1,10 ± 0,01	1,10 ± 0,02	1,11 ± 0,01	1,10 ± 0,03	1,11 ± 0,02	1,14 ± 0,01
33	1,15 ± 0,01	1,10 ± 0,02	1,11 ± 0,01	1,10 ± 0,02	1,09 ± 0,01	1,10 ± 0,01	1,10 ± 0,02	1,08 ± 0,03	1,12 ± 0,02	1,15 ± 0,01
35	1,15 ± 0,01	1,09 ± 0,02	1,11 ± 0,01	1,09 ± 0,02	1,09 ± 0,02	1,09 ± 0,01	1,11 ± 0,01	1,10 ± 0,02	1,12 ± 0,02	1,15 ± 0,01
37	1,15 ± 0,01	1,09 ± 0,02	1,10 ± 0,01	1,08 ± 0,01	1,08 ± 0,01	1,09 ± 0,01	1,10 ± 0,01	1,10 ± 0,02	1,12 ± 0,01	1,16 ± 0,02
39	1,13 ± 0,02	1,07 ± 0,02	1,08 ± 0,02	1,08 ± 0,01	1,07 ± 0,01	1,09 ± 0,02	1,10 ± 0,01	1,10 ± 0,02	1,13 ± 0,01	1,17 ± 0,01
41	1,09 ± 0,01	1,07 ± 0,01	1,09 ± 0,02	1,08 ± 0,02	1,07 ± 0,01	1,07 ± 0,01	1,09 ± 0,02	1,10 ± 0,01	1,10 ± 0,01	1,17 ± 0,01
43	1,08 ± 0,01	1,07 ± 0,01	1,08 ± 0,01	1,07 ± 0,01	1,07 ± 0,01	1,08 ± 0,02	1,09 ± 0,02	1,09 ± 0,02	1,11 ± 0,01	1,18 ± 0,01
45	1,08 ± 0,01	1,06 ± 0,00	1,08 ± 0,01	1,07 ± 0,01	1,06 ± 0,01	1,07 ± 0,02	1,09 ± 0,02	1,10 ± 0,01	1,13 ± 0,01	1,18 ± 0,01
47	1,07 ± 0,01	1,05 ± 0,01	1,08 ± 0,01	1,06 ± 0,01	1,07 ± 0,01	1,08 ± 0,02	1,07 ± 0,02	1,11 ± 0,01	1,13 ± 0,01	1,18 ± 0,01
49	1,06 ± 0,01	1,06 ± 0,01	1,07 ± 0,01	1,07 ± 0,01	1,06 ± 0,01	1,07 ± 0,02	1,08 ± 0,01	1,10 ± 0,02	1,12 ± 0,01	1,18 ± 0,01
51	1,07 ± 0,01	1,05 ± 0,01	1,06 ± 0,01	1,06 ± 0,01	1,06 ± 0,01	1,07 ± 0,02	1,08 ± 0,02	1,09 ± 0,01	1,12 ± 0,01	1,19 ± 0,01
53	1,06 ± 0,01	1,05 ± 0,01	1,07 ± 0,01	1,06 ± 0,01	1,06 ± 0,01	1,07 ± 0,02	1,07 ± 0,01	1,09 ± 0,02	1,12 ± 0,02	1,19 ± 0,02
55	1,06 ± 0,01	1,05 ± 0,02	1,06 ± 0,01	1,05 ± 0,01	1,05 ± 0,02	1,06 ± 0,02	1,08 ± 0,01	1,10 ± 0,01	1,13 ± 0,01	1,19 ± 0,01

Table VIII – Thermal variation of equivalent polarity values (I_1/I_3) for egg-Sphingomyelin (egg-SM)/ 1-palmitoyl-2-oleoyl-*sn*-glycero-3-phosphocholine (POPC) mixtures with different chemical compositions (represented in terms of average ± standard deviation).

	egg-SM/POPC (mol% / mol%)						
T **(ºC)**	**100/00**	**95/05**	**80/20**	**65/35**	**60/40**	**55/45**	**50/50**
15	-	1,21 ± 0,01	1,23 ± 0,01	1,21 ± 0,01	1,20 ± 0,01	1,20 ± 0,01	1,20 ± 0,01
17	-	1,21 ± 0,01	1,22 ± 0,01	1,20 ± 0,01	1,19 ± 0,02	1,20 ± 0,01	1,19 ± 0,02
19	-	1,19 ± 0,01	1,21 ± 0,01	1,19 ± 0,01	1,19 ± 0,01	1,19 ± 0,01	1,19 ± 0,02
21	-	1,18 ± 0,02	1,20 ± 0,01	1,18 ± 0,01	1,18 ± 0,01	1,18 ± 0,01	1,18 ± 0,02
23	-	1,17 ± 0,02	1,19 ± 0,01	1,17 ± 0,01	1,18 ± 0,02	1,17 ± 0,01	1,17 ± 0,02
25	1,18 ± 0,01	1,16 ± 0,02	1,18 ± 0,01	1,15 ± 0,00	1,17 ± 0,01	1,16 ± 0,01	1,17 ± 0,01
27	1,17 ± 0,01	1,15 ± 0,02	1,17 ± 0,01	1,15 ± 0,01	1,16 ± 0,01	1,16 ± 0,01	1,17 ± 0,02
29	1,15 ± 0,01	1,14 ± 0,02	1,16 ± 0,01	1,14 ± 0,01	1,16 ± 0,01	1,16 ± 0,01	1,16 ± 0,02
31	1,15 ± 0,01	1,13 ± 0,02	1,14 ± 0,02	1,13 ± 0,01	1,15 ± 0,01	1,15 ± 0,01	1,16 ± 0,02
33	1,15 ± 0,01	1,11 ± 0,02	1,14 ± 0,01	1,12 ± 0,01	1,14 ± 0,02	1,15 ± 0,01	1,15 ± 0,02
35	1,15 ± 0,01	1,10 ± 0,02	1,13 ± 0,01	1,12 ± 0,01	1,15 ± 0,01	1,15 ± 0,01	1,15 ± 0,02
37	1,15 ± 0,01	1,10 ± 0,01	1,13 ± 0,01	1,12 ± 0,01	1,14 ± 0,01	1,15 ± 0,01	1,14 ± 0,01
39	1,13 ± 0,02	1,09 ± 0,01	1,13 ± 0,02	1,12 ± 0,02	1,14 ± 0,01	1,15 ± 0,01	1,14 ± 0,02
41	1,09 ± 0,01	1,09 ± 0,02	1,12 ± 0,01	1,11 ± 0,02	1,14 ± 0,01	1,14 ± 0,01	1,14 ± 0,02
43	1,08 ± 0,01	1,08 ± 0,01	1,12 ± 0,01	1,11 ± 0,02	1,13 ± 0,00	1,13 ± 0,01	1,13 ± 0,01
45	1,08 ± 0,01	1,09 ± 0,01	1,12 ± 0,02	1,10 ± 0,02	1,12 ± 0,00	1,14 ± 0,01	1,14 ± 0,02
47	1,07 ± 0,01	1,08 ± 0,01	1,12 ± 0,01	1,10 ± 0,02	1,12 ± 0,00	1,13 ± 0,01	1,14 ± 0,02
49	1,06 ± 0,01	1,08 ± 0,01	1,11 ± 0,02	1,09 ± 0,02	1,13 ± 0,01	1,13 ± 0,01	1,12 ± 0,01
51	1,07 ± 0,01	1,08 ± 0,01	1,12 ± 0,01	1,09 ± 0,02	1,12 ± 0,01	1,12 ± 0,01	1,12 ± 0,02
53	1,06 ± 0,01	1,08 ± 0,01	1,11 ± 0,02	1,08 ± 0,01	1,12 ± 0,01	1,12 ± 0,00	1,12 ± 0,02
55	1,06 ± 0,01	1,08 ± 0,01	1,12 ± 0,01	1,08 ± 0,02	1,11 ± 0,01	1,12 ± 0,01	1,11 ± 0,02

Table IX – Thermal variation of equivalent polarity values (I_1/I_3) for egg-Sphingomyelin (egg-SM)/ 1,2-dioleoyl-*sn*-glycero-3-phosphocholine (DOPC) mixtures with different chemical compositions (represented in terms of average ± standard deviation).

	egg-SM / DOPC (mol% / mol%)						
T **(ºC)**	**100/00**	**95/05**	**80/20**	**65/35**	**60/40**	**55/45**	**50/50**
15	-	1,18 ± 0,01	1,19 ± 0,01	1,17 ± 0,01	1,18 ± 0,02	1,18 ± 0,02	1,18 ± 0,01
17	-	1,18 ± 0,01	1,18 ± 0,01	1,18 ± 0,01	1,18 ± 0,01	1,17 ± 0,01	1,18 ± 0,01
19	-	1,18 ± 0,01	1,16 ± 0,01	1,17 ± 0,02	1,17 ± 0,02	1,17 ± 0,01	1,17 ± 0,02
21	-	1,17 ± 0,01	1,17 ± 0,02	1,17 ± 0,02	1,17 ± 0,02	1,16 ± 0,01	1,17 ± 0,02
23	-	1,14 ± 0,01	1,16 ± 0,01	1,16 ± 0,02	1,15 ± 0,02	1,15 ± 0,01	1,15 ± 0,01
25	1,18 ± 0,01	1,16 ± 0,01	1,15 ± 0,02	1,15 ± 0,01	1,15 ± 0,01	1,14 ± 0,01	1,15 ± 0,02
27	1,17 ± 0,01	1,15 ± 0,01	1,13 ± 0,01	1,14 ± 0,01	1,13 ± 0,01	1,14 ± 0,02	1,15 ± 0,02
29	1,15 ± 0,01	1,13 ± 0,01	1,14 ± 0,02	1,13 ± 0,01	1,12 ± 0,01	1,13 ± 0,01	1,15 ± 0,01
31	1,15 ± 0,01	1,13 ± 0,01	1,12 ± 0,00	1,13 ± 0,01	1,14 ± 0,02	1,13 ± 0,01	1,15 ± 0,01
33	1,15 ± 0,01	1,11 ± 0,01	1,11 ± 0,01	1,12 ± 0,01	1,13 ± 0,01	1,13 ± 0,02	1,12 ± 0,01
35	1,15 ± 0,01	1,09 ± 0,02	1,09 ± 0,01	1,13 ± 0,01	1,12 ± 0,01	1,13 ± 0,01	1,13 ± 0,01
37	1,15 ± 0,01	1,08 ± 0,01	1,10 ± 0,01	1,13 ± 0,01	1,12 ± 0,02	1,14 ± 0,01	1,13 ± 0,01
39	1,13 ± 0,02	1,07 ± 0,02	1,10 ± 0,02	1,12 ± 0,01	1,11 ± 0,01	1,12 ± 0,01	1,12 ± 0,01
41	1,09 ± 0,01	1,07 ± 0,02	1,10 ± 0,01	1,11 ± 0,01	1,11 ± 0,01	1,12 ± 0,01	1,11 ± 0,01
43	1,08 ± 0,01	1,07 ± 0,01	1,10 ± 0,02	1,11 ± 0,01	1,11 ± 0,02	1,11 ± 0,02	1,11 ± 0,01
45	1,08 ± 0,01	1,07 ± 0,01	1,10 ± 0,01	1,10 ± 0,01	1,12 ± 0,01	1,12 ± 0,02	1,11 ± 0,01
47	1,07 ± 0,01	1,08 ± 0,02	1,09 ± 0,01	1,13 ± 0,01	1,11 ± 0,02	1,10 ± 0,02	1,12 ± 0,02
49	1,06 ± 0,01	1,07 ± 0,01	1,09 ± 0,01	1,12 ± 0,01	1,11 ± 0,01	1,11 ± 0,01	1,11 ± 0,01
51	1,07 ± 0,01	1,07 ± 0,01	1,10 ± 0,02	1,11 ± 0,01	1,11 ± 0,01	1,10 ± 0,01	1,11 ± 0,01
53	1,06 ± 0,01	1,06 ± 0,02	1,10 ± 0,01	1,11 ± 0,02	1,11 ± 0,01	1,09 ± 0,01	1,09 ± 0,01
55	1,06 ± 0,01	1,07 ± 0,03	1,09 ± 0,01	1,12 ± 0,02	1,12 ± 0,01	1,09 ± 0,02	1,10 ± 0,01

Table X – Thermal variation of equivalent polarity values (I_1/I_3) for 1-palmitoyl-2-oleoyl-*sn*-glycero-3-phosphocholine (POPC)/egg-Sphingomyelin (egg-SM)/Cholesterol (CHOL) mixtures with different chemical compositions (represented in terms of average ± standard deviation).

	POPC / egg-SM / Chol (mol% / mol% / mol%)		
T **(ºC)**	**(62.5 / 12.5 / 25.0)**	**(50.0 / 37.5 / 12.5)**	**(33.3 / 33.3 / 33.3)**
15	1,18 ± 0,02	1,15 ± 0,01	1,14 ± 0,01
17	1,16 ± 0,02	1,14 ± 0,02	1,14 ± 0,02
19	1,16 ± 0,01	1,13 ± 0,01	1,14 ± 0,01
21	1,15 ± 0,02	1,12 ± 0,01	1,13 ± 0,01
23	1,15 ± 0,01	1,12 ± 0,02	1,13 ± 0,01
25	1,15 ± 0,02	1,11 ± 0,01	1,12 ± 0,01
27	1,14 ± 0,02	1,11 ± 0,01	1,12 ± 0,01
29	1,13 ± 0,02	1,11 ± 0,01	1,11 ± 0,01
31	1,11 ± 0,01	1,10 ± 0,01	1,12 ± 0,01
33	1,12 ± 0,01	1,11 ± 0,02	1,10 ± 0,01
35	1,12 ± 0,01	1,10 ± 0,02	1,11 ± 0,02
37	1,12 ± 0,01	1,09 ± 0,01	1,11 ± 0,01
39	1,12 ± 0,01	1,10 ± 0,02	1,10 ± 0,01
41	1,12 ± 0,01	1,09 ± 0,03	1,11 ± 0,01
43	1,11 ± 0,01	1,09 ± 0,02	1,11 ± 0,01
45	1,11 ± 0,01	1,08 ± 0,03	1,10 ± 0,02
47	1,11 ± 0,01	1,09 ± 0,02	1,11 ± 0,02
49	1,11 ± 0,01	1,10 ± 0,01	1,10 ± 0,02
51	1,10 ± 0,01	1,09 ± 0,02	1,09 ± 0,01
53	1,11 ± 0,01	1,09 ± 0,02	1,12 ± 0,01
55	1,11 ± 0,01	1,12 ± 0,02	1,11 ± 0,01

Table XI – Thermal variation of equivalent polarity values (I_1/I_3) for egg-Sphingomyelin (egg-SM)/7-Dehydrocholesterol (7DHC) mixtures with different chemical compositions (represented in terms of average ± standard deviation).

	egg-SM / 7DHC (mol% / mol%)						
T **(ºC)**	**95/05**	**90/10**	**80/20**	**70/30**	**65/35**	**60/40**	**55/45**
25	1,06 ± 0,01	0,97 ± 0,01	0,95 ± 0,04	0,95 ± 0,03	1,05 ± 0,01	1,00 ± 0,04	1,06 ± 0,01
27	1,05 ± 0,01	0,96 ± 0,03	0,96 ± 0,02	0,97 ± 0,03	1,07 ± 0,02	0,98 ± 0,03	1,06 ± 0,02
29	1,03 ± 0,01	0,94 ± 0,02	0,97 ± 0,01	1,00 ± 0,03	1,01 ± 0,02	0,99 ± 0,04	1,08 ± 0,02
31	1,04 ± 0,02	0,95 ± 0,01	0,96 ± 0,03	0,99 ± 0,03	1,03 ± 0,01	1,00 ± 0,03	1,06 ± 0,03
33	1,02 ± 0,01	0,95 ± 0,02	0,94 ± 0,02	0,94 ± 0,03	1,03 ± 0,04	1,01 ± 0,03	1,08 ± 0,03
35	1,01 ± 0,01	0,93 ± 0,02	0,94 ± 0,02	0,93 ± 0,04	1,01 ± 0,02	0,98 ± 0,03	1,06 ± 0,03
37	0,98 ± 0,02	0,92 ± 0,01	0,92 ± 0,02	0,92 ± 0,03	1,00 ± 0,02	1,00 ± 0,03	1,09 ± 0,02
39	0,98 ± 0,01	0,92 ± 0,02	0,93 ± 0,01	0,90 ± 0,02	1,03 ± 0,01	0,95 ± 0,02	1,07 ± 0,01
41	0,98 ± 0,01	0,91 ± 0,02	0,95 ± 0,02	0,92 ± 0,01	1,02 ± 0,02	0,97 ± 0,03	1,07 ± 0,01
43	0,98 ± 0,02	0,89 ± 0,01	0,93 ± 0,02	0,94 ± 0,02	1,04 ± 0,02	1,01 ± 0,01	1,09 ± 0,04
45	0,98 ± 0,01	0,89 ± 0,01	0,94 ± 0,02	0,94 ± 0,03	1,03 ± 0,03	1,00 ± 0,03	1,14 ± 0,01
47	0,98 ± 0,00	0,93 ± 0,01	0,94 ± 0,03	0,96 ± 0,03	1,02 ± 0,01	0,99 ± 0,02	1,11 ± 0,03
49	0,99 ± 0,01	0,90 ± 0,01	0,96 ± 0,03	0,97 ± 0,04	1,03 ± 0,02	1,02 ± 0,03	1,14 ± 0,02
51	0,98 ± 0,01	0,93 ± 0,03	0,95 ± 0,03	0,98 ± 0,03	1,10 ± 0,04	1,01 ± 0,02	1,12 ± 0,02
53	0,99 ± 0,02	0,91 ± 0,02	0,94 ± 0,03	0,97 ± 0,04	1,09 ± 0,04	1,03 ± 0,01	1,15 ± 0,02
55	0,99 ± 0,01	0,92 ± 0,02	0,96 ± 0,03	0,99 ± 0,02	1,08 ± 0,04	1,02 ± 0,02	1,13 ± 0,03

Table XII – Thermal variation of equivalent polarity values (I_1/I_3) for egg-Sphingomyelin (egg-SM)/Cholestanol (DCHOL) mixtures with different chemical compositions (represented in terms of average ± standard deviation).

	egg-SM / DCHOL (mol% / mol%)						
T **(ºC)**	**95/05**	**90/10**	**80/20**	**70/30**	**65/35**	**60/40**	**55/45**
25	1,04 ± 0,01	1,03 ± 0,02	1,02 ± 0,01	1,03 ± 0,02	1,00 ± 0,02	1,02 ± 0,02	1,02 ± 0,02
27	1,03 ± 0,01	1,02 ± 0,01	1,01 ± 0,02	1,01 ± 0,01	1,00 ± 0,02	1,03 ± 0,01	1,00 ± 0,02
29	1,03 ± 0,01	1,02 ± 0,02	1,01 ± 0,02	1,00 ± 0,02	1,02 ± 0,01	1,03 ± 0,02	1,01 ± 0,02
31	1,01 ± 0,01	1,01 ± 0,02	1,00 ± 0,02	1,00 ± 0,01	1,00 ± 0,03	1,03 ± 0,02	1,02 ± 0,01
33	1,01 ± 0,01	1,00 ± 0,02	1,00 ± 0,01	0,98 ± 0,02	1,01 ± 0,02	1,02 ± 0,01	1,03 ± 0,02
35	1,01 ± 0,01	0,99 ± 0,01	0,98 ± 0,02	1,00 ± 0,01	0,98 ± 0,02	1,04 ± 0,01	1,04 ± 0,01
37	0,99 ± 0,01	1,00 ± 0,02	0,97 ± 0,01	0,99 ± 0,02	1,00 ± 0,02	1,04 ± 0,02	1,04 ± 0,01
39	0,97 ± 0,02	0,99 ± 0,01	0,96 ± 0,02	0,99 ± 0,01	1,00 ± 0,02	1,05 ± 0,02	1,04 ± 0,02
41	0,97 ± 0,02	0,97 ± 0,01	0,95 ± 0,01	0,98 ± 0,01	0,98 ± 0,03	1,05 ± 0,02	1,05 ± 0,02
43	0,97 ± 0,02	0,98 ± 0,01	0,96 ± 0,01	0,98 ± 0,01	0,99 ± 0,01	1,06 ± 0,01	1,05 ± 0,02
45	0,98 ± 0,01	0,98 ± 0,02	0,97 ± 0,02	0,99 ± 0,02	0,97 ± 0,02	1,06 ± 0,02	1,05 ± 0,01
47	0,97 ± 0,01	0,97 ± 0,01	0,96 ± 0,02	0,98 ± 0,01	0,99 ± 0,02	1,07 ± 0,02	1,06 ± 0,01
49	0,98 ± 0,01	0,97 ± 0,01	0,96 ± 0,01	0,97 ± 0,01	1,00 ± 0,02	1,08 ± 0,02	1,05 ± 0,01
51	0,98 ± 0,01	0,97 ± 0,01	0,96 ± 0,02	0,97 ± 0,02	0,99 ± 0,02	1,08 ± 0,02	1,07 ± 0,02
53	0,97 ± 0,01	0,98 ± 0,01	0,97 ± 0,02	0,97 ± 0,01	0,99 ± 0,02	1,08 ± 0,02	1,08 ± 0,01
55	0,98 ± 0,01	0,98 ± 0,01	0,96 ± 0,01	0,96 ± 0,01	0,99 ± 0,01	1,08 ± 0,02	1,06 ± 0,01